Factors influencing overbreak in narrow vein longitudinal retreat mining

By

Rory Hughes, B.ASc

A thesis submitted to McGill University in partial fulfillment of the requirements for the Degree of Master of Engineering

Department of Mining and Materials Engineering

McGill University

Montreal, Quebec, Canada

January, 2011

Abstract

Limiting the amount of ore dilution prior to entering the process stream is the goal of any mining operation. Narrow vein longitudinal retreating mining methods are especially susceptible to hanging wall and footwall dilution due to the wall overbreak. Understanding the factors which influence the stability of these walls can help a mining engineer design stopes that minimize dilution. This thesis presents the results of a study to examine these influential factors and reveals the process used to construct an empirical model capable of estimating dilution for a specific stope. This work is centered on a case study of Agnico Eagle Mines Ltd. Lapa mine located in Preissac, Quebec.

Possessing a means to properly measure and quantify dilution is an essential part of this study. An in depth review of the various techniques is presented with the concept of Dilution Density being chosen as a means to quantify dilution. In order to determine which factors influence dilution, a review of existing literature, including modelling studies is undertaken. With careful review of the mining practice and geological environment, the most important of these factors are identified. One of these factors, stope strike length in narrow vein retreat mining, is not thoroughly explored by existing publications; and, in order to better understand this factor a numerical model is constructed.

Before constructing this numerical model it is necessary to find an adequate means to organize and interpret the copious amounts of data retrieved from the mine site. Data such as geotechnical drill holes, stope reconciliation data, and stope construction details are integrated into a purpose-built geomechanical database. Named the *"Data Integrator for Mine Analysis and Design (DIMAND)"* the database software package provides easy access to important data and eases the construction of numerical models.

In order to fully understand the influence of stope strike length on unplanned ore dilution, a numerical model is constructed. Due to the geometry of the problem, it is necessary to perform the analysis in three dimensions. The finite difference code FLAC3D is employed to construct a model based on rock mass properties and stope constructions present at Lapa mine. With strain softening behaviour common in rock masses and the Lapa rock mass being one regularly

subjected to large strains, a strain-softening constitutive model is employed in the FLAC3D model. This model reveals that larger stope strike lengths are prone to generate larger volumes of dilution into a newly opened stope whereas shorter strike lengths are less prone to dilution. The model also explores the effects of a retreat sequence on overbreak; revealing that primary stopes are slightly more prone to overbreak than secondary stopes.

These studies aided in the development of an empirical model that provides estimates for stope overbreak tonnages. The development of the empirical model is explored in detail from early models with small sample groups and simple mathematical constructions, to the final model which employed 86 stopes and statistical software to identify important relationships between seemingly independent factors. Through the use of this model engineers can now plan stopes with knowledge of how each parameter influences overbreak and production and scheduling personnel can plan production goals with increased confidence.

Résumé

Limiter le montant de dilution dans le flux de processus est l'objectif de toute exploitation minière. Les méthodes d'exploitation minière en veine mince par retraite longitudinal sont particulièrement sensible à la dilution en raison de la forme élancée des chantiers. Comprendre les facteurs qui influencent la stabilité de ces murs peuvent aider un ingénieur des mines a réduire au minimum la dilution. Cette thèse présente les resultants d'une étude visant à examiner ces facteurs d'influence et révèle les processus utilizes pour construire un modèle empirique permettant d'estimer la dilution pour un chantier spécifique. Ce travail est centré sur une étude de cas de la mine Lapa de Agnico Eagle Mines Ltd, situé à Preissac, Québec.

Avoir en sa possession un moyen de bien mesurer et de quantifier la dilution est une partie essentielle de cette étude. Un examen approfondi des différentes techniques est présentée avec le concept de Densité de Dilution choisi comme un moyen de quantifier la dilution. Afin de déterminer les facteurs qui influencent la dilution, une revue de la littérature existante, et les études de modélisation est effectuée. Avec un examen attentif de la pratique des mines et de l'environnement géologique, les plus importants de ces facteurs sont identifiés. Une de ces facteurs, la longueur du chantier dans le secteur minier veine mince retraite, n'est pas exploré par la publication en vigueur, en vue de mieux comprendre ces facteurs un modèle numérique est construit.

Avant de construire ce modèle numérique, il est nécessaire a trouver un moyen approprié pour organiser et interpréter la grande quantité de données extraites de la mine. Les données telles que les trous de forage géotechnique, la réconciliation des données du chantier, et les détails de construction du chantier sont intégrés dans une base de données. Nommé le *"Data Integrator for Mine Analysis and Design (DIMAND)"* le logiciel permet d'accéder facilement à des données importantes et facilite la construction de modèles numériques.

Pour bien comprendre l'influence de la longueur du chantier sur la dilution, un modèle numérique est construit. A cause de la géométrie du problème, il est nécessaire d'effectuer l'analyse en trois dimensions. Le code FLAC3D différences finies est utilize pour construire un modèle basé sur les propriétés de la masse rocheuse et constructions chantier présents à la mine

Lapa. Avec des comportements adoucissement commune dans les roches et la masse rocheuse Lapa régulièrement soumis à une grande souches, une modèle d'adoucissement de comportement est utilisé dans le modèle FLAC3D. Ce modèle révèle que les grandes longueurs du chantier sont susceptible d'introduire des volumes plus élevés de dilution dans un chantier récemment ouvert alors que la grève des longueurs plus courtes sont moins sujettes à la dilution. Le modèle examine également les effets d'une séquence de retraite sur la profil du dilution, révélant que les chantiers primaires sont légèrement plus enclins au dilution que les chantiers secondaires.

Ces études ont contribué au développement d'un modèle empirique qui donne des estimations de dilution. Le développement de ce modèle est étudié en détail à partir des premiers modèles avec des petites groupes de chantiers et des simples constructions mathématiques, le modèle final, qui employait 86 chantiers et des logiciels statistiques pour identifier les relations importantes entre les facteurs en apparence indépendants. Grâce à l'utilisation de ce modèle ingénieurs peuvent maintenant planifier les chantiers avec une connaissance de la façon dont chaque paramètre influence la dilution et de la cote production et planification ils peuvent planifier les objectifs de production avec une confiance accrue.

Acknowledgement

I thank my supervisor, Professor Hani S. Mitri, for his unwavering support and thoughtful guidance throughout my studies. I thank Eric Lecomte of Agnico Eagle Mines for his contributions to the project and his enthusiasm during our meetings. Thanks to the members of the Mine Design Lab group for their assistance on countless occasions.

Table of Contents

List of Figures

List of Tables

Nomenclature

c	cohesion
DD	dilution density
DD_{MAX}	maximum distance DD extents into the wall at the centroid of the face
E	Young's modulus
E_i	Young's modulus for intact rock
E_{rm}	Young's modulus for rock mass
ELOS	equivalent linear overbreak/slough
GSI	geological strength index
G	shear modulus
K	bulk modulus
K_{MIN}	minimum horizontal to vertical stress ratio
K_{MAX}	maximum horizontal to vertical stress ratio
m, s, a	material constants of Hoek-Brown failure criterion
m_i	intact rock material constant of Hoek-Brown failure criterion
N'	modified stability number
Q	rock tunneling index
RMR	rock mass rating
RQD	rock quality designation

γ material unit weight

ε strain

ε_{MAX} maximum elastic strain

θ angle of internal friction

ν Poison’s ratio

ρ material density

σ stress

σ_1, σ_2, σ_3 major, intermediate, and minor principal stress, respectively

σ_c uniaxial compressive strength of intact rock (UCS)

σ_{bc} uniaxial compressive strength of rock mass

σ_t tensile strength

ψ angle of dilation

Chapter 1 – Introduction

1.1 General

Longitudinal retreat mining methods are commonplace in narrow vein Canadian mines. The slender shape of the stopes created using this method can cause instability along the walls. Due to the fact that height is often the largest dimension, this instability can cause large amounts of waste rock, or dilution, to slough into a newly blasted stope. Since sorting waste rock from ore material at a drawpoint is nearly impossible, this waste rock is often unintentionally fed into the production stream. The addition of this worthless material to the process stream lowers the overall expected grade. Should this continue unchecked, it could threaten the economic viability of a mining operation. Understanding the factors which influence overbreak in narrow vein longitudinal retreat mining can lead to the development of practices that reduce unplanned dilution.

A geotechnical and stope reconciliation database was developed for Lapa mine, Agnico Eagle Mines Ltd., to help acquire the data necessary to examine factors influencing overbreak.

This data allowed for the development of a three dimensional numerical model designed to assess the influence of stope strike length on stope stability. Numerical modelling results, from the strike study, as well as other studies, aided in the development of an empirical model designed to estimate unplanned dilution at Lapa mine.

This thesis introduces a methodology for developing an empirical dilution model for a specific mine.

1.2 Research objectives

There are three major goals in the research of unplanned ore dilution in narrow vein longitudinal mining:

- Develop a geotechnical and stope reconciliation database capable of storing and interpreting data from the mine site. This database must provide features which allow the generation of numerical modelling input as well as features which aid in the analysis of past stopes and the design of new stopes.

- Construct a three dimensional finite difference model in order to assess the effects of stope strike length on stope stability. The model should be constructed in a fashion which allows for the effects of mining sequence to be considered.
- Develop an empirical model which can be used to predict dilution based on a set of measurable factors.

1.3 Thesis structure

Chapter 1 is a general introduction to the research problem, the methodology employed, and the objectives of this research.

Chapter 2 reviews literature pertaining to measuring, quantifying, and modelling dilution. It examines literature which explores factors influencing dilution.

Chapter 3 presents the features and functionality of the database software package developed using *Visual Basic .Net*.

Chapter 4 reveals the development of the three dimensional numerical model designed to evaluate the effects of strike length and sequence.

Chapter 5 describes the methodology and steps employed in the creation of an empirical model that estimates unplanned ore dilution at Lapa mine.

Chapter 6 summarizes the findings of this research and makes recommendations for future studies.

Chapter 2 – Dilution

2.1 Introduction

Dilution is a measure of unwanted material in the mine material process stream. This unwanted material can be barren waste rock or ore material which is below cut-off grade. At times, this unwanted material must be included within planned stope boundaries. While this remains undesirable, in bulk mining methods geometric constraints necessitate the inclusion of this so called planned dilution.

Planned dilution occurs when equipment or mining method limitations force it to be incorporated into the planned stope outline. When bulk mining methods are employed in irregular, small thickness or narrow vein deposits poor equipment sizing can result in planned dilution (Trevor 1991). In cases where the ore and waste materials have a complex contact surface it can be impractical to follow that contact surface in detail. Limitations in drilling machines and blasting techniques are unable to follow these complex surfaces and instead, simple surfaces which incorporate the minimal amount of dilution are employed (Elbrond 1994).

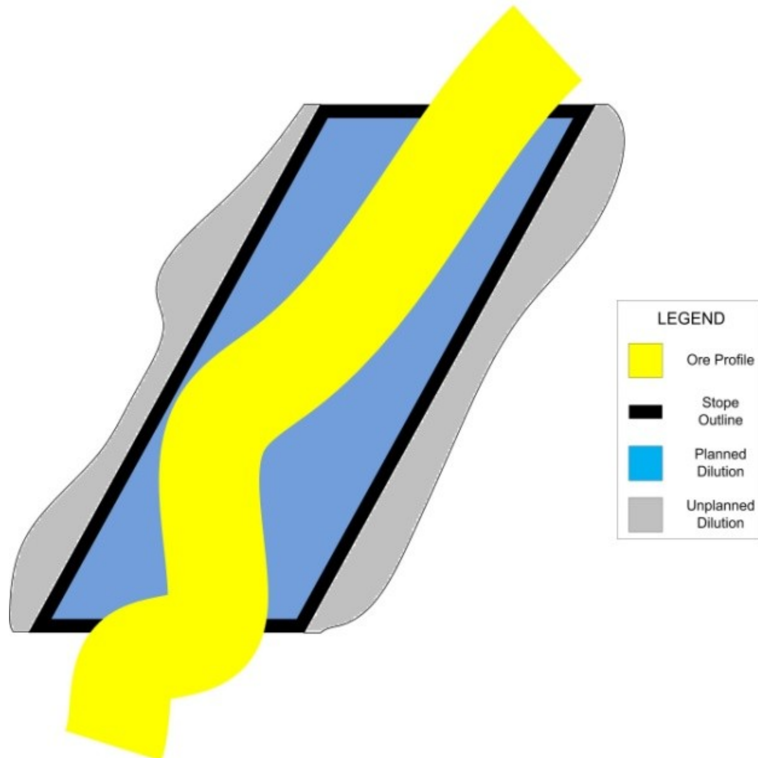

Figure 2.1 Schematic of planned and unplanned dilution.

Unplanned dilution is caused by instability of the exposed rock face. This instability leads to caving and sloughage of the exposed wall rock. Several factors have been shown to affect this stability and are discussed in this chapter. This caved rock is then unknowingly mucked out and enters the ore material handling stream. Once in the ore material handling stream, this worthless material is handled in the same way as profitable ore. The costs of hauling, crushing, hoisting as well as associated milling costs can be enormous and the additional waste material can displace profitable ore from the handling and milling stream (Henning and Mitri 2008). Time costs associated with the additional time required to muck and backfill greater than anticipated stope volumes can be significant enough to disrupt the mining schedule.

2.2 Quantifying and reporting dilution

To fully assess the impact of unplanned dilution on an operation it is necessary to have a means to quantify and report dilution values. Modern mining operations are equipped with highly accurate survey equipment such as total stations and cavity monitoring surveys (CMS). The development of the CMS in the 1980s has provided mine operators with the ability to accurately survey the shape of an underground cavity. By performing a CMS on a recently excavated stope it is possible to estimate the volume of material extracted and to also locate the source of any unplanned dilution.

The ability to locate the source of dilution (i.e. to identify which wall it fell from) allows dilution to be reported based on a specific location rather than just for a stope in general.

2.2.1 Percentages

Dilution is often presented as a percentage of waste rock to ore material but, as shown by Pakalnis (1986), is reported in a variety of ways in Canadian mines.

$$Dilution = \frac{Tonnes\ waste\ mined}{Tonnes\ ore\ mined} \times 100\% \quad (1)$$

$$Dilution = \frac{Tonnes\ waste\ mined}{Tonnes\ ore\ mined + Tonnes\ waste\ mined} \times 100\% \quad (2)$$

$$Dilution = Backfill\ tonnage\ actually\ placed - Backfill\ tonnage\ theoretically\ required \quad (3)$$

$$Dilution = \frac{Meters\ of\ footwall\ slough + Meters\ of\ hanging\ wall\ slough}{Ore\ Width} \quad (4)$$

Vallée et al. (1992) explain how narrow longhole stopes may fall victim to misleading results using the equations presented above. Due to their slender shapes, these types of stopes are often prone to large amounts of dilution. For example, consider a case where a 2 meter wide stope, 30 meters high, and 12 meters long contains about 2,000 tonnes of ore. If the footwall and hanging wall each show dilutions of 750 tonnes then a dilution of 75% is found (using Equation 1). If the overbreak on both the footwall and hanging wall remains the same, yet the stope width increases to 4 meters the new stope tonnage is about 4,000 tonnes and the dilution plunges to 37.5%.

2.2.2 Equivalent linear overbreak/sloughage (ELOS)

In order to overcome the problems caused by using percentages and to better reflect the actual size of overbreak, Dunne and Pakalnis (1996) proposed that dilution should be calculated in average meters of wall slough per square meter of wall.

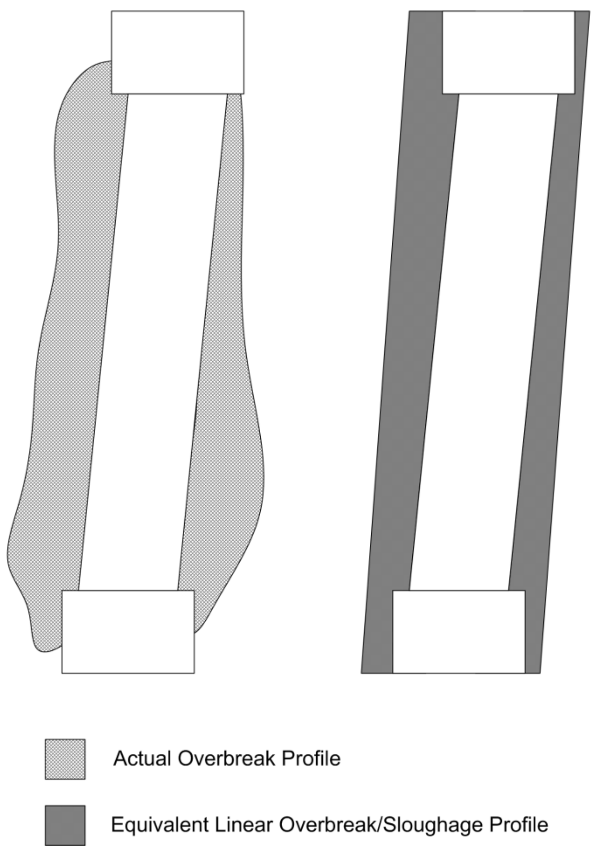

Figure 2.2 Equivalent linear overbreak/sloughage (ELOS).

ELOS can be calculated by using Equation 5.

$$ELOS = \frac{Volume\ of\ slough\ from\ stope\ surface}{Stope\ Height\ \times Wall\ Strike\ Lenght} \quad (5)$$

2.2.3 Dilution density

While ELOS is a very useful tool, in that it assigns a location to overbreak but also that it is actually a physical representation of the size of this overbreak, it assumes that the shape of the overbreak envelope is a rectangle with uniform thickness along all sections of the stope face. Examination of CMS profiles by Henning and Mitri ([7]2007, 2008) revealed that overbreak profiles are more accurately generalized as a half-prolate ellipsoid, refer to Figure 2.1.

Figure 2.3 Plan view mid-stope height CMS profile.

The concept of Dilution Density, presented by Henning and Mitri (2007, 2008) considers the origin of the overbreak and provides a means to better report dilution. In this strategy, overbreak is described by the volume of a half-prolate ellipsoid, refer to Figure 2.4.

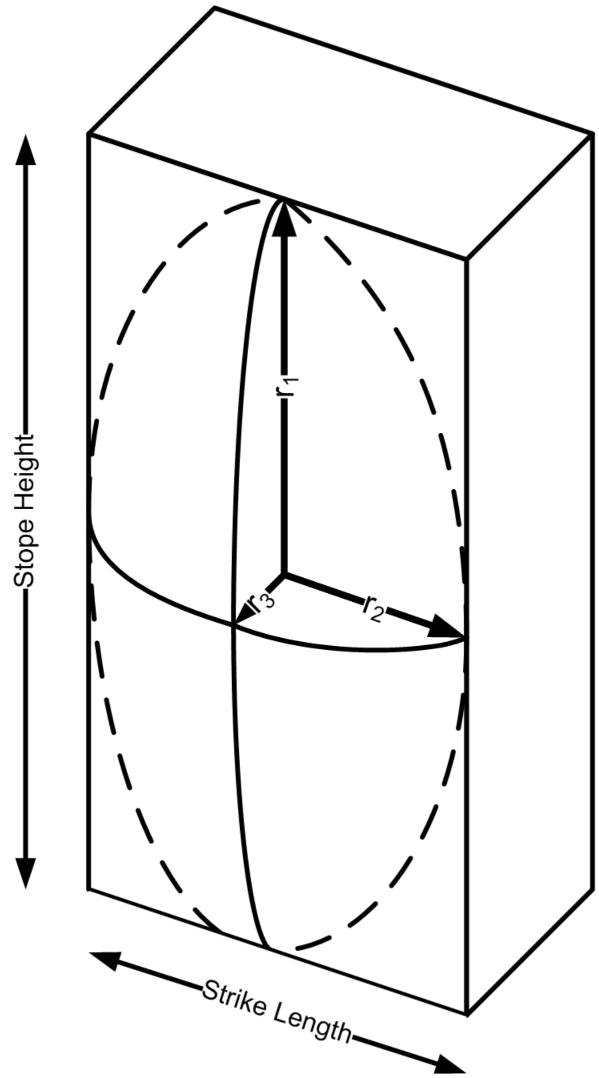

Figure 2.4 The dilution density half-prolate ellipsoid.

The volume of the ellipsoid can be calculated using Equation 6.

$V = \frac{2\pi}{3} r_1 r_2 r_3 (m^3)$ (6)

Where r_1, r_2, and r_3 refer to the perpendicular and horizontal radius distances from the center of the stope wall contact. The ellipsoid makes it possible to calculate dilution density at any point on the stope wall. The maximum values occurs at the center where DD=r_1. For the purposes of this thesis, this will be referred to as DD_{MAX}.

2.3 Factors influencing unplanned dilution

By exploring factors perceived to influence unplanned dilution it is possible to gain a better understanding of their impact on the degree of overbreak. As factors are better understood it becomes possible to plan stopes in such a way as to minimize the potential for unplanned dilution.

Instability of rock faces are typically driven by two broad failure types. Stress driven failure is a situation where the applied stress is greater than the material strength. Failure criteria described by Coulomb (1776) and Hoek and Brown (1980) are commonly used in the evaluation of rock strengths. Stresses cause failure in both compression; when concentrated stresses surrounding an opening exceed the strength of the rock and in tension; when stress redistribution surrounding an opening created tensile stresses in the rock (shown in Figure 2.5). In large underground stopes, the development of low stress or tensile stress zones is common. These zones of stress relaxation reduce the clamping forces which would otherwise prevent the rock mass from sloughing or unraveling (Henning and Mitri 2007).

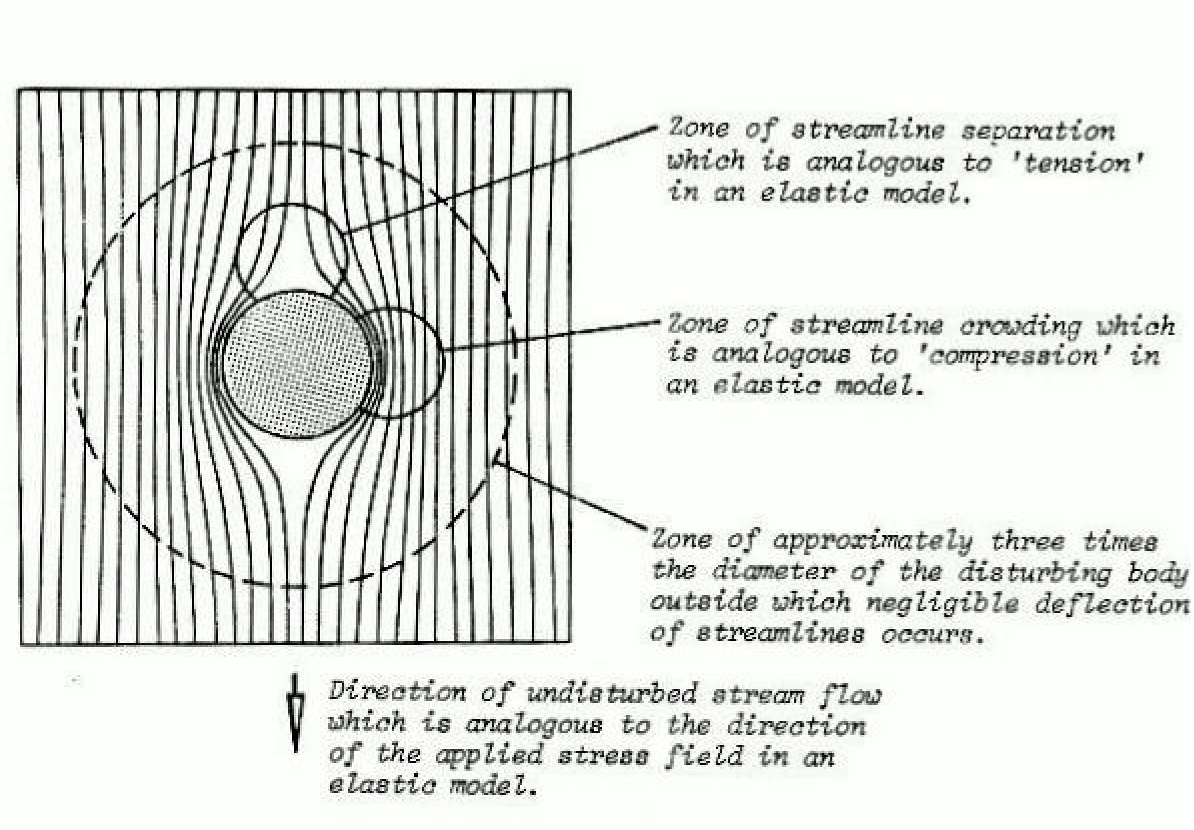

Figure 2.5 Deflection of stress lines around a circular opening after Hoek and Brown (1980).

It is this type of low stress environment that allows for the second failure type to occur. Gravity driven failure describes how wedges of rock can slide or fall from a free surface. The orientation of the free surface as well as the jointed nature of a rock mass can help determine the susceptibility of a face to gravity driven failure.

With an understanding of the failure mechanism, it is possible to create a list of factors which influence this mechanism and through the use of numerical modelling and back analysis, their importance can be determined.

2.3.1 Rock mass mechanical strength

Since unplanned ore dilution is the product of wall instability it is apparent that the mechanical properties of the rock mass would have a significant influence. The empirical stope design methods presented by Mathews et al (1981) and extended by Potvin (1988) are based largely on the modified stability number, N'.

This stability number is used as a measure of the rock mass strength with respect to the orientation between critical joint surfaces and stope face. The modified stability number, N', presented by Potvin (1988) is the product of four factors as shown in Equation 7:

$$N' = Q' \times A \times B \times C \quad (7)$$

Q' is an indication of rock mass quality, A incorporates the effects of induced stress, B accounts for weakness due to the direction of the dominant joint system, and C takes into account the orientation of the critical face and the impact of gravity upon it. The value of Q' is based on the Rock Tunnelling Index, Q, introduced by Barton et al. (1974) as described by the following equation:

$$Q = \frac{RQD}{J_n}\frac{J_r}{J_a}\frac{J_w}{SRF} \quad (8)$$

In the above, RQD is the rock quality designation, Jn is the joint set number, Jr is the joint roughness number, Ja is the joint alteration number, Jw is the joint water reduction factor, and SRF is the stress reduction factor. The modified rock tunnelling Index, Q', sets the values of Jw and SRF both equal to 1, which results in the following equation provided by Potvin (1988):

$$Q' = \frac{RQD}{J_N}\frac{J_R}{J_A} \quad (9)$$

In effect, the parameters Jw and SRF representing the effects of active stress on stability, are replaced by the Rock Stress Factor, A, within the modified stability number, N'.

The modified stability number is an example of a means to assess the resistance of a rock mass to failure. It attempts to incorporate the effects of both stress and gravity driven failure; unfortunately, it is also very simple in nature, making it ideal only for preliminary studies.

In order to properly assess the effects of rock strength and stress it is necessary to construct numerical models. Properly constructed and designed models can provide insight into the stress distributions around excavations. These types of models also allow the exploration of other factors such as stope geometry and construction.

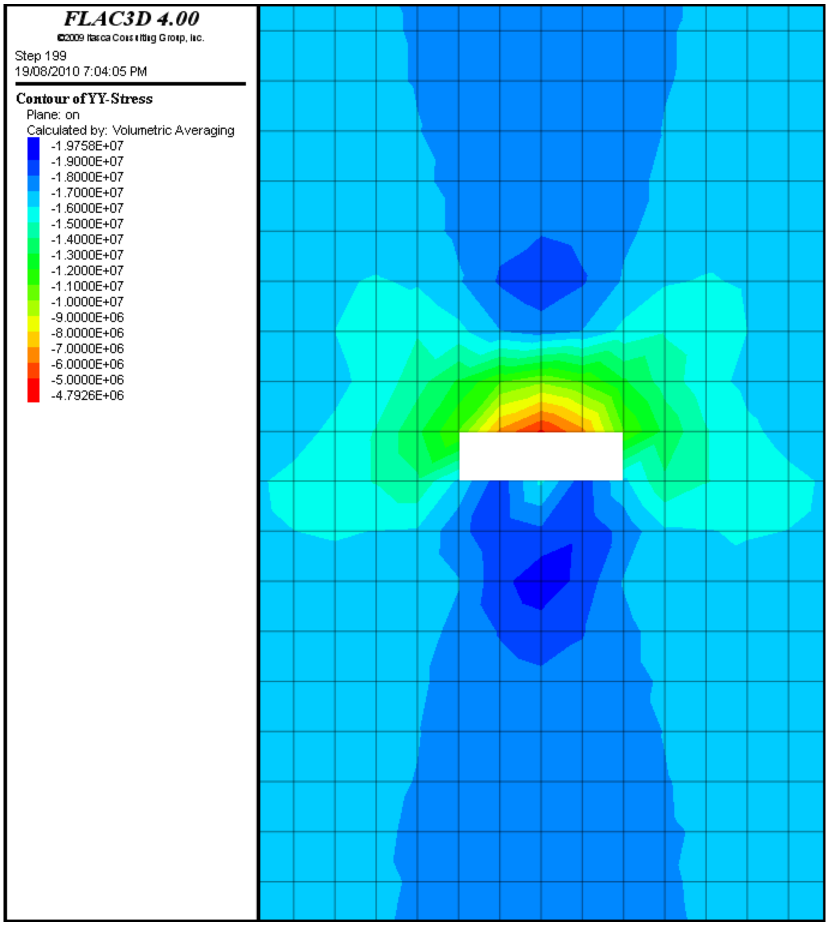

Figure 2.6 A three-dimensional finite difference model constructed using FLAC3D in order to determine the maximum stress on the stope skin at its mid-height.

2.3.2 Stope geometry

The dimensions of a stope have an enormous influence on its stability. The greater the span of the unsupported face the higher the strength requirement and the greater the chance for failure. Mathews (1980) and Potvin (1988) both used hydraulic radius as a measure of the effects of dimensions. The hydraulic radius is the quotient of the area to the perimeter of the face under examination. For example, if the roof was being examined:

HR = $\frac{Length \times Width}{2 \times Length + 2 \times Width}$ (10)

In longhole and other bulk mining methods, the height is normally the largest dimension with the length and width depending on the thickness of the ore seam and whether the sequence is transverse or longitudinal. With that in mind, it is the stope walls which are of the most concern with regards to unplanned dilution.

Stope height is determined in the early stages of mine design and is usually based on the mining method, production drilling equipment capabilities, and open stope stability. From a stability perspective, in narrow vein longitudinal mining the stope height (and predominantly the hanging wall), is the face most susceptible to overbreak. The hanging wall face is often the largest span and is more heavily influenced by the effects of gravity.

The influence of gravity is heavily affected by the dip of the stope. Steeply dipping orebodies shed vertical stresses around their perimeter and are less influenced by the effects of gravity.(see Figure 2.7 90 degree dipping stope shedding vertical stresses.) As the dip becomes shallower, vertical stresses cannot as easily pass around and they create zones of relaxation and potential caving. Thus, in shallower dipping stopes, the hanging wall becomes increasingly prone to the effects of gravity; see Figure 2.8.

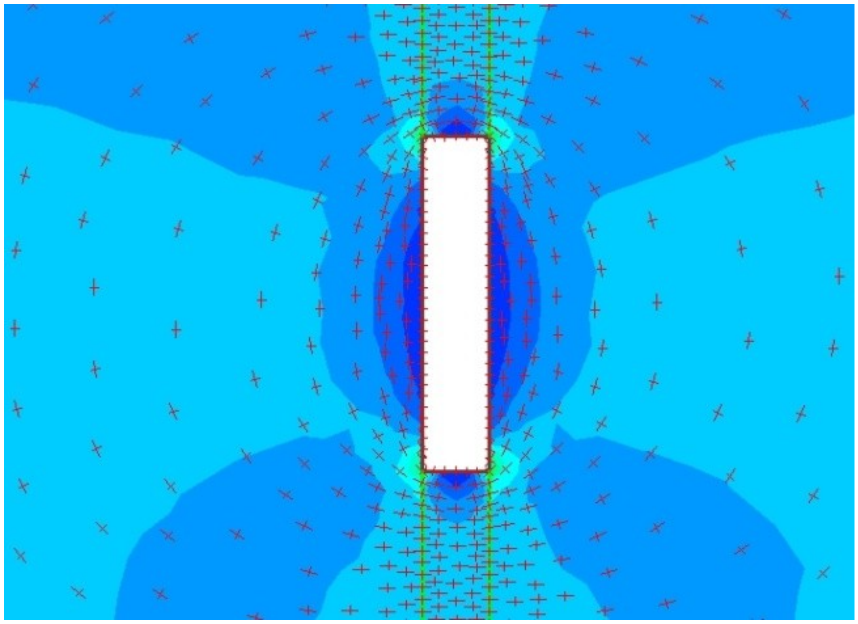

Figure 2.7 90 degree dipping stope shedding vertical stresses.

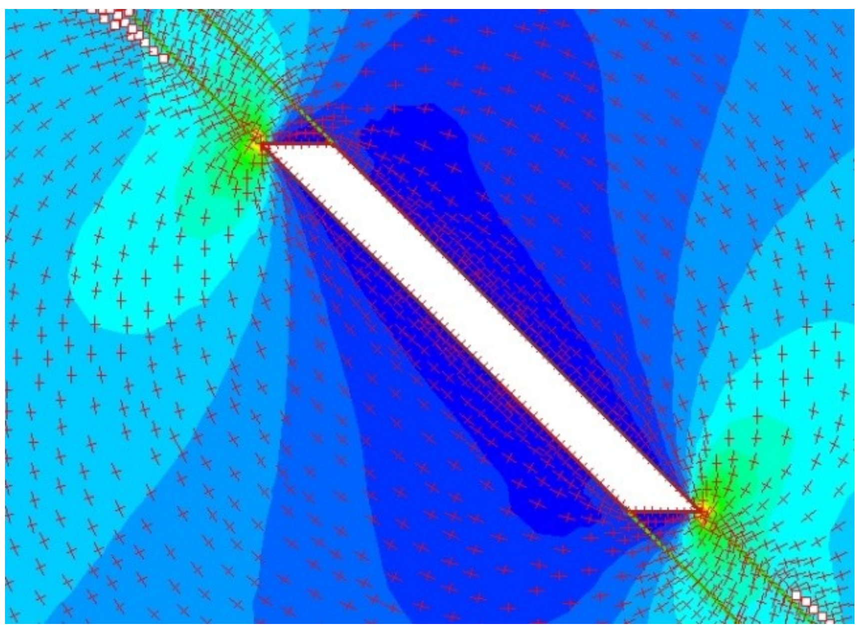

Figure 2.8 Shallow dipping stope showing large zones of relaxation.

Henning and Mitri (2007) examined the effects of stope dimensions as well as dip on transverse stopes. A relaxation criterion was employed as a means to describe the degree of overbreak that could be expected for each set of variables. This type of criteria is based on the size of the relaxation enveloped formed by the contour of $\sigma_3 \leq 0$ MPa. The concept behind this criterion is that the minor principal induced stress is providing a clamping force which keeps the rock mass from unraveling. This criterion assumes that the rock mass has no tensile strength.

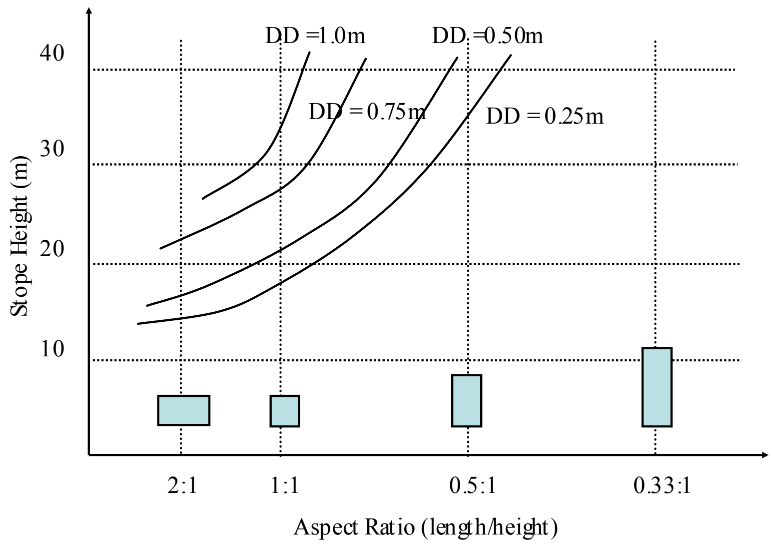

Figure 2.9 Dilution density associated with stope height and aspect ratio for the base case stope, σ_3=0MPa contour after Henning and Mitri (2007).

Figure 2.9 shows how short stopes with short strike lengths generate the lowest DD values. As the aspect ratio approaches 1 and, as stope heights increase the degree of overbreak also increases.

In narrow vein longitudinal mining, the stope length is frequently the second largest dimension, along with the fact that it also influences the hydraulic radius of the hanging and footwalls make it another important factor. Chapter 4 examines the effect of stope strike length in detail.

Stope width (again, in narrow vein longitudinal mining) is governed by the thickness of the seam. This largely limits the ability of the engineer to adjust it yet it is a dimension which has an influence on overbreak. While it represents the span of the back (which is supported and not of major concern with respect to overbreak) it also influences the post mining stress regime. The extent to which it influences the post mining stress regime depends largely on the orientation of the in-situ stress regime in relation to the opening as well as the ratio of horizontal to vertical stresses.

2.3.3 Undercutting

Undercutting occurs often in longhole narrow vein longitudinal retreat mining, since the vein is so narrow it becomes necessary to drill parallel production holes instead of fanning them.

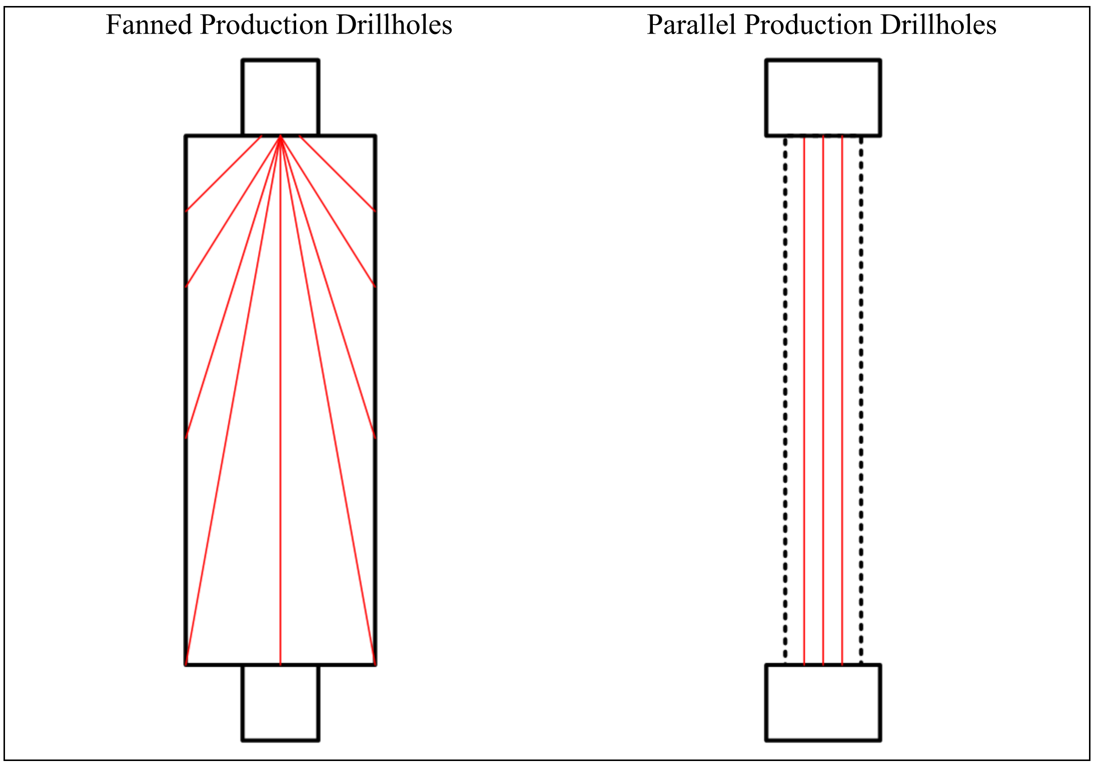

Figure 2.10 Undercutting due to production drilling requirements.

In order to allow for safe clearance around the drill boom, the overcut drift (i.e. where the drill operates) needs to be wider than the vein. Since mining progresses upwards in retreat mining, the overcut of the lower level stope becomes the undercut of the stope above it. Wang (2004) explains that undercutting has a significant impact on the stability of a wall rock mass in that:

1) An additional free face is developed with the creation of the undercut
2) Confinement of the immediate wall is reduced which allows a jointed rock mass to "loosen up"
3) The beam created by the immediate wall is broken

4) There is an increased zone of relaxation associated with wall undercutting.

A study by Zniber et al. (2009) showed that the effect of moving from no undercut to even a slight undercut has a significant impact on the stability of a stope wall.

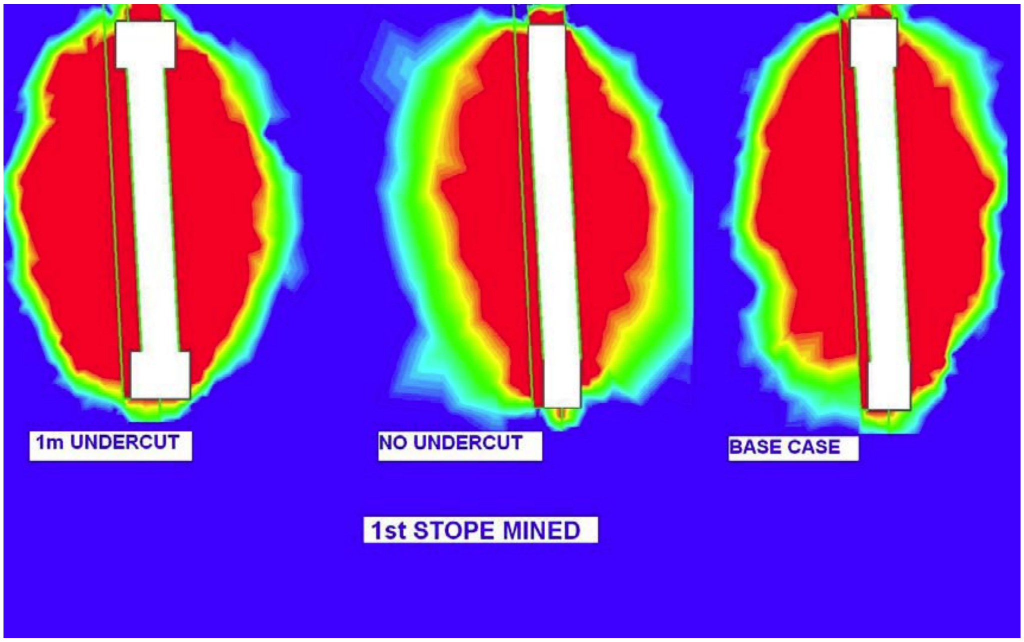

Figure 2.11 Changes in yielded material surrounding stopes with various degrees of undercutting (Zniber et al., 2009)

Undercutting can also be caused by extensive failure in a previously mined lower stope. If not kept in check, as mining progresses upwards, this type of failure driven undercutting can worsen throughout the sequence. Minimizing undercut is essential to reducing the degree of overbreak.

2.3.4 In-situ stress fields

Henning and Mitri (2007) performed numerical studies to show the influence of in-situ stress field magnitude, orientation as well as the effect of stope dip on transverse stopes. In the examination of stress field magnitude a base case (30m vertical height, 80° dip, GSI=65, σ_1° perpendicular to hanging wall) with strike lengths ranging between 10 to 40 meters was modeled at three different mining depths.

Henning and Mitri (2007) again employed a relaxation criterion as a means to describe the degree of overbreak that could be expected for each set of variables. This criterion assumes that the rock mass has no tensile strength but Henning and Mitri (2007) also examined the effect of depth if the rock mass is assumed to have a tensile strength of -0.5MPa. In that case, DD_{MAX} is described by the contour of σ_3=-0.5 MPa.

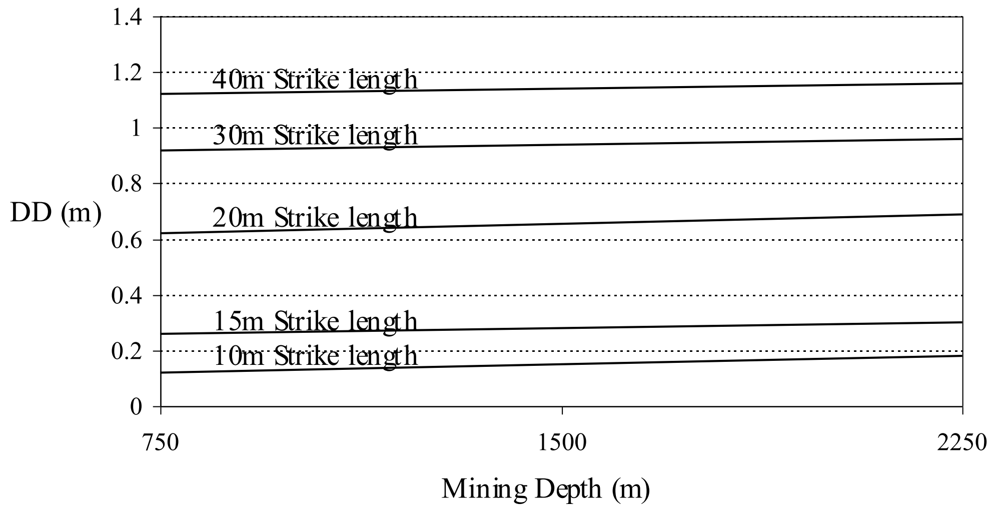

Figure 2.12 Modelled dilution density trend lines as a function of mining depth, σ_3=0MPa contour after Henning and Mitri (2007).

Figure 2.12 uses the zero-tensile strength relaxation criterion to describe overbreak and very little change in DD is seen with increasing mining depth. If the rock is assumed to have a tensile strength of 0.5MPa and a -0.5MPa σ_3 contour is employed (refer to Figure 2.13) then the effect of mining depth becomes more pronounced.

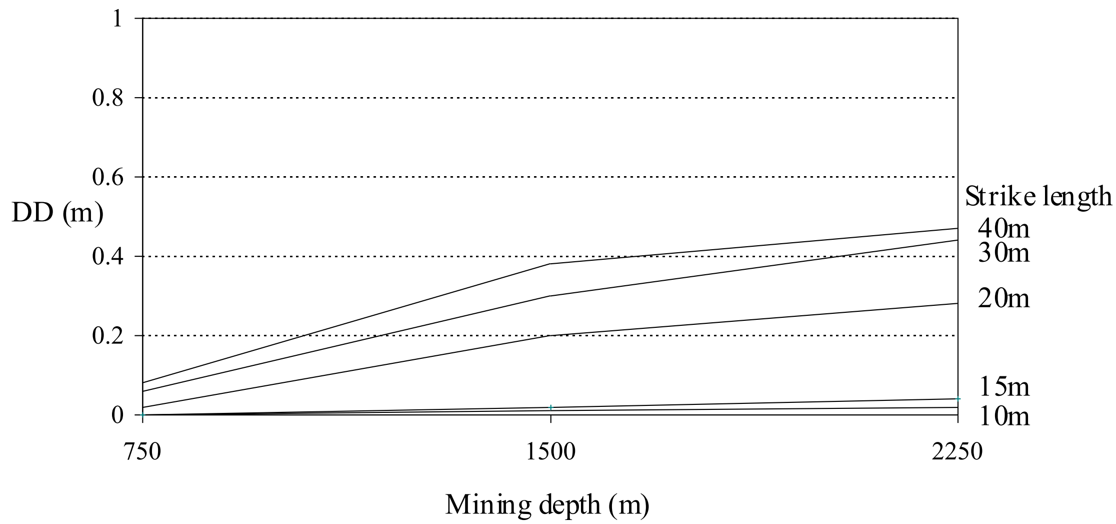

Figure 2.13 Modelled dilution density trend lines as a function of mining depth, σ_3=-0.5MPa contour after Henning and Mitri (2007).

Henning and Mitri (2007) also explored the effects of rotating the in-situ stresses on transverse stopes. In this study the in-situ stress magnitudes were kept constant and the maximum horizontal to vertical stress ratio was held at 1.6, the minimum horizontal to vertical stress ratio was 1.2. Figure 2.14 shows that when the major principal pre-mining stress is oriented perpendicular to the stope strike length (strike length being variable while width was constant at 10m) the overbreak is greater in every case with the exception to the case where length and width are equal. When the maximum stress is oriented perpendicular to the largest open face it is expected to see the greatest stress disturbance on that face. In this case, as the stresses are forced around the opening they create relaxation in the walls.

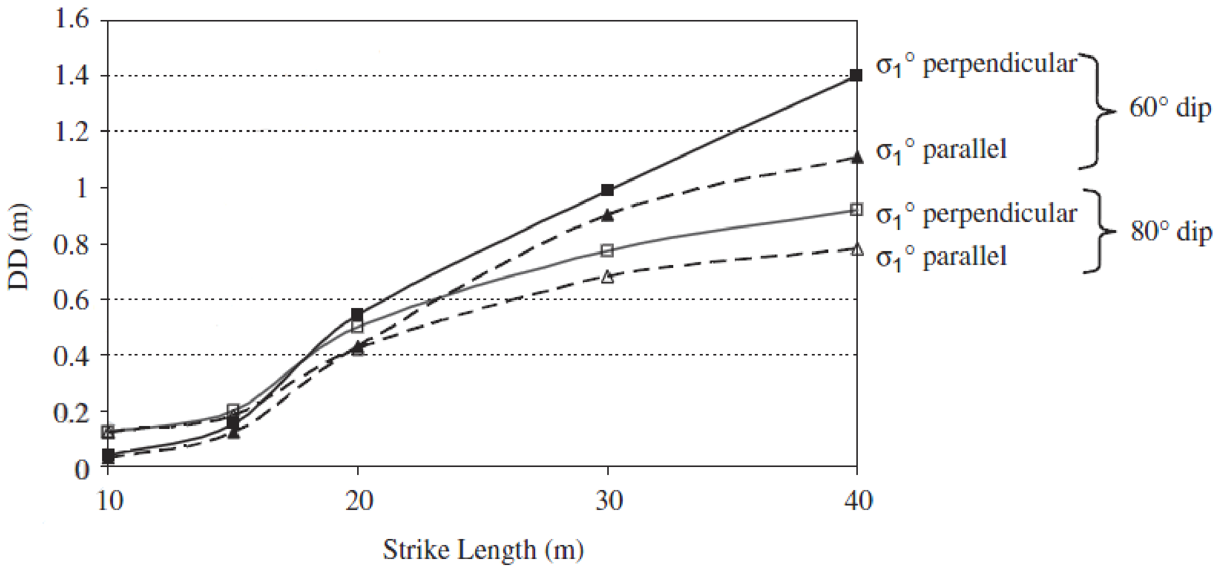

Figure 2.14 Influence of major principal stress orientation on overbreak. Base-case stope, σ_3=0 MPa contour after Henning and Mitri (2007)

Wang (2004) examined the effects of horizontal to vertical stress ratio (such that K_{MIN} and K_{MAX} were equal) on a variety of transverse stope sizes. The major principal in-situ stress was oriented normal to the strike length-stope height face with the minor principal stress in the vertical direction. Using a constant stope width of 10m, stope heights which varied between 20 and 100m, and strike lengths which varied between 10 to 100m a set of models with increasing hydraulic radiuses were created. Figure 2.15 shows the findings of this study. Wang (2004) showed that increasing the K value resulted in a larger zone of relaxation ($\sigma_3 \leq 0$MPa) and that increasing the hydraulic radius also increases the zone of relaxation.

This was expected for the same reason as before. When the largest stress is oriented normal to the largest face it will generate a large relaxation zone along that face as the stresses are forced to flow around the opening.

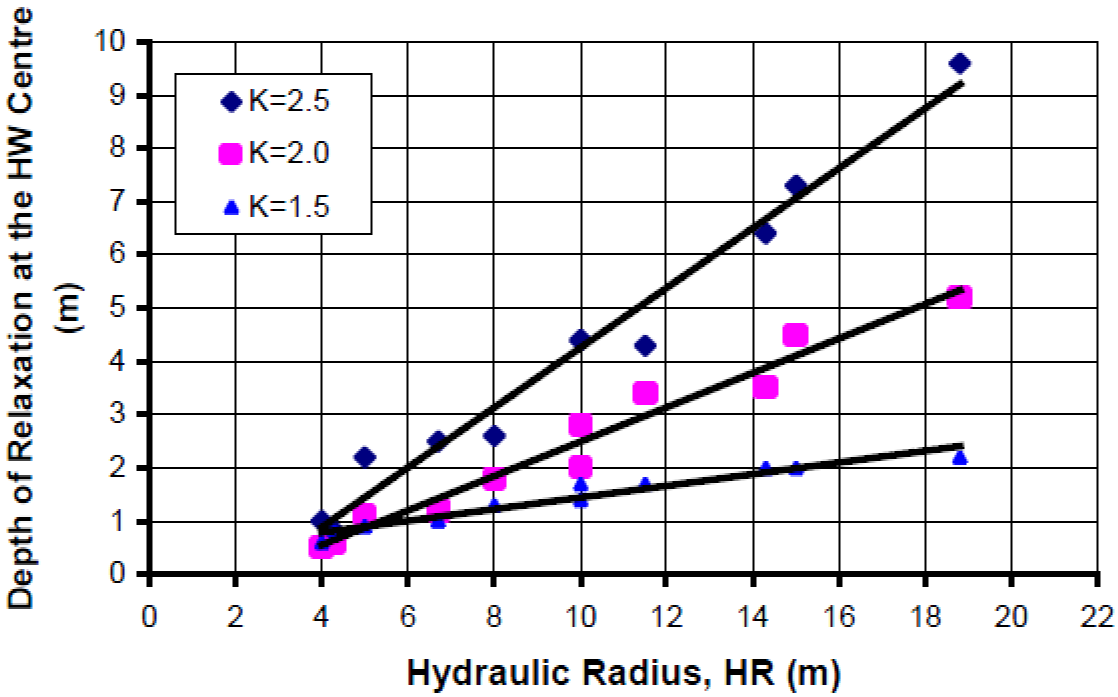

Figure 2.15 The depth of relaxation at the center of the stope HW vs. hydraulic radius (HR) for different stress ratios for rectangular shaped stopes after Wang (2004).

2.3.5 Stope sequence

Local stope sequence has been shown to have a significant impact in transverse sequences (Henning and Mitri 2007). In transverse mining a variety of stope types are created due to the sequence; primary stopes (P1) are surrounded by rock on both walls and secondary stopes have backfill on one (S1) or both (S2) sides. As the mining sequence progresses upwards, there is another stope type (sublevel stopes) which have already had the stope(s) below them mined out. Henning and Mitri (2007) showed that primary stopes show significantly lower degrees of overbreak than secondary stopes, also, that sublevel primary (P2 and P3) stopes show more overbreak than level primary stopes (P1). S2 stopes have the highest overbreak because the mining of two stopes on either side has created a larger zone of disturbance which allows for a greater degree of relaxation. A similar phenomenon explains the increase between P1 and P2 stopes; with P2 stopes, a disturbance has been created by the stope mined out below.

In longitudinal retreat mining, a primary stope exists at the start of the sequence but then it is followed by a series of secondary stopes with backfill only on one side (refer to Figure 2.17). Mining then progresses upwards in a repeating pattern. Unfortunately, very little literature exists on the effects of sequence on overbreak in narrow vein longitudinal retreat mining.

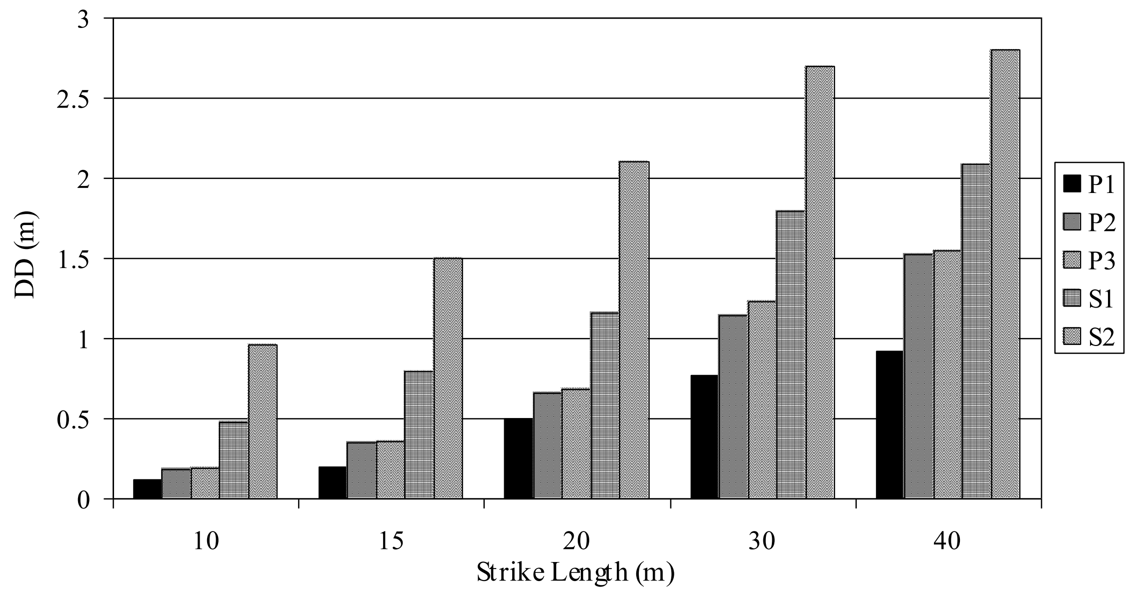

Figure 2.16 Influence of stope type on Dilution Density. Base-case stope at σ3=0MPa contour after Henning and Mitri (2007).

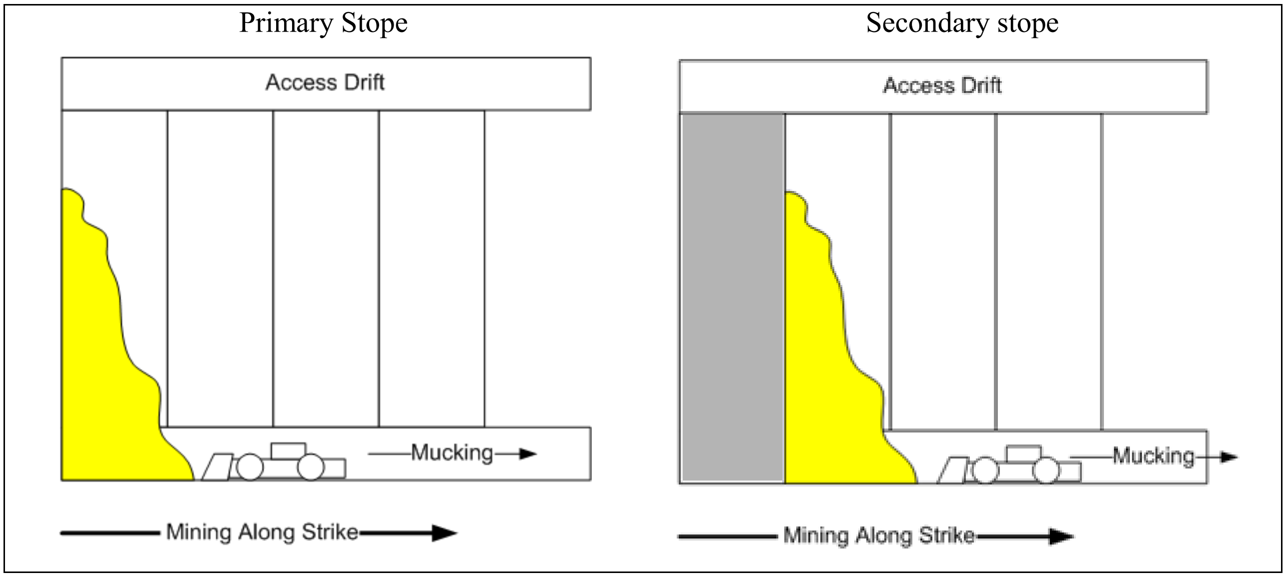

Figure 2.17 Longitudinal retreat mining long section.

Chapter 4 presents a three dimensional numerical model which examined the effect of strike length on overbreak at Lapa mine. These models comprise of a mine and fill sequence which indicates that secondary stopes see a smaller amount of relaxation than their primary counterparts. While this is somewhat in conflict with the findings of Henning and Mitri (2007), the stress regime at Lapa is primarily vertical with the lowest in-situ stress oriented in the horizontal and normal to the stope strike length. At Lapa, the extraction of the primary stope results in a large stress disturbance which (due to the backfill and in-situ stress orientation) is not as significant in subsequent stopes. The model presented in Chapter 4 does not examine the effects of vertical sequence. A study by Mitri et al. (2010) explored the effect of stope height at Lapa mine and also included a one sublevel sequence.

The model presented by Mitri et al. (2010) showed that the level stope had a higher degree of overbreak than the secondary stope. This finding corresponded to actual field data for the modeled stopes. Once again, the discrepancy between the Lapa case studies and the work of Henning and Mitri (2007) is caused by different mining methods and a completely different in-situ stress regime.

2.3.6 Blast design

Good blast design is necessary to break the ore such that it flows freely into drawpoints and also to ensure that blocks of broken rock are easily handled by equipment. Wang (2004) points out how the conflicting goals of blast design (i.e. damage the ore to such a degree to ensure that unbroken ore does not remain in the stope and to minimize damage to adjacent walls) make good blast design a crucial tool in controlling overbreak. Blast damage loosens the rock mass and can introduce new fractures, this in turn degrades the quality of the rock mass which results in increased risk of slough or overbreak (Wang 2004).

Wang (2004) also describes the problems associated with drill hole deviation (refer to Figure 2.18) which can result in improper and unexpected explosive concentrations. Should these concentrations be too close (or within) one of the walls then overbreak will most definitely occur. Forsyth et al. (1994) explain that drill hole deviation is caused by both external and internal deviation. External deviation refers to inaccurate surveying, drill set up errors, and poor hole collaring. Internal deviation is caused by the drilling equipment, its operation, varying geological composition, and geological structures.

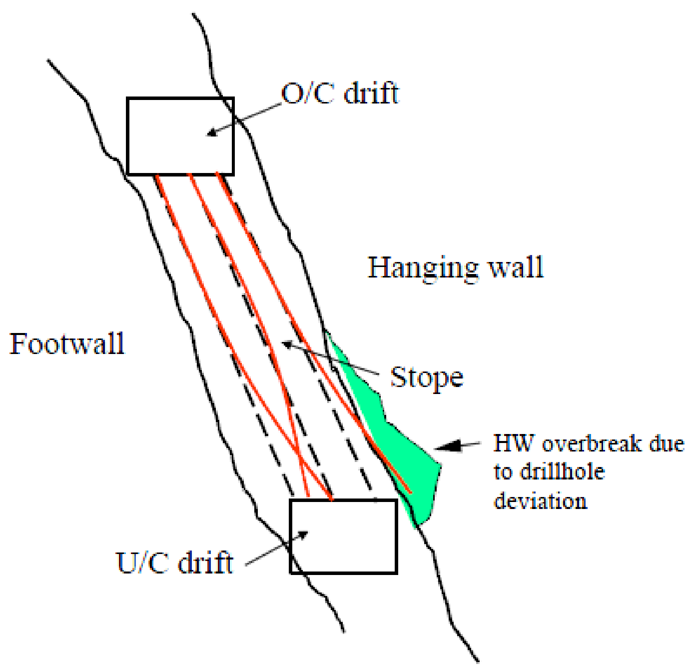

Figure 2.18 Cross-section showing drillhole deviation causing overbreak after Wong (2004).

Chapter 3 – A Geotechnical Database for Lapa Mine

3.1 Introduction

Modern mining operations are equipped with highly accurate survey equipment (such as Total Stations, Cavity Monitoring Surveys, etc) which are often used to measure overbreak off specific stope walls. Operations often undertake extensive diamond drilling programs and lab testing to provide the modern engineer with extensive data regarding the rock mass. This, along with data from various types of instrumentation, such as seismic systems, SMART Cables, and MPBX's provide mining operations with enormous amounts of electronic data.

While it is relatively simple to collect enormous amounts of data, it is only by processing this information that we can truly gain from it. Unfortunately, often this data is scattered around within many departments and is not kept current or maintained on a regular basis. By integrating data within a central database and designing tools to aid in updating and maintaining this database it is possible to resolve these problems and gain more from existing data.

Numerical modelling requires a variety of input data which should be as representative as possible of the actual conditions. Gathering this data from a variety of sources can be time consuming and without a standard practice can result in misinformation. Once again, the need for a geotechnical database arises.

The project with Lapa mine included the development of one such database. The goal was to integrate stope reconciliation data and diamond drill hole data in order to aid in the development of the empirical dilution model, the construction of various numerical models, and to provide the mine with a useful tool moving forward into the future.

3.2 Components of the database

The database is composed of four key parts:

1) A Graphical User Interface
2) The Stope Reconciliation Database
3) The Drillhole Database
4) Background Computations

These components work together to provide a simple interface, ease of use, and functionality to the user. The two databases were created as two tables within a single Access Database file. Database files can be accessed and manipulated using application programming interfaces such as the *Object Linking and Embedding, Database* (OLEDB) and a database engine. The JET Database engine developed by Microsoft was employed in this project.

Visual Basic .NET 4.0 was used to develop the Graphical User Interface and performs the background computations as well as the communication with the database. The API (application programming interface) that allows .NET to interact with the Microsoft Office suite of software (such as Access and Excel) is well documented and supported. Since these libraries are developed by Microsoft they are readily available and easily distributed to host machines. These features, the widespread use of the .NET Framework, and powerful development tools make .NET an excellent choice for this project.

3.3 Structure of the database

The database, called Data Integrator for Mine ANalysis and Design (DIMAND) is represented in Figure 3.1.

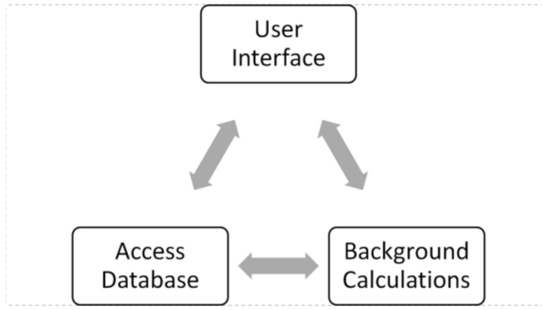

Figure 3.1 The structure of DIMAND.

The components of DIMAND work together to provide data to the user but also to add and edit data found within the Access Database. DIMAND provides data to the user either within the GUI itself or by outputting data to Excel spreadsheets.

Communication with the database is achieved programmatically through the use of the JET database engine. An example of this communication is presented below. In this section of code, a structured query string (Query) is sent to the database as a means to retrieve relevant data. The program then establishes a connection to the database file (lines 8-15). The rest of the code loads the database into memory while properly managing null database values. Database fields which are used in calculations require that null values be negative (i.e.:" -1") to allow for easier error trapping in later sections of the code.

```
 1.  Sub DatabaseQuery(ByVal Query As String)
 2.
 3.          Dim Cmd As OleDb.OleDbCommand
 4.          Dim Con As OleDb.OleDbConnection
 5.          Dim eReader As OleDb.OleDbDataReader
 6.          Dim Field As String = Nothing
 7.          Dim n As Integer = 0
 8.          Con = New OleDb.OleDbConnection(ConStr)
 9.
10.          Cmd = New OleDb.OleDbCommand(Query.ToString, Con)
11.          Try
12.              Con.Open()
13.          Catch ex As Exception
14.              MsgBox(ex.ToString)
15.          End Try
16.
17.
18.          eReader = Cmd.ExecuteReader
```

```

        Array.Clear(MasterHolder, 0, MasterHolder.Length)

        While eReader.Read

            For Col = 0 To eReader.FieldCount - 1
                If eReader.Item(Col) Is DBNull.Value Then
                    If Col >= 35 Then
                        Field = "-1"
                    Else
                        Field = ""
                    End If

                Else
                    Field = eReader.Item(Col)
                End If

                ReDim Preserve MasterHolder(69, n)

                MasterHolder(Col, n) = Field

            Next

            n = n + 1
        End While
        Con.Close()

    End Sub
```

More advanced functionality with the Access database file involves a similar communication procedure. The program is capable of reading data from the database, editing entries within the database, creating new data entries, and deleting unwanted records.

The program has been designed in such a way that the full installation of Microsoft Access is not required to fully benefit from the program. Microsoft provides the OLEDB drivers required by the DIMAND to fully manipulate the Access Database file. User output is generated either graphically within the GUI itself or it is outputted to Microsoft Excel using the built in API. An example of this exchange is shown below. This section of code executes once a user has defined the advanced query they wish to perform. Lines 3 to 30 are translating user input into command lines that can be understood by the database. Lines 32 to 48 are the DIMAND communicating with Excel in order to launch Excel, create a new workbook and prepare needed variables. Lines 50 to 61 are the actual query being pushed to the database and the results being copied into the Excel workbook.

```
1.  Private Sub btnRunQuery_Click(ByVal sender As System.Object, ByVal e As System.EventArgs) Handles btnRunQuery.Click
2.
3.          Dim SB As New StringBuilder
4.
5.          Dim Filters As String
6.
7.          If lstAppliedFilters.Items.Count > 0 Then
8.              For i = 0 To lstAppliedFilters.Items.Count - 1
9.                  SB.Append(lstAppliedFilters.Items.Item(i).ToString)
10.                 SB.Append(" AND ")
11.             Next
12.
13.             SB.Remove(SB.Length - 5, 5)
14.
15.             Filters = SB.ToString
16.         Else
17.             Filters = Nothing
18.         End If
19.
20.         If My.Settings.CustomOutput.ToString = "" Then
21.             For p = 0 To FieldBoolean.Length - 1
22.                 FieldBoolean(p) = True
23.             Next
24.         Else
25.             OutputFields(My.Settings.CustomOutput.ToString)
26.         End If
27.
28.         Dim q As String
29.
30.         q = QueryStringBuilder(FieldBoolean, Filters)
31.
32.         Dim xlApp As New Excel.Application
33.         Dim xlWorkbook As Excel.Workbook
34.         Dim xlWorksheet As Excel.Worksheet
35.         Dim xlRange As Excel.Range
36.         Dim misValue As Object = System.Reflection.Missing.Value
37.
```

```
        xlWorkbook = xlApp.Workbooks.Add(misValue)
        xlWorksheet = CType(xlWorkbook.Worksheets(1), Excel.Worksheet)
        xlRange = CType(xlWorksheet.Range("A1"), Excel.Range)

        If xlApp Is Nothing Then
            MsgBox("Cannot load Excel.", MsgBoxStyle.Critical, "ERROR!")
            End
        End If

        xlApp.Visible = True
        xlWorkbook.Activate()

        Dim QryTable As Excel.QueryTable
        Try
            QryTable = xlWorksheet.QueryTables.Add(qConStr, xlRange, q)
            With QryTable
                .Refresh()
                .RefreshOnFileOpen = True
            End With

            MsgBox("Finished!", MsgBoxStyle.Information, "SUCCESS!")
        Catch ex As Exception
            MsgBox(ex.ToString)
        End Try

        QryTable = Nothing
        xlWorksheet = Nothing
        xlWorkbook = Nothing

    End Sub
```

3.4 Features and functionality

The Lapa DIMAND has been designed specifically with the needs of Lapa mine and a rock mechanics engineer in mind. A variety of user-friendly tools allow for everything from quick data viewing to advanced queries to report generation and failure criterion calculation. This section will describe the features build into this software package.

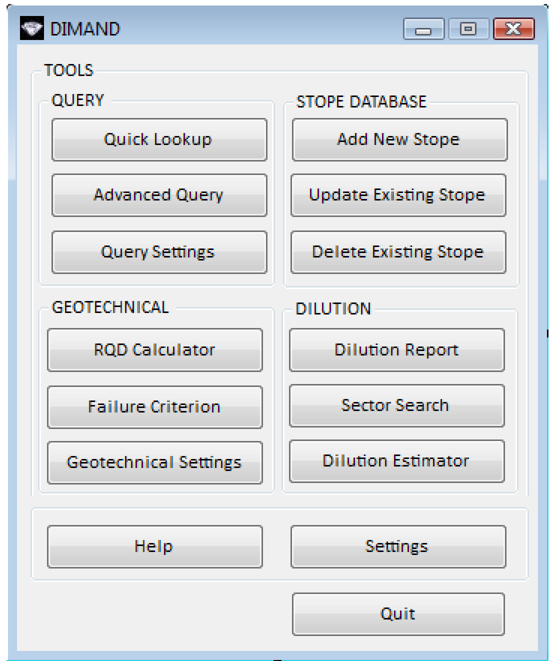

Figure 3.2 Lapa DIMAND home screen.

3.4.1 Start-up

The Lapa DIMAND has been developed with a start-up sequence designed to validate available data and to attempt to resolve missing values. It has been designed to allow for property changes (i.e. changing the average density of the footwall rock, changing the rock mechanics properties from the defaults, etc) to be automatically reflected in the data. User-controllable settings can change the behaviour of the start-up sequence. Two settings exist:

1) ENABLE Database Auto Refresh
2) DISABLE Database Auto Refresh

Enabling this feature will cause the database to recalculate all UCS, RQD, Rock Type, and dilution data for each stope. This feature greatly increases start-up time but as mentioned previously, updates all values with modified properties and will also allow for updated diamond drill hole data to be reflected in the stope database. Disabling this feature greatly reduces start-up time and is the default setting. Even with the feature disabled, DIMAND will still attempt to calculate missing values but will not recalculate existing values. Figure 3.3 shows the flowchart of the start-up sequence.

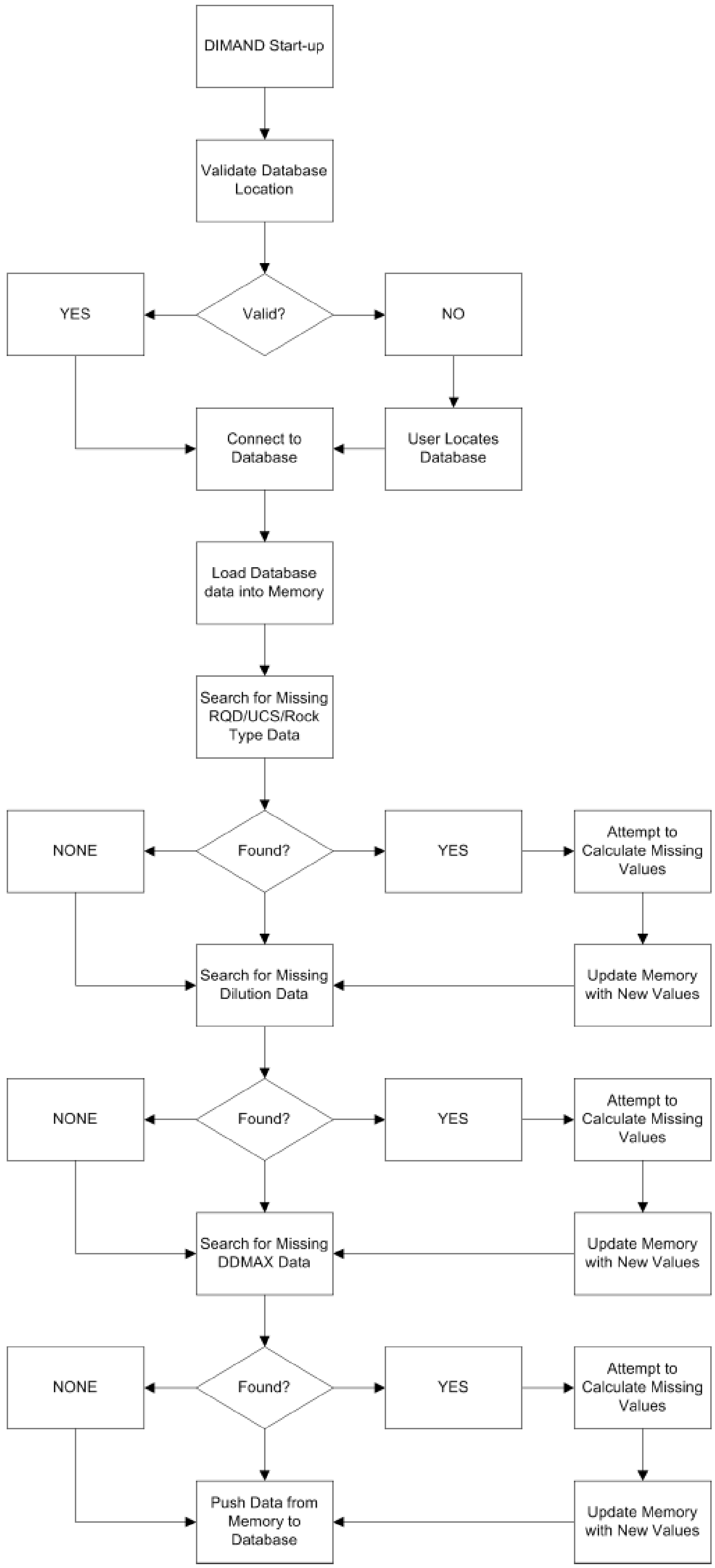

Figure 3.3 The start-up flowchart for DIMAND.

3.4.2 Quick Lookup

The Quick Lookup feature was designed to allow for quick and easy access to all the data available for each stope. A user needs only to highlight the stope they wish to view and the GUI is populated with all the data available for the selected stope. This data is presented in five tabs:

1) General – Includes basic stope geometry, dates, coordinates, etc.
2) Geotechnical – Presents the rock composition, RQD, and UCS for the South Wall, Ore, and North Wall blocks.
3) Dilution Locations – Shows the user-entered dilution data
4) Dilution Totals – Presents the calculated dilution percentages and compares stope values to mine-wide averages.
5) DDMAX – Shows the DDMAX values for the North and South Wall as well as a sketch showing a scale representation of the overbreak ellipsoid.

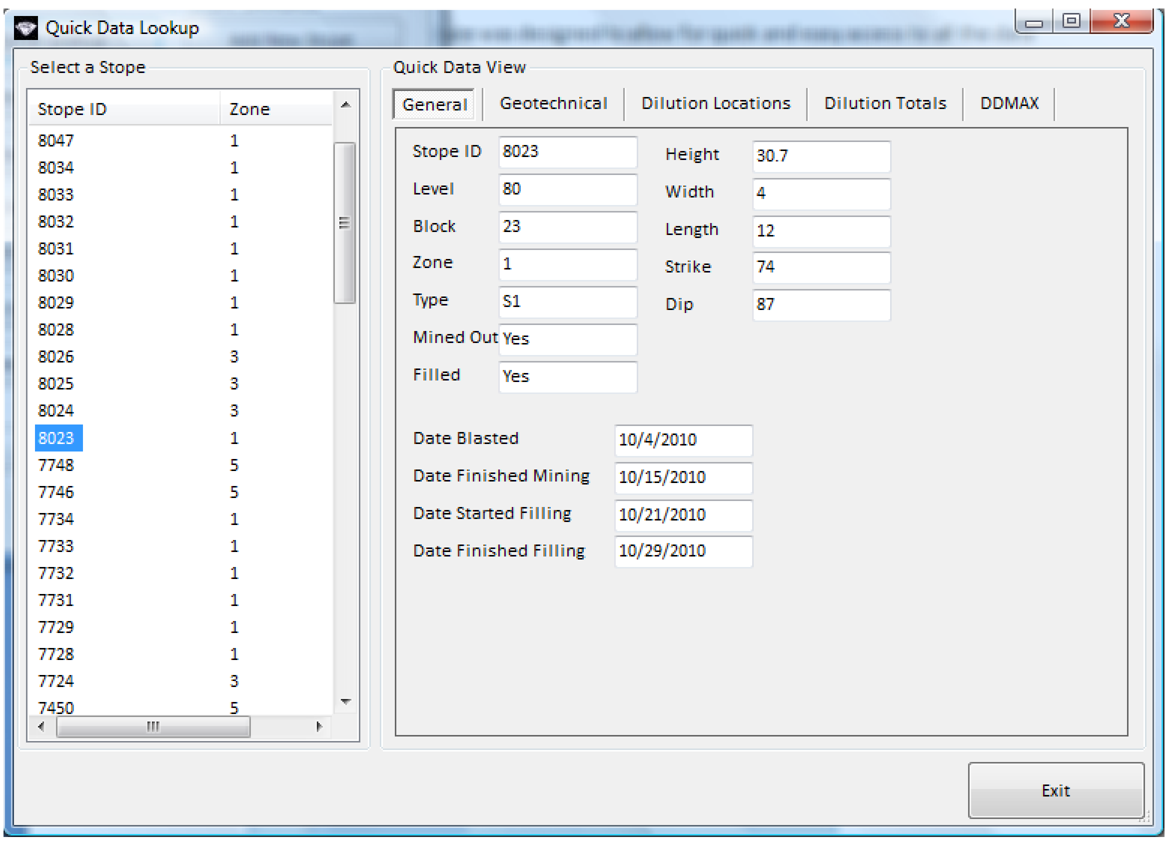

Figure 3.4 The General data tab within the Quick Lookup feature.

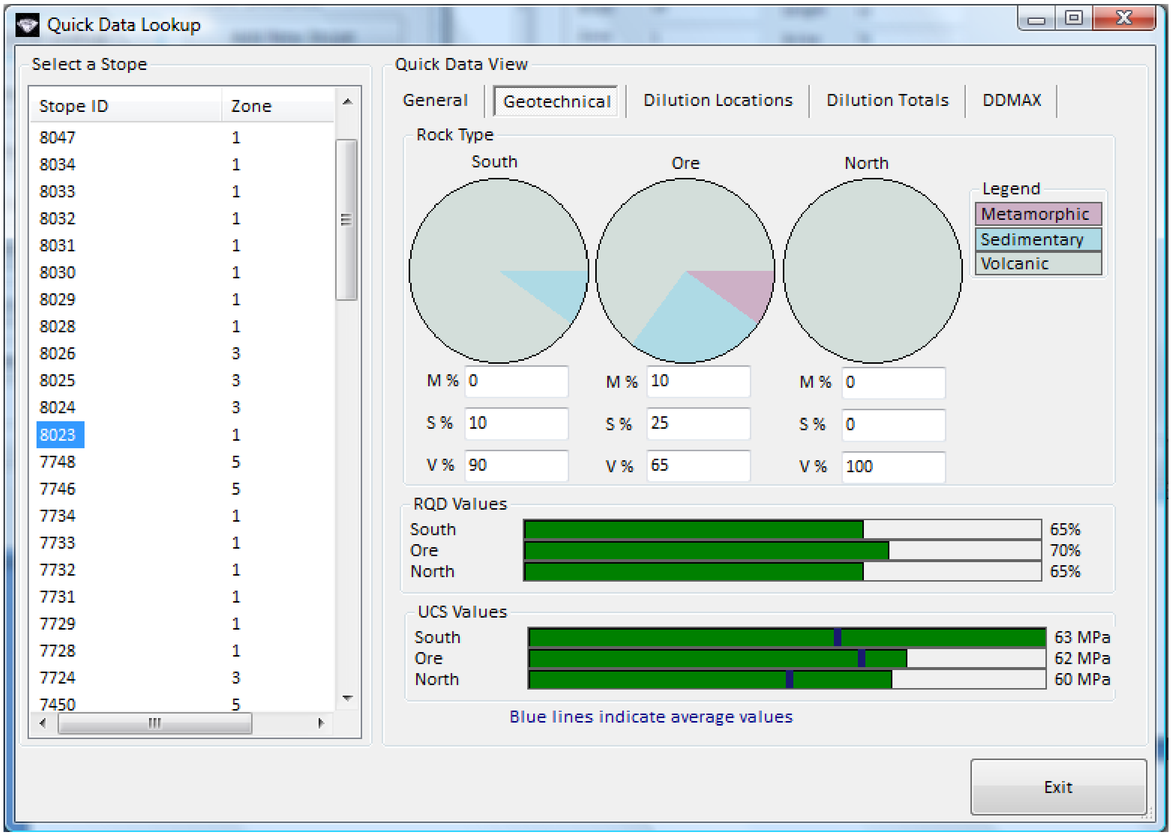

Figure 3.5 The Geotechnical data tab within the Quick Lookup feature.

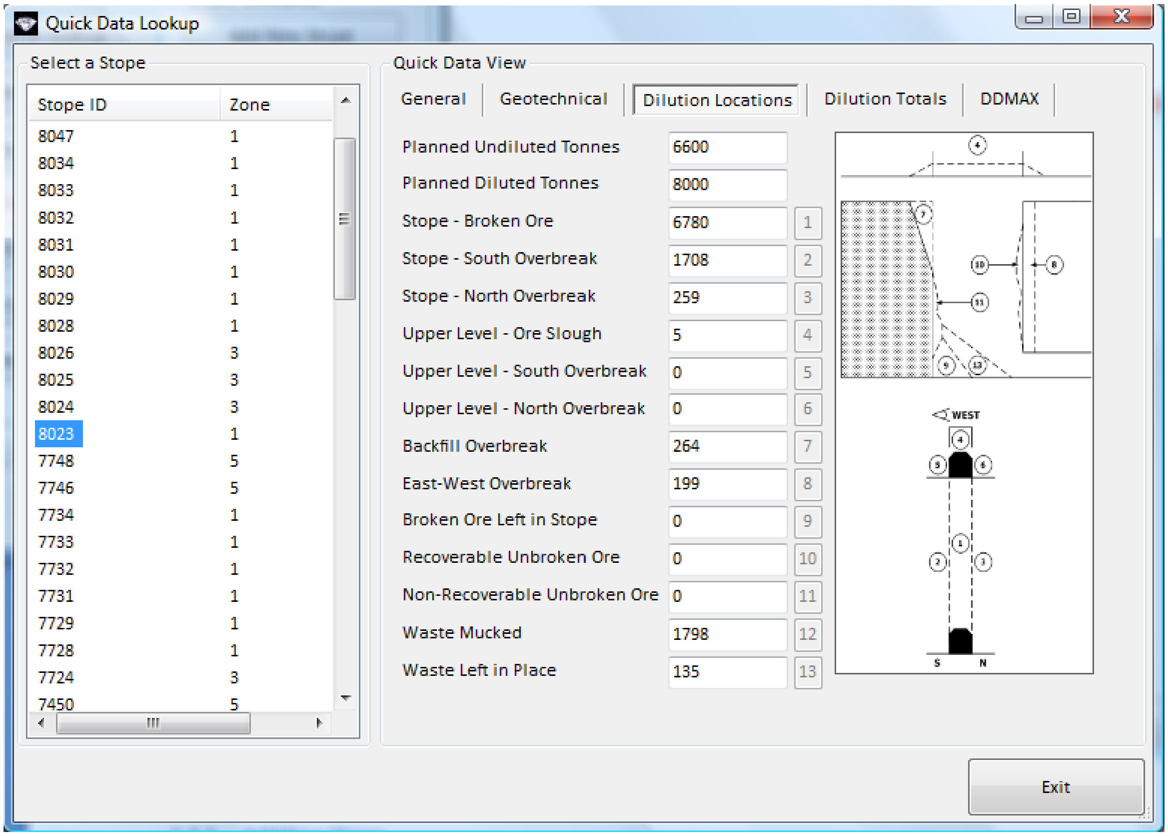

Figure 3. 6 Dilution Locations data tab within the Quick Lookup feature.

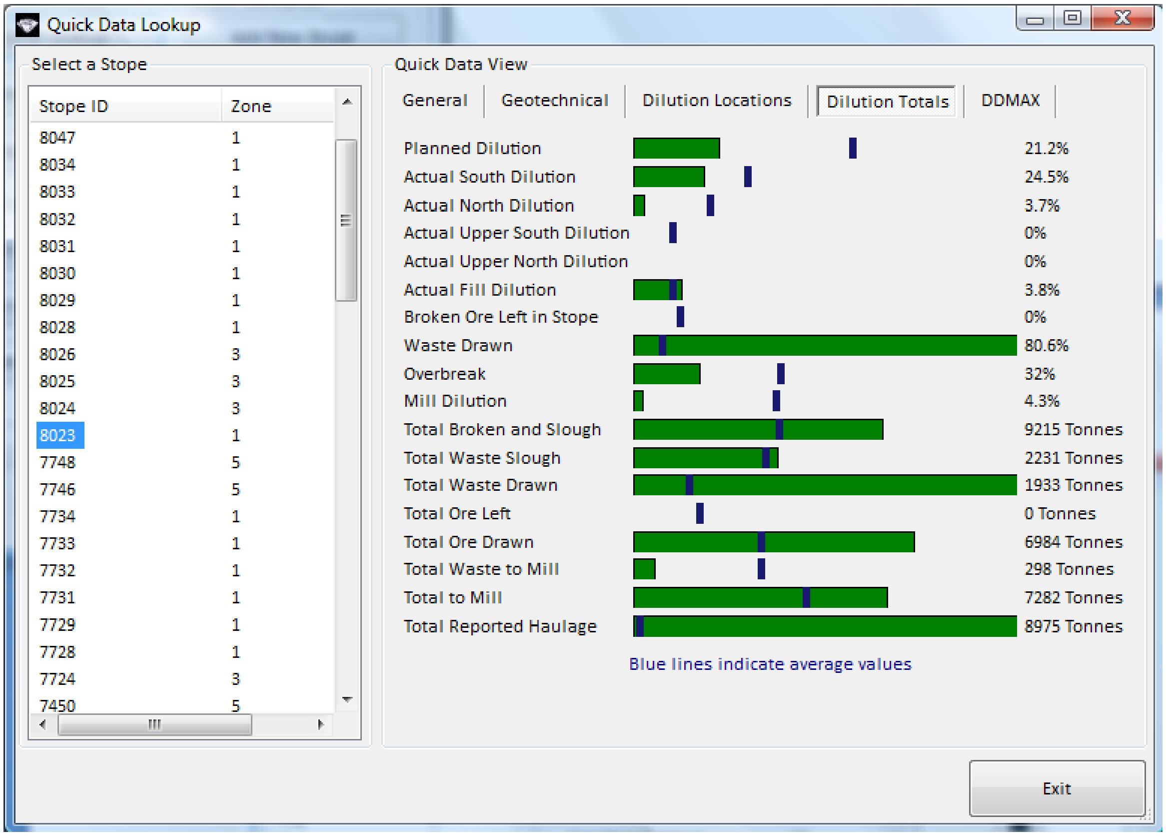

Figure 3.7 The Dilution Totals data tab within the Quick Lookup feature.

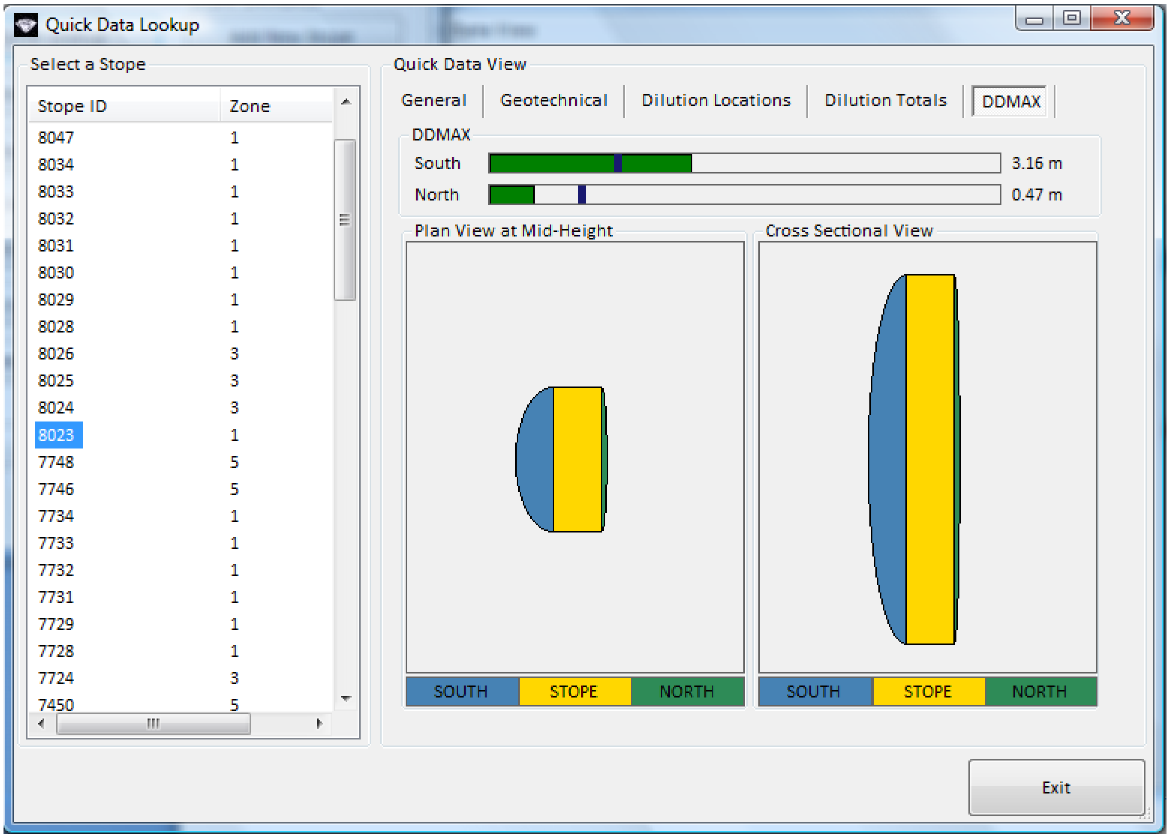

Figure 3.8 The DDMAX data tab within the Quick Lookup feature.

3.4.3 Advanced Query

The Advanced Query allows the user to create, save, and load custom queries. All fields within the database are subject to query and a simple editor uses radio buttons to select the constraint. The GUI changes the language of the constraints with respect to the selected field. The constraints per field data type are presented below in Table 3.1.

Table 3.1 Constraints per field data type.

Data Type	Constraints
Text String	Equals, Does Not Equal
Boolean	Equals, Does Not Equal
Numerical	Equals, Less Than, Greater Than, Between, Outside
Date	On, Before, After, Between, Outside

In addition to this interface feature, each constraint entry box is a dropdown menu which contains all the values for the selected field. This allows the user to best tune their query and helps prevent accidental input. The entry field will accept either a selection from the dropdown menu or a value entered by the user. This feature is shown below in Figure 3.9.

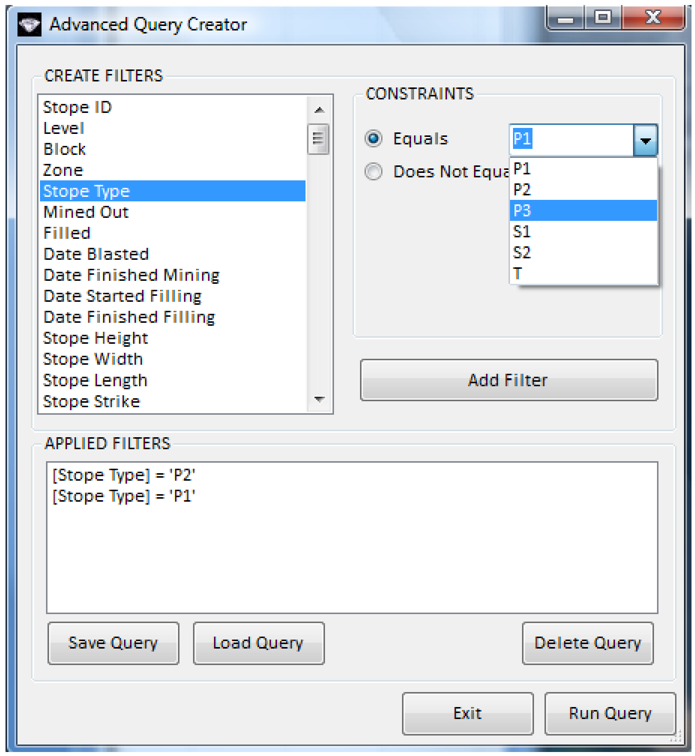

Figure 3.9 Advanced Query functionality.

A user is free to add as many filters as they wish and if a complex query is constructed the user can opt to save this query for future use. These saved query files (ASCII files with the extension .diaq) can be reloaded at a later time.

Running the Advanced Query Creator will generate an Excel file with the results of the query. By default, this feature will return all of the data fields within the database. If a user desires to streamline the output from the Advanced Query Creator then the Query Settings feature (available from the Home Screen) allows the user to specify which fields (and their order) they require in output. Changing the format of the output does not have any impact on the query itself. Query Settings are saved each time and preserved through program termination and restart.

3.4.4 Add New Stope

An important feature of the Lapa DIMAND is its ability to accept new stope entries. The Add New Stope feature allows for the creation of a new data record. By completing the fields in the the GUI and clicking the Launch Geotechnical Calculator button, the DIMAND will attempt to calculate rock types, UCS, and RQD for the new stope. This feature uses the same procedure as outlined in Section 3.4.6. If values cannot be determined (or if the user is unhappy with the provided values) it is possible to manually specify them. Once the form is completed and the user entries have been validated (i.e. checked against potential duplicate stopes, data types checked, etc.) the new stope is added to the Access database file using a database command connection.

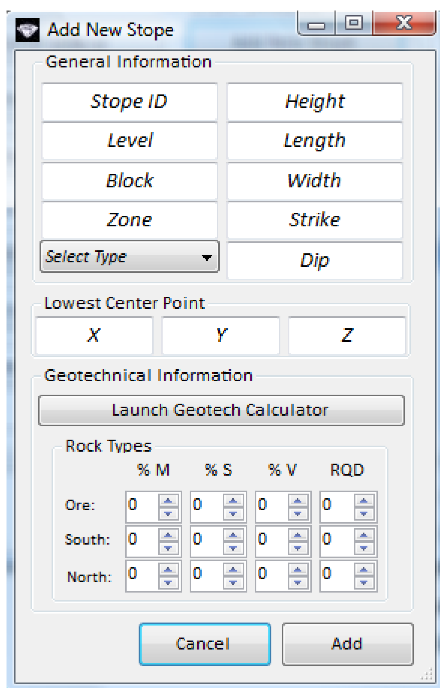

Figure 3.10 The Add New Stope GUI.

This feature allows for the input of basic stope geometry and is designed to be completed after a stope has been outlined and planned. The addition of sequence data and stope reconciliation data is achieved using the Update Existing Stope feature.

3.4.5 Update Existing Stope

Once a stope has been added to the database it is still possible to edit the basic data using this feature, but more importantly the Update Existing Stope feature is used to add in all the data obtained through post-mining CMS analysis. The interface functions similarly to the Quick Data Lookup feature in that the user selects the stope they wish to update in a pane on the left and then the fields are spread across several tabs. In the Update Existing Stope window there are three tabs:

1) General – Includes basic stope geometry dates, etc.
2) Geotechnical – Edit the stope coordinates, the rock composition, RQD, and UCS for the South Wall, Ore, and North Wall blocks.
3) Dilution Locations –Enter dilution data

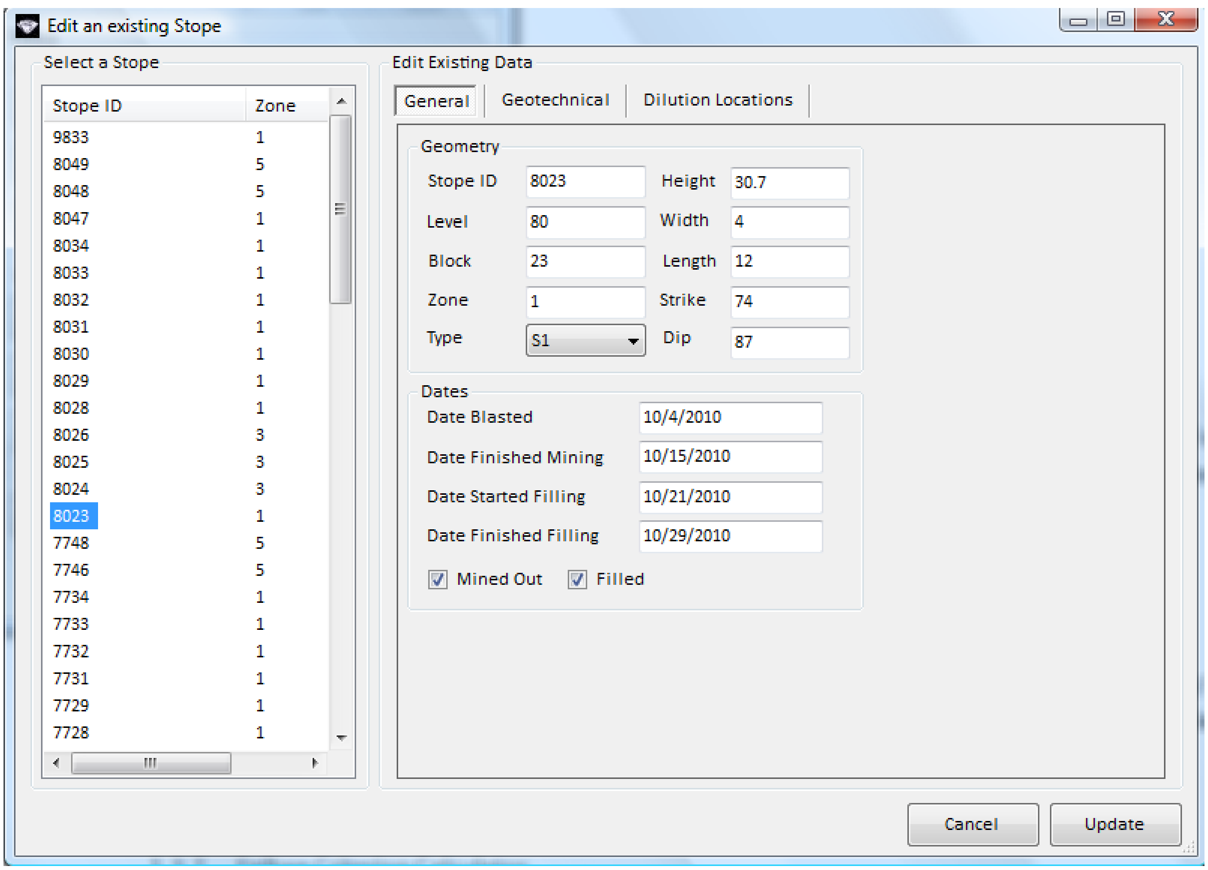

Figure 3.11 The General tab within the Update Existing Stope feature.

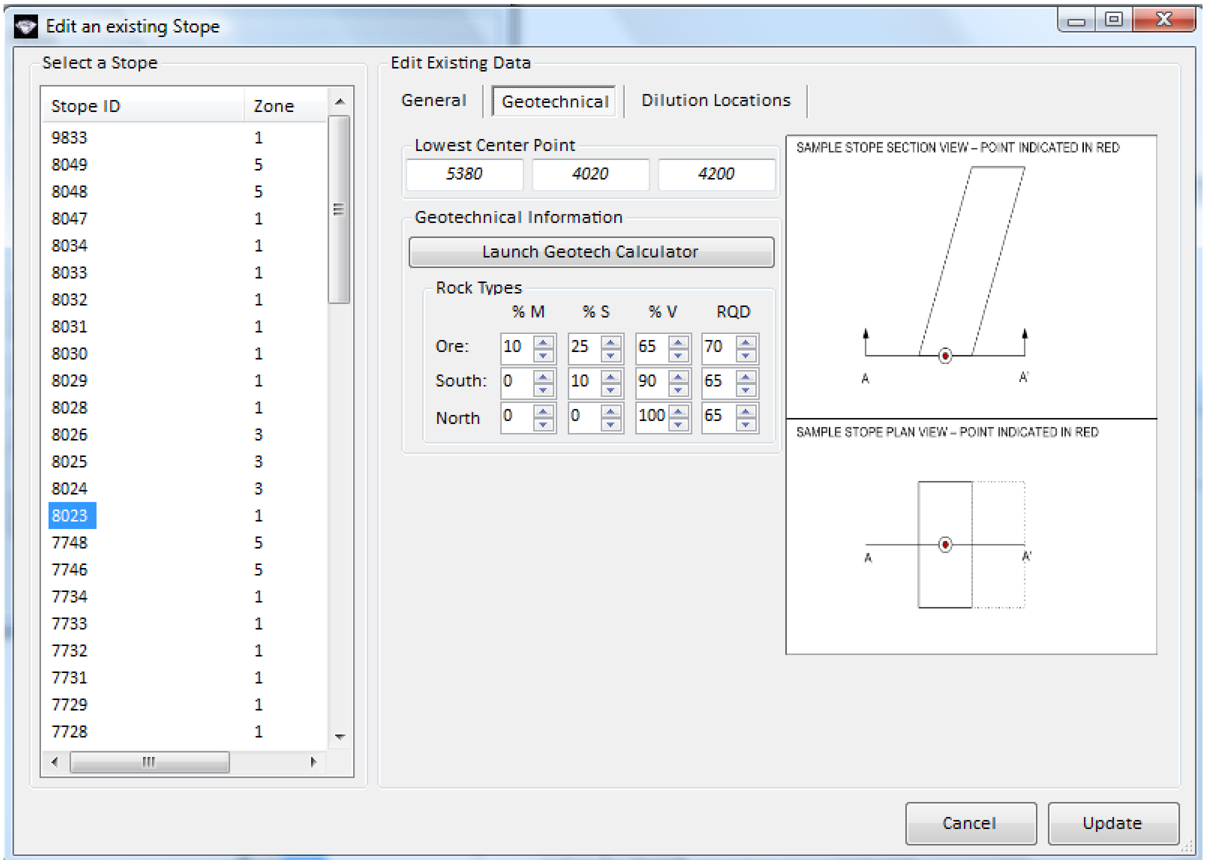

Figure 3.12 The Geotechnical tab within the Update Existing Stope feature.

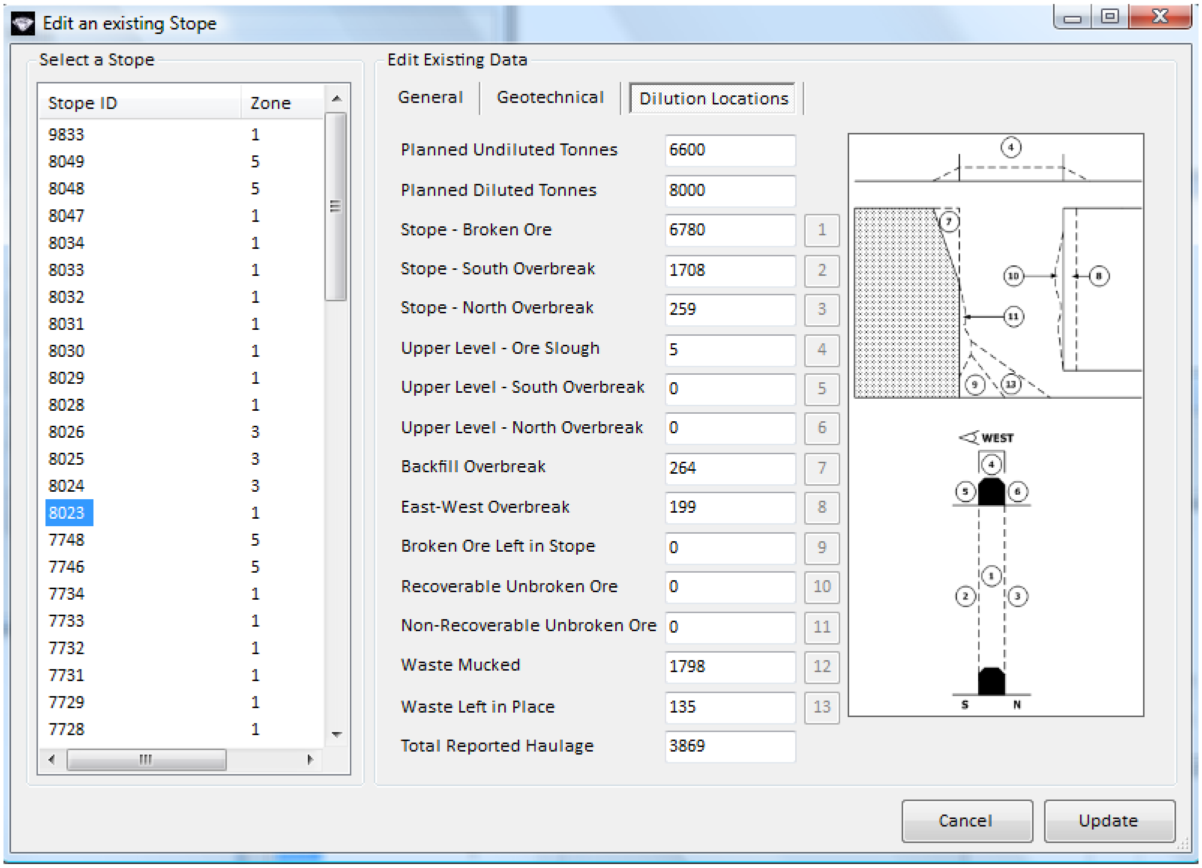

Figure 3.13 The Dilution Locations tab within the Update Existing Stope feature.

Once the user completes the information they wished to update the program communicates with the Access Database in order to update the fields within the specified record.

3.4.6 RQD Calculator

The RQD Calculator is both an internal and user-accessible feature. This algorithm is employed to calculate rock composition, UCS, and RQD for a representative volume of space within which relevant drill hole data may exist. Diamond drill hole data has been provided as a series of lines oriented somewhere in the coordinate system. Each of these short sections of line are assigned a RQD and rock type and are each of varying length. A single diamond drill hole is broken into many of these small samples.

Using a coordinate point within a planned stope outline, the stope height, length, width, dip, and strike it is possible to create a 3 dimensional parallelogram shaped block which represent the ore, south wall, and north wall materials. Now, by finding the drill hole samples which lie within these blocks it is possible to use a weighted average (based on sample length) to estimate values which would be representative of the rock materials. Unfortunately, in order to create a search it is necessary to approximate the geometry of the 3 dimensional parallelogram into 9 smaller sub-blocks.

Since the 3 dimensional parallelogram most likely has a dip and a strike which make the shape oblique when compared to the Cartesian coordinate system used to locate the drill hole samples it is necessary to create these smaller sub-blocks which are coplanar with the coordinate system. These coplanar blocks allow for a search to be performed on the drill hole samples. By subdividing the larger shape into smaller sub-blocks it is possible to slightly offset these smaller blocks from each other in order to mirror the dip and strike of the stope. This is shown below in Figure 3.14 Showing the blocks used to approximate dip and strike (dark blue, yellow, and light blue representing the footwall, ore, and hanging wall respectively).

.

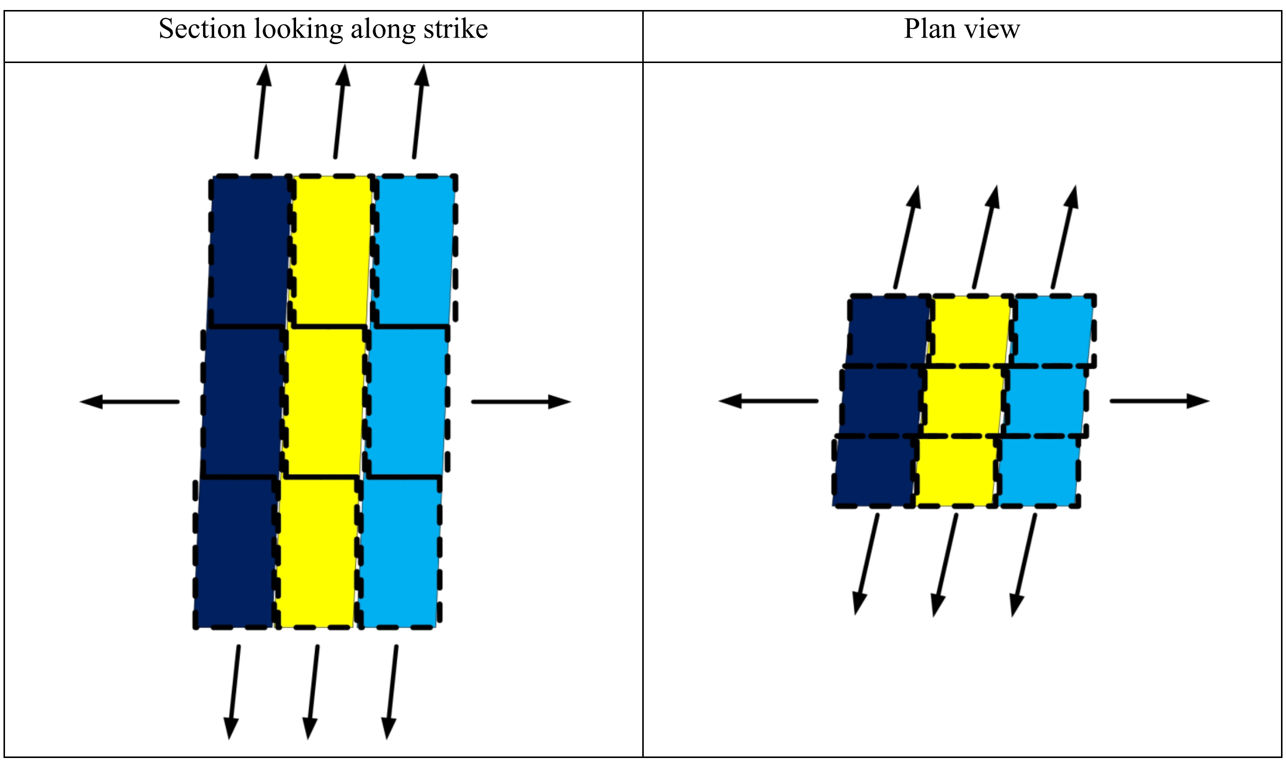

Figure 3.14 Showing the blocks used to approximate dip and strike (dark blue, yellow, and light blue representing the footwall, ore, and hanging wall respectively).

The South and North wall blocks are originally the same dimensions of the stope blocks but the expansion sequence is somewhat different. If the 9 blocks do not meet the user specified minimum threshold for total sample length then an expansion algorithm is applied. This algorithm expands the dimensions of these sub-blocks in an effort to capture more samples. The expansions taken by the north and south wall sub-blocks differs from that employed in the ore blocks. The north and south wall sub-blocks expand along strike and dip and outwards further into their respective walls. The ore blocks on the other hand expand only along strike and dip because if they were to widen they would become increasingly representative of the north and south walls. The user can control several search parameters, such as the previously mentioned minimum total sample length but can also adjust the maximum and minimum allowable sample lengths as well as the maximum expansion factor.

The algorithm can be represented by the flowchart presented below in Figure 3.15.

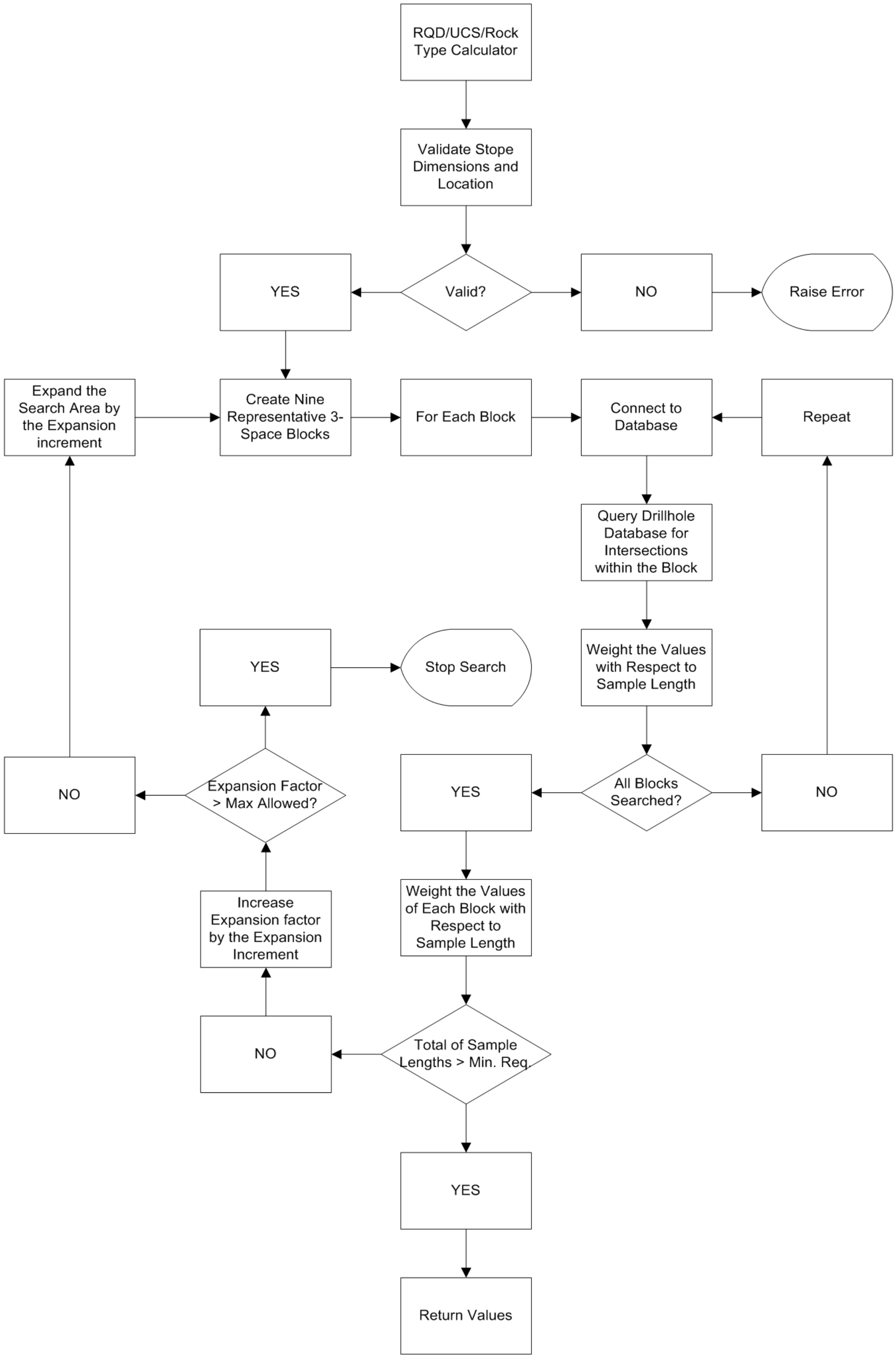

Figure 3.15 Flowchart describing the logic employed in the RQD Calculator algorithm

As explained earlier, this algorithm is often employed in background calculations, for example during the start-up sequence or upon clicking the Launch Geotechnical Calculator button within the Add New Stope and Update Existing Stope windows. In these cases the calculator is using stope geometries belonging to stopes which are found within (or about to be added to) the database. If the user wishes to use Geotechnical Calculator without having to add or edit an existing entry then it can be accessed through the RQD Calculator feature found on the Home screen.

The RQD Calculator requires only the required information to be provided. By entering the stope dimensions, dip, strike, and base coordinates the feature will search the existing drillhole database for relevant samples and will provide estimates.

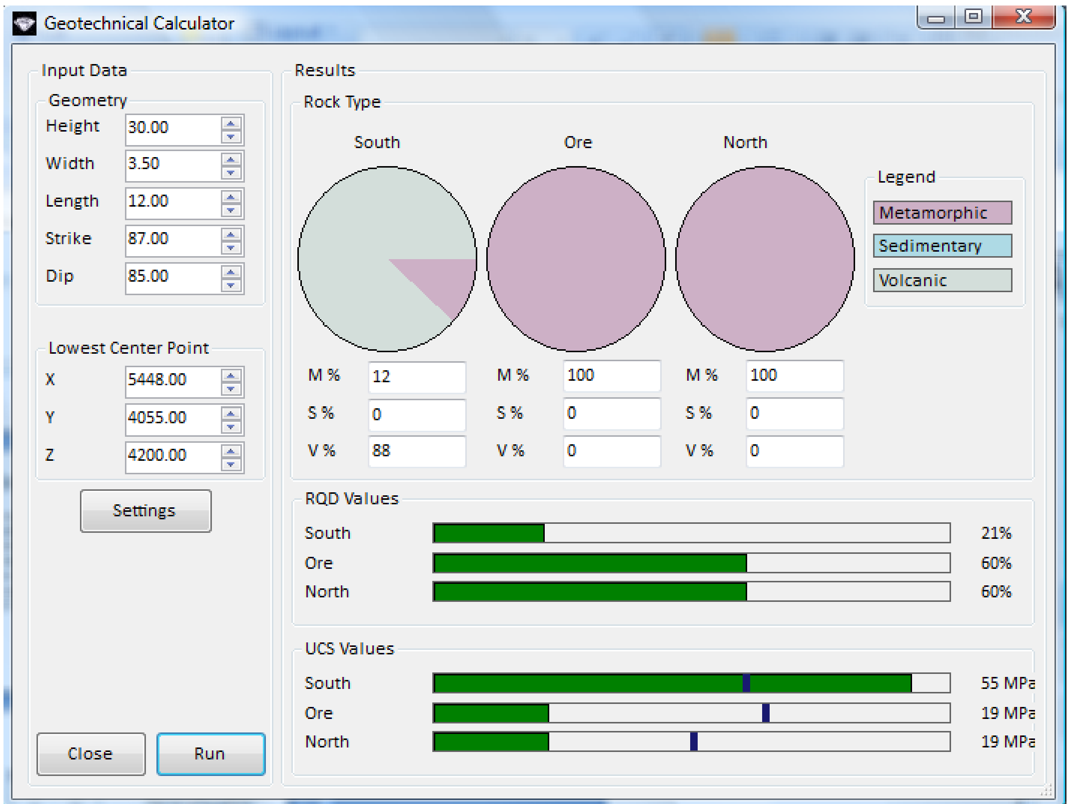

Figure 3.16 The GUI for use of the RQD Calculator.

3.4.7 Failure Criterion Calculator

Throughout the course of this project, a variety of numerical models have been developed. Gathering the required data to build these models can be very challenging and time consuming. Stope geometries, rock types, rock mechanical properties, and stope reconciliation data are all required to build and tune a numerical model. The development of the Lapa DIMAND was partly driven by the need to gather all of this type of information in one place and to be able to easily withdraw rock mechanics properties.

The Failure Criterion calculator provides rock mass mechanical properties and failure criterion for stopes selected by a user. By using the rock type and intact properties for all three rock types, a weighted average of these properties (based on the weight of each rock type) is calculated. In order to convert these intact values to rock mass values, it is necessary to determine the Rock Mass Rating (RMR) as per Bieniawski (1989). Based on the RMR criteria, a simple function was developed to reflect the influence of varying RQD, UCS, and rock face. The scores assigned for joint spacing (60-200mm spacing, 8) and groundwater (Completely dry, 15) were kept constant for all rock masses. The joint condition scores were adjusted for each the south, north, and ore rockmasses in order to reflect their relative condition. The joint condition scores for the south (or FW) was set to 7, the north (or HW) was set to 23, and the ore was set to 20. The RMR Calculator function shown below uses the UCS of the intact rock, the RQD rating of the face, and the face type to calculate and return a RMR rating.

```
Public Function RMRCalulator(ByVal ucsr As Double, ByVal rqdr As Double, ByVal facer As String)
        Dim score As Double = 0

        Select Case ucsr 'ucs
            Case Is > 250
                score = score + 15
            Case 100 To 250
                score = score + 12
            Case 50 To 99.9999
                score = score + 7
            Case 25 To 49.9999
                score = score + 4
            Case 5 To 24.9999
                score = score + 2
            Case 1 To 4.9999
                score = score + 1
        End Select

        Select Case rqdr 'rqd
```

```
            Case 90 To 100
                score = score + 20
            Case 75 To 89.9999
                score = score + 17
            Case 50 To 74.9999
                score = score + 13
            Case 25 To 49.9999
                score = score + 8
            Case Else
                score = score + 3
        End Select

        score = score + 5 'spacing

        Select Case facer 'condition
            Case "FW"
                score = score + 7
            Case "HW"
                score = score + 23
            Case "Ore"
                score = score + 20
        End Select

        score = score + 13 'groundwater

        Return score

    End Function
```

Next, using the calculated RMR value for the rock mass along with the intact properties it is possible to determine both the Hoek-Brown and Mohr-Coulomb Failure criteria for the rock mass using the formulae described by Hoek, E., Carranza-Torres, C., & Corkum, B.(2002). For the purposes of calculating the equivalent Mohr-Coulomb failure envelope σ'_{3MAX} is based on the tunnel case and depth underground is determined based on the stope level. The relationship between GSI and RMR is described by Hoek E, Brown ET (1997). The formula used to reduce the intact Young's modulus is described by Hoek, E. and M.S. Diederichs (2006). Below is the section of code that executes these calculations and returns the Hoek-Brown, Mohr-Coulomb, RMR, and E_{RM}.

```
    Public Function GeotechCalc(ByVal mi As Double, ByVal ucs As Double, ByVal rqd As
    Double, ByVal d As Double, ByVal depth As Double, ByVal E As Double, ByVal den As
    Double, ByVal face As String) As Double()
            Dim CalculatedParams() As Double
            Dim gsi As Double
            Dim k As Double = 1
            Dim rmr As Double

            den = den * 9.81 / 1000
```

```
E = E * 1000
rmr = RMRCalulator(ucs, rqd, face)
gsi = rmr - 5
Dim mb As Double
mb = mi * Math.Exp((gsi - 100) / (28 - 14 * d))
Dim s As Double
s = Exp((gsi - 100) / (9 - 3 * d))
Dim a As Double
a = 1 / 2 + 1 / 6 * (Exp(-gsi / 15) - Exp(-20 / 3))
Dim ocrm As Double
ocrm = ucs * (s ^ a)
Dim Erm As Double
Erm = E * (0.02 + (1 - (d / 2)) / (1 + Exp((60 + 15 * d - gsi) / 11)))
Dim ocm As Double
ocm = (mb / 4 + s) ^ (a - 1)
ocm = ocm * (mb + 4 * s - a * (mb - 8 * s))
ocm = ocm / (2 * (1 + a) * (2 + a))
ocm = ocm * ucs
Dim sig3max As Double
sig3max = ocm * 0.47 * (ocm / ((depth * den) / k)) ^ (-0.94)
Dim sig3n As Double
sig3n = sig3max / ucs
Dim phi As Double
phi = 6 * a * mb * ((s + mb * sig3n) ^ (a - 1))
phi = phi / (2 * (1 + a) * (2 + a) + 6 * a * mb * ((s + mb * sig3n) ^ (a - 1)))
phi = Asin(phi) * 180 / PI
Dim c As Double
c = ((1 + 2 * a) * s + (1 - a) * mb * sig3n)
c = c * ((s + mb * sig3n) ^ (a - 1))
c = c * ucs
c = c / ((1 + a) * (2 + a))
c = c / Sqrt(1 + (6 * a * mb * ((s + mb * sig3n) ^ (a - 1))) / ((1 + a) * (2 + a)))
```

```

                ReDim CalculatedParams(7)
                CalculatedParams(0) = Round(mb, 6)
                CalculatedParams(1) = Round(s, 6)
                CalculatedParams(2) = Round(a, 6)
                CalculatedParams(3) = Round(ocrm, 1)
                CalculatedParams(4) = Round(Erm, 0)
                CalculatedParams(5) = Round(phi, 2)
                CalculatedParams(6) = Round(c, 3)
                CalculatedParams(7) = Round(rmr, 1)


                Return CalculatedParams

            End Function
```

This sequence of calculations is performed for all three rock masses for each user selected stope. The user is free to select as many stopes as they desire. The DIMAND will present each stope's data set as a sheet in an Excel workbook. Should the required data not be available for a specific stope rock mass then the user is notified and the missing data is left out of the spreadsheet.

An example of this report is provided below in Figure 3.17.

Stope - 7734 1

General	Footwall	Ore	Hanging wall
Disturbance Factor	0	0	0
UCS, MPa	49	79	86
Poisson's Ratio	0.3	0.3	0.3
Constant, mi	11	11	11
Density, tonnes/cu.m	2.86	2.86	2.86
Young's Modulus, MPa	26431.1	40561.2	44750

Rock Mass	Footwall	Ore	Hanging wall
RQD	50	71	73
RMR	37	58	61
Young's Modulus, MPa	2451	14848	19246
UCS, MPa	1	5.6	7.3

Mohr-Coulomb Failure Criterion	Footwall	Ore	Hanging wall
Cohesion, MPa	1.554	2.746	3.022
Angle of Friction, Degrees	27.94	37.89	39.45

Hoek-Brown Failure Criterion	Footwall	Ore	Hanging wall
mb	0.96979	2.053045	2.28523
s	0.000523	0.005395	0.00753
a	0.519528	0.504656	0.503773

Figure 3.17 Sample Failure Criterion Report.

3.4.8 Dilution Report

The Dilution Report tool uses reconciliation data within the database to quickly produce "Stope Dilution Reports" for Lapa mine. The mine uses a specific format for these reports and the program can quickly output an Excel version for any number of selected stopes. The necessary calculations are simple in nature yet are performed programmatically as to speed the process even further. An example of this report is shown below in Figure 3.18.

STOPE 8023 1

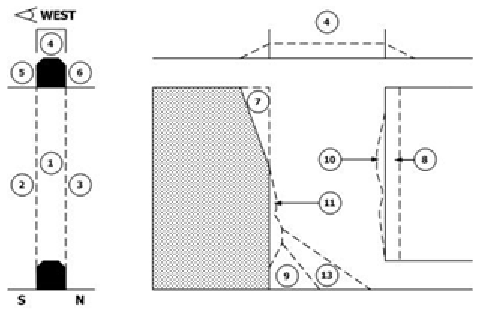

Planned	Undiluted Tonne	Diluted Tonne:	% Dilution
	6600	8000	21.20%

First Blast	October 4, 2010
Finished Mining	October 15, 2010
Started Filling	October 21, 2010
Finished Filling	October 29, 2010

Stope		Tonnes	% Dilution
1	Ore Broken	6780	
2	South Overbreak	1708	24.50%
3	North Overbreak	259	3.70%
Upper Level			
4	Ore Overbreak	5	
5	South Overbreak	0	0.00%
6	North Overbreak	0	0.00%
Other			
7	Fill Sloughed	264	3.80%
8	Ore Sloughed East/West	199	
9	Broken Ore Left in the Stope	0	0.00%
10	Unbroken Ore (Recoverable)	0	
11	Unbroken Ore (Non-Recoverable)	0	
12	Waste Mucked	1798	8060.00%
13	Waste Left in Place	135	
	Total Broken and Sloughed	**9215**	
	Total Waste Sloughed	**2231**	**32.00%**
	Total Waste Mucked	**1933**	
	Total Ore Left in Place	**0**	
	Total Ore Mucked	**6984**	
	Total Waste sent to Mill	**298**	
	Total Tonnes sent to Mill	**7282**	**4.30%**
	Total Reported Haulage	**8975**	
DDMAX Values			
	South Wall	3.16	
	North Wall	0.47	

Figure 3.18 A sample dilution report.

3.4.9 Sector Search

The concept of the Sector Search tool was developed directly with the engineering staff at Lapa mine. While planning a stope it is common practice for the planners to examine nearby mined-out stopes in an effort to understand local geology and any other regionalized trends. The Sector

Search tool was designed to search the database for stopes within a certain region and then average values from relevant stopes to create regional averages.

The user defines a central search point using the level (vertical) and block number (East-West along strike) and can then search for stopes within user-definable ranges which are independently adjustable in four directions (above, below, East, and West). The program then populates a list with all the stopes found within the search range and the user can opt to select some or all of the search results to be included in the regional averages. This allows for the user to exclude stopes if they felt that they were abnormal cases and not representative of the overall region. An example of a set of regional averages is shown below in the next figure.

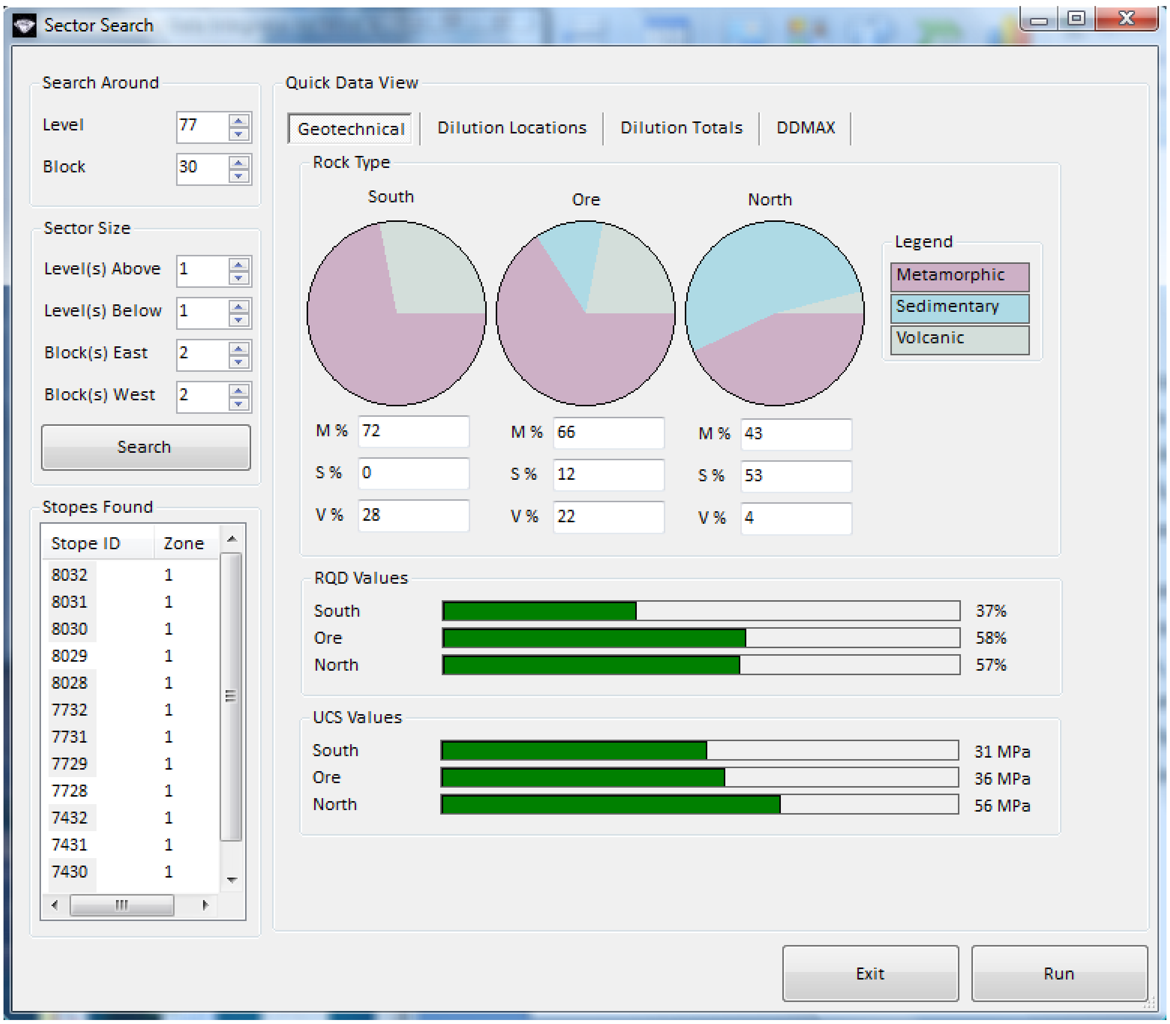

Figure 3.19 An example of Sector Search results - Geotechnical.

This feature presents the results on four tabs:

1) Geotechnical – Presents the average rock composition, RQD, and UCS for the South Wall, Ore, and North Wall blocks.
2) Dilution Locations – Shows the average dilution data
3) Dilution Totals – Presents the average calculated dilution
4) DDMAX – Shows the average DDMAX values for the North and South Wall as well as a sketch showing a scale representation of the overbreak ellipsoid.

3.4.10 Dilution Estimator

The Dilution Estimator is a simple tool which, based on the empirical dilution model (presented in Chapter 5), the expected stope geometry, stope type, and north and south wall RQD values, provides an estimate to the degree of overbreak that is to be expected. The estimate is provided in terms of both DD_{MAX} in meters and tonnes.

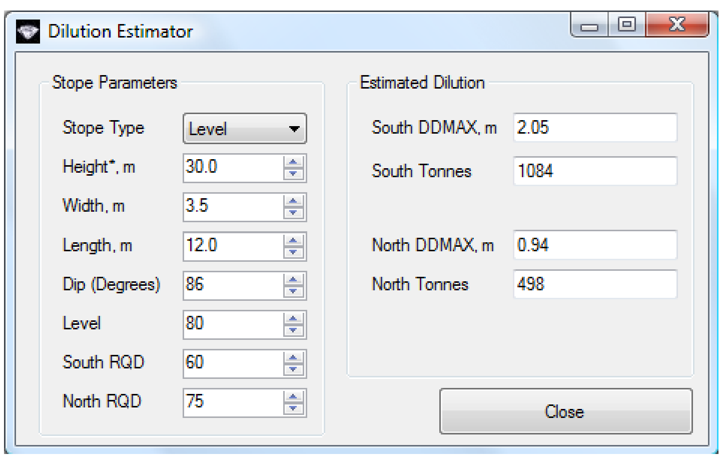

Figure 3.20 The Dilution Estimator.

3.4.11 User settings

DIMAND was programmed in a way such that hard-coded values or factors are minimized. Default values have been provided for all settings but the user is free to adjust them to their needs. All of these settings are saved and restored following program termination.

The General Settings tab allows the user to Enable/Disable the Database Auto Refresh feature described in Section 3.0. This tab also allows the user to view and change the database file path.

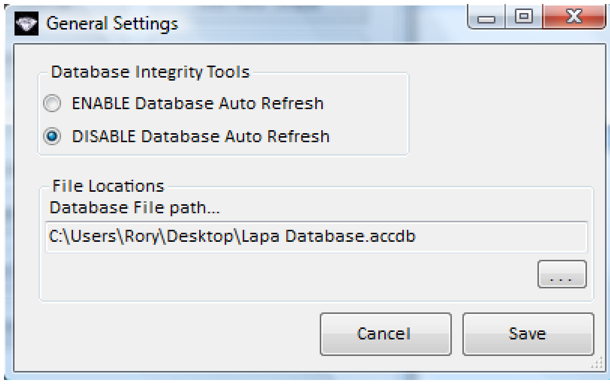

Figure 3.21 General settings.

The Geotechnical Settings window allows the user to define the intact properties for the three rock types used in the database. A user should note that in order to have changes to UCS or densities reflected in the database data it is necessary to save the new Geotechnical Settings, Enable Database Auto Refresh, and then restart DIMAND (forcing it to revise all the necessary values). This is necessary because values such as DD_{MAX} and UCS are stored within the database records. Changing any other settings does not require this step since they are accessed only when called and not stored in the database records.

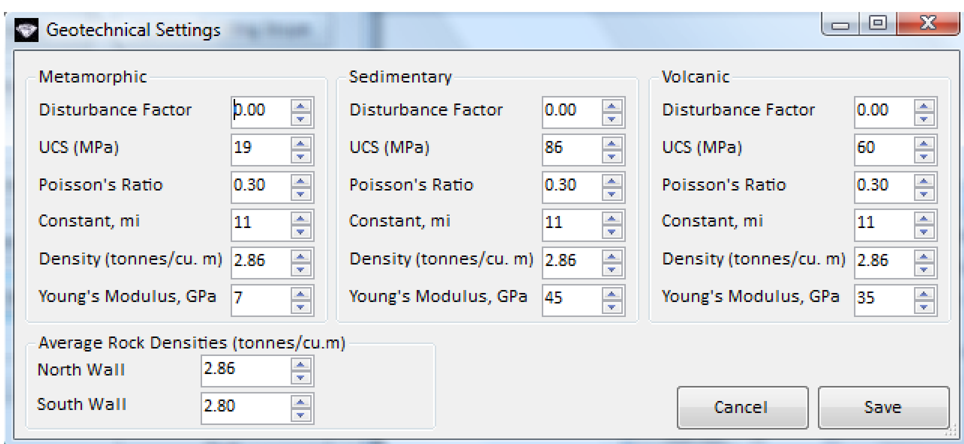

Figure 3.22 Geotechnical settings.

The Geotechnical Calculator Settings can also be modified. The minimum and maximum sample lengths can be adjusted. There are several samples in the database which are excessively long (greater than 50 m) or very short (less than 10cm), while the short samples do not present significant problems to the algorithm, very long samples are not representative of the fairly small regions which are being described. Minimum Total Length per Sample sets the lower threshold for sample length required to characterize a block. Increasing this value will likely increase run time since more expansions will likely be required. The Maximum Expansion Factor is the largest expansion of the blocks. The very first iteration has block at a scale of 1.0. Each iteration increases the scale of these blocks by 0.05. Increasing this value increases run time but also leads to less accurate representations of the block.

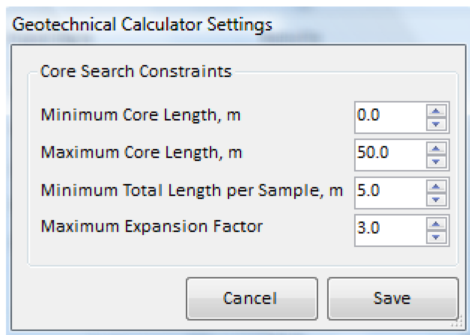

Figure 3.23 Geotechnical Calculator settings.

3.5 Error-trapping

The Lapa DIMAND has been designed to be as stable as possible and to protect the database from corruption. In most cases where user input is involved there are two levels of error-trapping. The first level occurs within the GUI as a user in entering data. Data fields which require specific formats (i.e. dates) or data types (i.e. whole numbers only, decimals, text, etc.) limit acceptable keystrokes accordingly. In the case of dates it is not possible to manually enter digits and slashes, instead an interactive calendar launches when the field is clicked and the user selects a date from the calendar. An example of keystroke limiting code is as shown below.

```
Private Sub txtY_KeyPress(ByVal sender As Object, ByVal e As System.Windows.Forms.KeyPressEventArgs) Handles txtY.KeyPress
        If Char.IsNumber(e.KeyChar) Or Char.IsPunctuation(e.KeyChar) Or Char.IsControl(e.KeyChar) Then
```

```
            e.Handled = False
        Else
            e.Handled = True
        End If
    End Sub
```

The previous selection of code will allow a user to enter numbers, decimals, and use the delete or backspace keys on their keyboards. Other logical tests are used to ensure that user input is acceptable before erroneous data is fed into other subroutines. An example of these tests is shown below. In this section of code if the ore composition does not sum to 100%, the user is notified using an error alert and a specific error message is returned. The subroutine is immediately exited, which in this case would return them to the data entry form and allow them to correct the specific error without recompleting the entire form.

```
If OreTot > 0 Then
            If OreTot < 100 Then
                MsgBox("Ore Composition must sum to 100", MsgBoxStyle.Exclamation, "ERROR!")
                Exit Sub
            ElseIf OreTot > 100 Then
                MsgBox("Ore Composition must sum to 100", MsgBoxStyle.Exclamation, "ERROR!")
                Exit Sub
            End If
        End If
```

Another style of error trapping using within subroutines is the Try...Catch...Finally trap. This error trap allows a programmer to place a block of code within the Try block; the compiler will attempt to execute the code, if an exception (i.e. error) is thrown the code jumps to the Catch block. There can be several Catch blocks per Try with each Catch block for a specific type of error or there can be a single generic Catch block. The code within the Catch block will then be executed. The programmer can also choose in include a Finally block (but it is optional), this block is a section of code which runs after a successful Try block or an unsuccessful Try and a successful Catch block (i.e. no matter what). A sample of a generic Catch block is shown below.

```
Try
      Con.Open()
      Cmd.ExecuteNonQuery()
      Cmd.Parameters.Clear()
Catch ex As Exception
      MsgBox(ex.ToString)
Finally
      Con.Close()
End Try
```

3.6 Recommended improvements

The Lapa DIMAND has undergone several developmental iterations. Each step has brought increased stability and functionality. Nevertheless, there is always room for improvement and expanding and adding functionality adds value to the software. While there are surely a variety of small modifications and features which could be modified or added, this section will focus on larger goals.

The current version of DIMAND was designed specifically with Lapa mine in mind. Revising several features could enable the software to be more flexible. Once of the principal limitations of the Lapa DIMAND is the fact that only three rock types are employed. Increasing the number of usable rock types would not be very challenging and making them user-customizable (i.e. the name of the rock type, properties, etc.) is achievable. It would be necessary to revise the GUI layouts (to accommodate for a variable number of rock types) and to make slight changes to the Geotechnical Calculator algorithm.

Another limitation of the DIMAND software is the inability for the end-user to add to the diamond drill hole database. Currently, samples must be appended manually to the Access Database file. While the process of adding these samples to the Access Database file is not time consuming nor complicated, if a user does not have Access (and some basic familiarity with it) installed on their PC they are unable to add samples. The addition of this type of functionality greatly enhances the ability of the software to remain up to date moving forward. Allowing the user to expand the drill hole database with ease is a feature that could be added with relative ease. A CSV (comma separated value) file could easily be created by the user (i.e. by using

Excel or a text editor) which could then be read by the DIMAND and appended to the drill hole database.

The Geotechnical calculator algorithm, while very useful, is not incredibly efficient. Steps could certainly be made which could reduce the run-time required to execute the algorithm. It is possible that very simple adjustments such as increasing the expansion step interval or reducing the maximum allowable expansion factor could have a significant impact on run time but adjustments to the code itself may present better opportunity for improvement.

Lastly, general improvements in the realm of error-trapping and exemption handling within the code itself would increase overall stability and reduce unnecessary crashes. While simple to use, the development of a software documentation (i.e. Help) feature could aid the end-user in understanding the features and limitations of the software.

3.7 Discussion and recommendations

The development of the Lapa DIMAND was an exhaustive process but the benefits and ease of use of the software make it a very useful tool. Being able to quickly view and extract a wide variety of data was an invaluable asset in the construction of the numerical model (Chapter 4) and the empirical model (Chapter 5).

Expanding the capabilities of this software to increase functionality and accessibility will add value to work already accomplished.

Chapter 4 – Effect of Stope Strike Length

4.1 Introduction

Lapa mine is located in the Abitibi region of north-western Quebec near the midway point between the cities of Val D'Or and Rouyn-Noranda. The operation straddles the extensive Cadillac-Larder Lake Fault Zone which hosts economic mineralization previously exploited by other nearby operations. Within the Lapa property exists the Contact Zone, the focus of this paper. This tabular shaped zone of steeply dipping (nearly vertical) gold vein and veinlet mineralization is hosted by biotite altered sulphide mineralized volcanics. The Contact Zone is located at the altered and weakly deformed north contact between a footwall composed of Piché Group sediments (comprised of volcanic rock and talc-chlorite schist) and a hanging wall composed of Cadillac Group sediments (greywacke). The Contact Zone has been traced up to 600 metres horizontally and ranges between 490 metres and 1280 metres below surface. The strike of the orebody runs approximately East-West with the footwall being located on the Southern side. The Contact Zone is narrow (approximately 3 metres in thickness) at the eastern extents but widens to thicknesses approximating 8 meters along the western extent. The stopes are 30 meters in height.

Production is achieved using a longitudinal mining method based on the Eureka method. Overcut and undercut drifts are driven the length of the orebody along the direction of strike. Mining is started with either a retreating or a centre-out sequence. In a traditional Eureka method Styrofoam 'slots' are left in place after mining and backfilling a stope. These slots are required for production blast fragmentation and heave. The modified Eureka method used at Lapa mine does not involve installing these styrofoam sheets but instead relies on the development of a slot at the center of the stope extending from the overcut down to the undercut. The creation of this slot is achieved by drilling a large hole and reaming it to 762 mm. Production blasting progresses outwards from the slot and material is mucked from the undercut. Once the stope is mucked out it is backfilled with cemented rockfill.

Managing overbreak at Lapa mine is difficult for two reasons. Firstly, as explored by Zniber et al. (2009), the drifts at Lapa are typically wider than the stope width. This was necessary in order to allow production drilling equipment adequate room to operate. Since the orebody is narrow it is not possible to fan the production drill holes, instead they must be drilled nearly vertical and this requires the drill holes to be positioned along the sidewall. This necessitates that the stope walls be undercut, leading to increased potential for unplanned dilution. This potential for overbreak is exaggerated by the poor quality of the footwall rock at Lapa is and the steeply dipping orebody causes the footwall to be a significant concern.

4.2 Case study

During the development of this project, stope strike length was identified as a controllable parameter. Undercutting, stope height, and stope width have been shown to influence stope wall overbreak (Zniber El Mouhabbis, Mitri et al. 2009; Mitri, Hughes et al. 2010), it is unfeasible to change these dimensions at Lapa mine. Undercutting is a necessary operational practice to allow for equipment access and safety. With sublevels developed at 30 meter intervals, it is uneconomic to change stope height. Stope width is defined by the width of the orebody and cannot be designed. Changing stope strike length requires only an adjustment of drilling patterns and modifying schedules to account for new stope tonnages.

A previous phase of this project saw the development of a two-dimensional elasto-plastic model to assess the impact of stope strike length and sequence on overbreak. While this yielded promising results, two-dimensional models assume that the model geometry normal to the modelled coordinates is infinitely extensive. This often results in exaggerated values and may not capture the expected behaviour.

This phase of the project presents a three-dimensional finite difference elasto-plastic model, designed to fully examine the effect of stope strike length and sequence on footwall overbreak. Also, the use of advanced modelling software has allowed for the incorporation of a strain-softening constitutive model. Strain-softening behaviour is widely observed in rock materials.

4.3 Numerical Model setup

In order to both examine the effects of stope strike length and stope sequence it is necessary to provide a model geometry which can be used for all cases. Average stope dimensions at Lapa mine are: 30 meters in height, 12 meters in length, and 3.5 meters wide. These dimensions represent a planned stope tonnage of about 3,600 tonnes. If stope strike length is changed it will result in changes in stope tonnage, these changes are presented below in Figure 4.1.

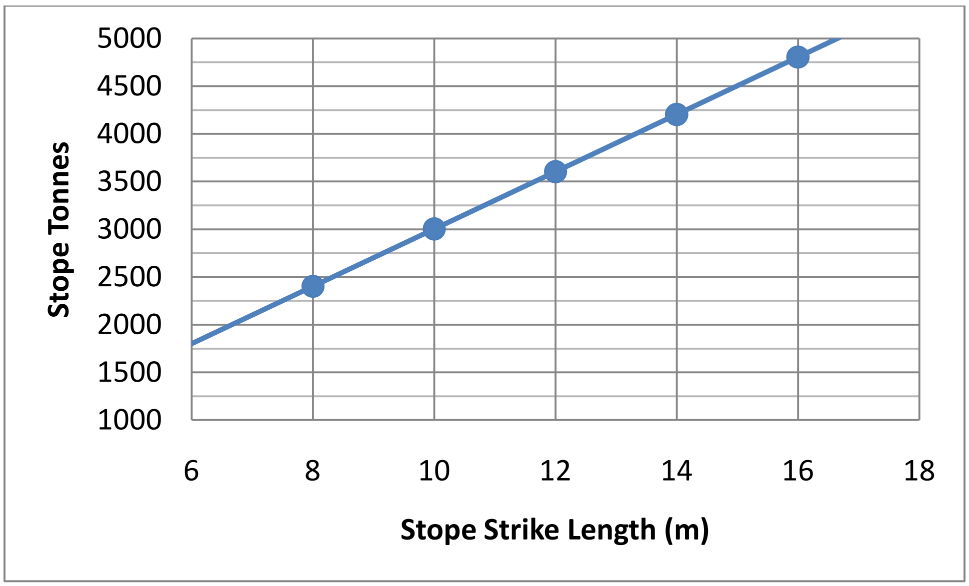

Figure 4.1 The influence of strike length on stope tonnage.

In the non-oxidizing ore found at Lapa mine increasing stope tonnage does not have a significant drawback. Decreasing stope tonnages impacts a mine's ability to reach production targets; if tonnages are reduced significantly then it may become necessary to increase the number of stopes in production. Due to the nature of the longitudinal retreat mining method employed at Lapa mine, opening up additional mining fronts is very difficult. With that in mind it was decided that the shortest possible strike length is 8 meters. This represents a 33% decrease in stope tonnages. With that in mind, a total of 5 models will be run, representing strike lengths of 8, 10, 12, 14, and 16 meters.

The model will comprise of a mine and fill sequence for three stopes mined in retreat, as shown below in Figure 4.2. Mining begins at the end of the overcut and undercut drifts and progresses in retreat, the extent of the over and undercuts in the retreat direction are long as to best simulate their effects. Figure 4.3 shows the dimensions for the 12 meter strike length model. The overcut and undercut drifts extend 50 meters past Block 3 in the direction of mining. Stope height, width, dip, and drift dimensions are held constant for all models.

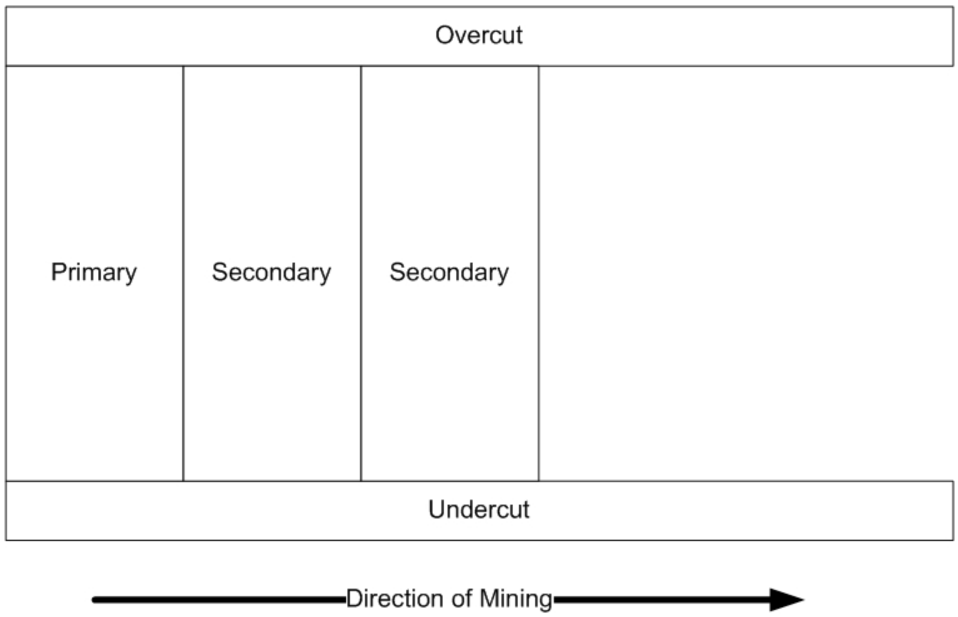

Figure 4.2 Retreat mining sequence.

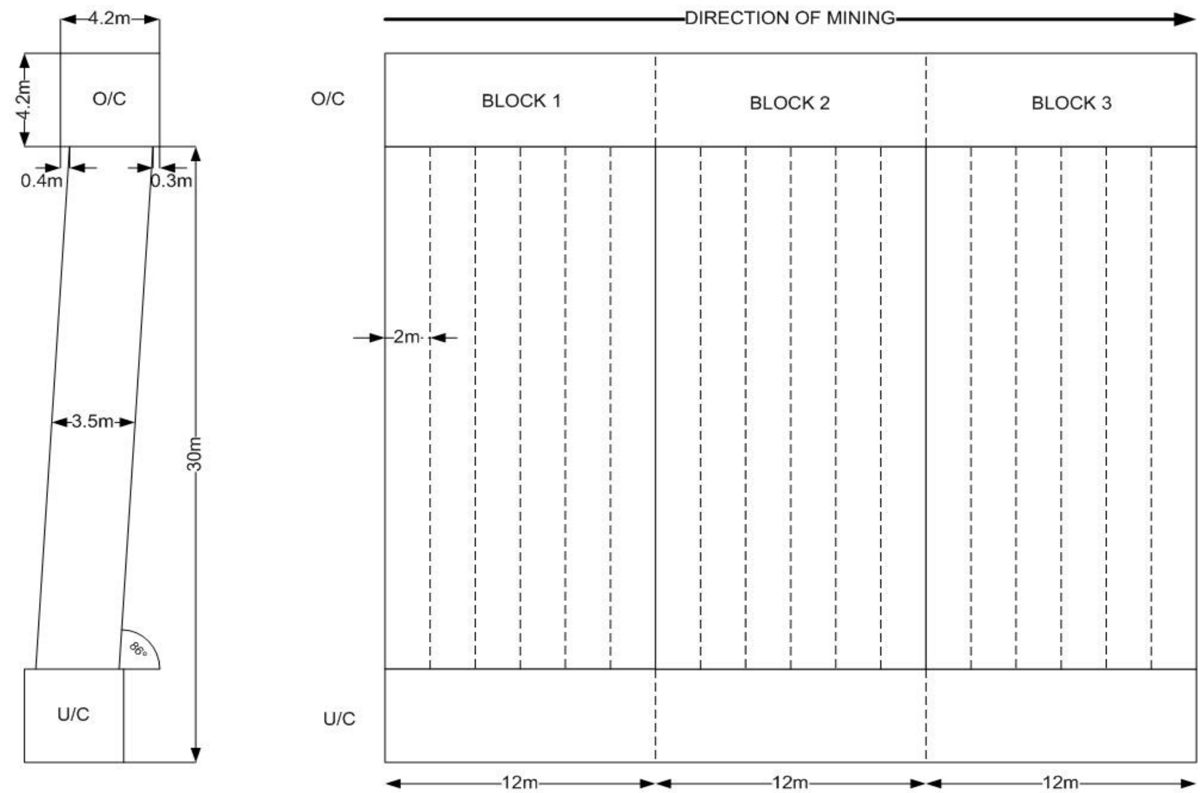

Figure 4.3 12-meter strike length model geometry.

Based on laboratory testing and field data, a set of failure criterion were established for the three rock mass types. Since a mine and fill sequence is being modelled it is also necessary to include a backfill material (Hassani and Archibald 1998). These parameters can be found below in Table 4.1.

Table 4.1 Rock mass properties.

Property	Footwall	Ore	Hanging wall	Cemented Rockfill
UCS (MPa)	30	65	80	3
GSI	45	55	60	
E_{intact} (MPa)	37000	37000	44750	2500
Cohesion (MPa)	1.67	2.81	3.63	0.1
Angle of Friction (°)	27.86	38.12	43.95	35
Angle of Dilation (°)	6.97	9.53	10.99	0
Rock Mass Bulk Modulus (MPa)	4597	8392	12927	2777
Rock Mass Shear Modulus (MPa)	3447	6294	9695	925

In order to implement a strain softening constitutive model in FLAC3D it is necessary to define the functions which represent angle of friction, angle of dilation, and cohesion with respect to the strain that the specimen has undergone. Tri-axial testing of various types of rock (Zhao and Cai 2010) allude to the characteristic shape presented below in Figure 4.4.

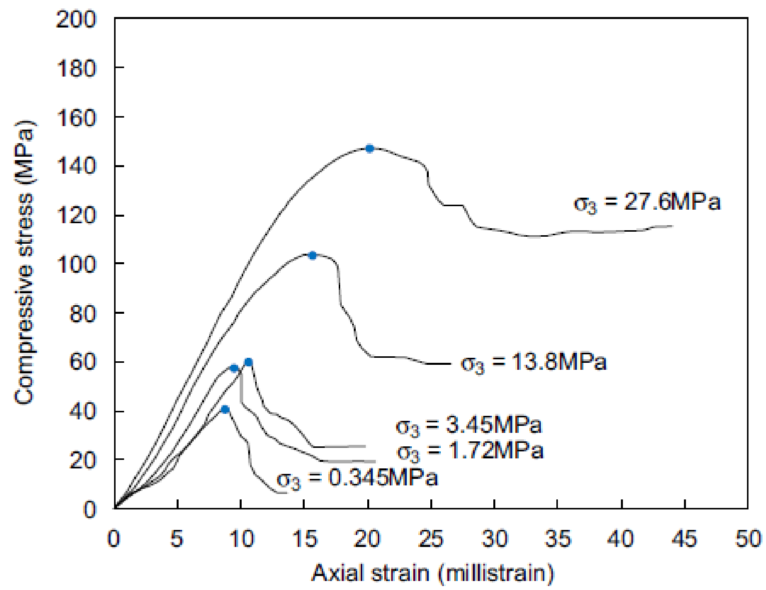

Figure 4.4 Post-peak strain softening behaviour of rock materials after Zhao and Cai (2010).

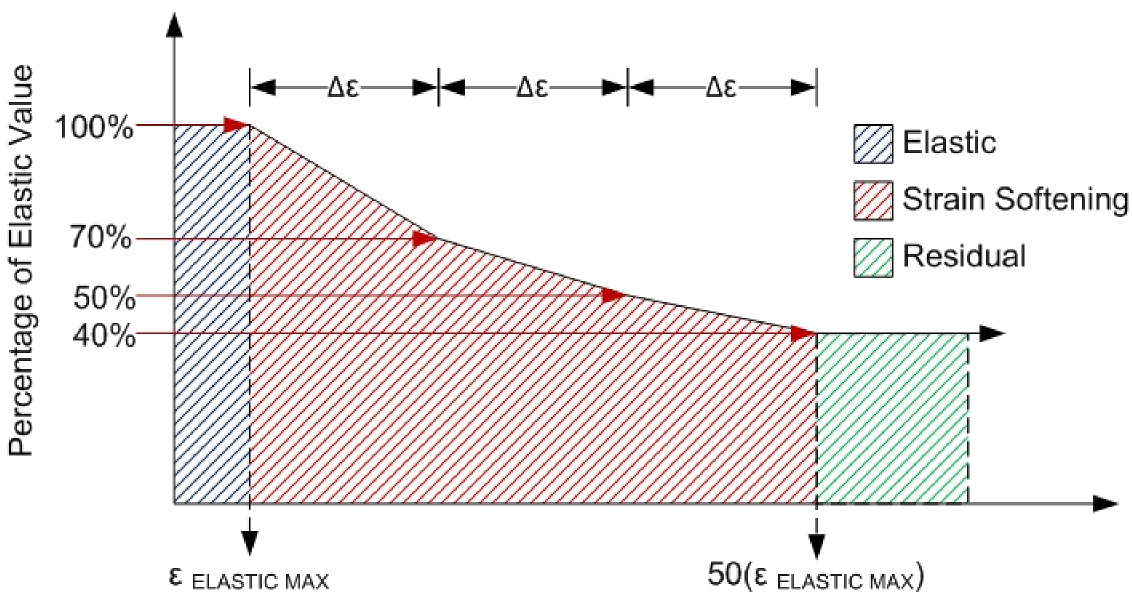

Figure 4.5 Strain softening characterization in FLAC3D.

This softening behaviour can be reflected the shape shown in Figure 4.5 where the parameters should have their full values in the elastic region. This region refers to all strains less than the maximum elastic strain ($\varepsilon_{ELASTIC\ MAX}$) which is described by Equation 11.

$$\varepsilon_{ELASTIC\ MAX} = \frac{\sigma_{CRM}}{E_{RM}} \quad (11)$$

Where σ_{CRM} is the uniaxial compressive strength of the rock mass and E_{RM} is Young's modulus of the rock mass.

Once the rock mass is strained beyond this elastic region it begins to undergo the softening process defined by four points that describe the change in property values as an element is strained. Fifty times the maximum elastic strain is considered to be the end of the softening process with properties have been reduced to 40% of their elastic values, this is the final residual strength. An example of how this concept affects properties is shown below in Figure 4.6.

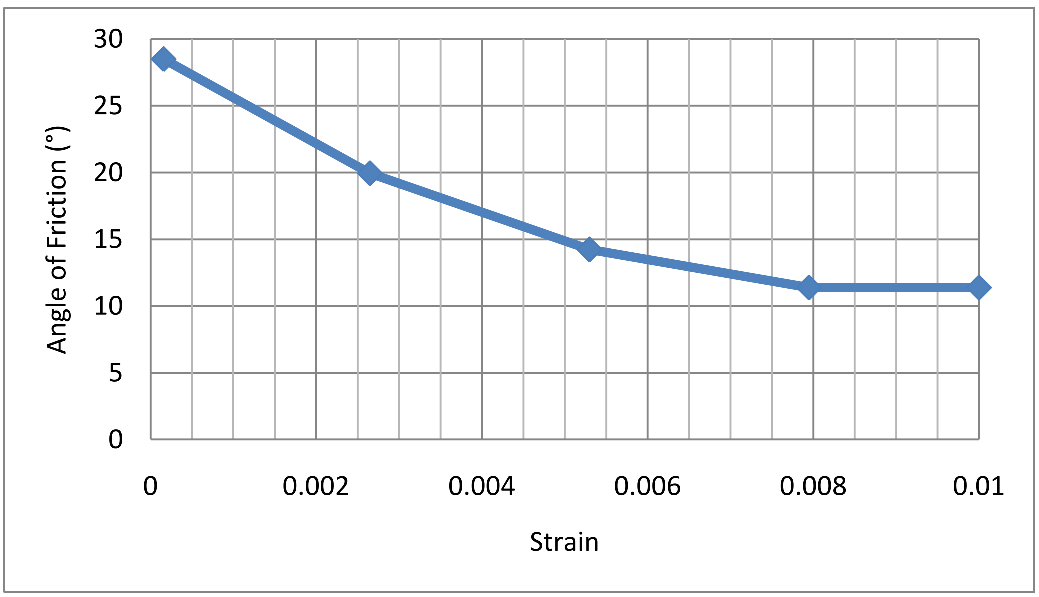

Figure 4.6 Strain softening response of friction angle for the footwall rock mass.

As seen in Figure 4.6, the elastic region is very small compared to the strain softening regime. As the footwall rock mass is strained, the angle of friction decreases from 27.86° down eventually to 11.14°. The same scheme was used to develop functions for cohesion and angle of dilation for all three rock mass types. The backfill material is not subjected to this strain softening model.

Local in-situ stress fields are oriented vertical and horizontally parallel and perpendicular to the orebody strike. A high degree of nearly vertical dipping foliation exists throughout the rock mass. These conditions suggest a low stress regime, thus the horizontal to vertical stress ratio is assumed to be 0.9 normal to the strike of the orebody. The horizontal to vertical stress ratio along the strike of the orebody is assumed to be 1.0.

4.4 Numerical modelling

The model is composed of around 3.2 million zones with ultimate boundaries large enough to prevent any unwanted boundary effects. The undercut and overcut drifts extend 50 meters beyond the end of the stopes to reduce any of their unwanted effects. The modelling stages are shown below in Table 4.2.

Table 4.2 Modelling stages.

Stage Number	Stage
1	Initial Equilibrium
2	Extract Undercut and Overcut Drifts
3	Mine First Stope
4	Fill Fist Stope
5	Mine Second Stope
6	Fill Second Stope
7	Mine Third Stope

The small-strain model was employed with the effect of gravity used to create the in-situ stresses. Model run time was between 8-10 hours.

Field observations at Lapa mine reveal that the footwall is a very soft material whereas the hanging wall is much more competent. Figure 4.7 shows how the footwall (on the right) deforms while the hanging wall (left hand side) more or less retains its designed contour.

Figure 4.7 Footwall closure at Lapa mine.

By running a variety of models with slightly different parameters each time it was possible to find properties which reflect these observations in the model. Parameters were varied by adjusted GSI values. Figure 4.8 shows the result of this effort, large displacements (about 55 cm of closure) occur on the footwall side while the hanging wall does not see deformation to the same degree.

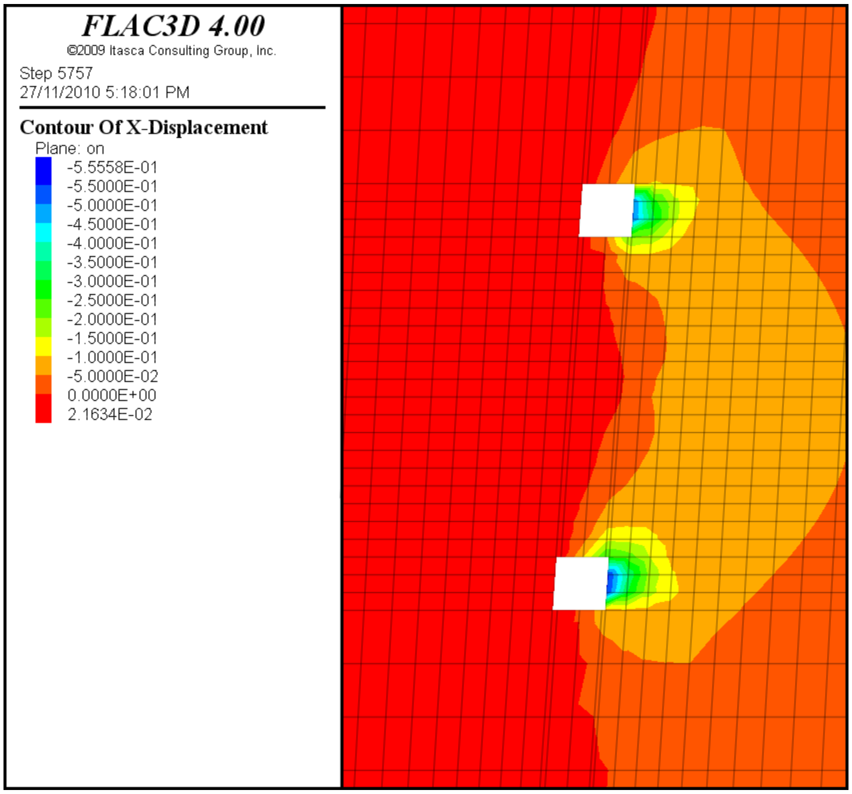

Figure 4.8 Deformation contours after opening the undercut and overcut.

Figure 4.9 shows the effect of the strain softening model in terms of changes in the angle of friction. The footwall sees a fair amount of softening occurring once a stope is mined. The stronger hanging wall does not see as much softening which is expected due to the fact that it does not undergo as much displacement.

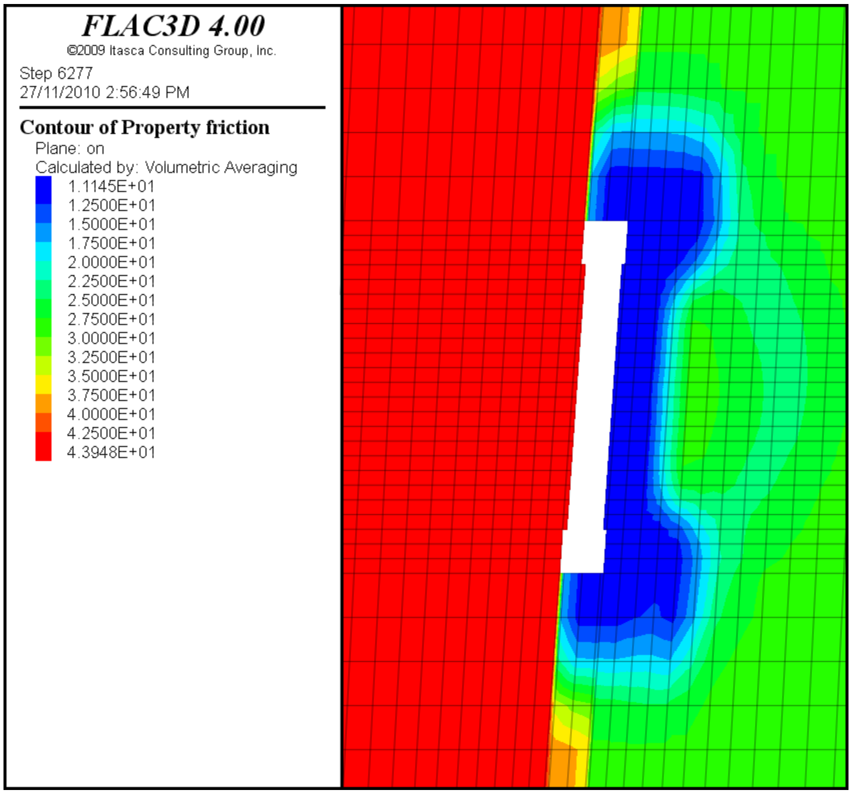

Figure 4.9 Strain-softening

4.5 Modelling results

Past numerical models showed a zone of relaxation (where the minor principal stress is less than 0 MPa) along the footwall and hanging wall faces. The size of this zone was used as the criteria for estimating the size of the DD_{MAX} envelope. These models were performed using two dimensional analyses. The FLAC3D model did not show these envelopes of relaxation; instead only very small local pockets would appear, as shown in black in Figure 4.10. Note that FLAC3D treats compressive stresses as negative values and has thus reversed the minimum and maximum principal stresses.

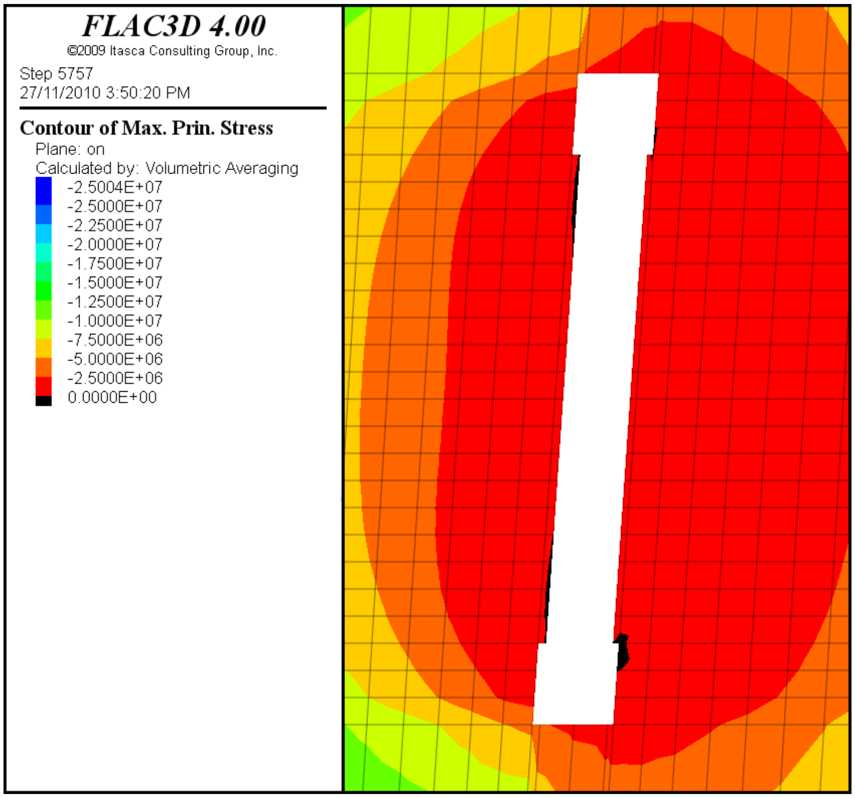

Figure 4.10 Relaxation in the FLAC3D model.

It is necessary to establish different criteria to describe overbreak. With a large stope database in hand it is possible to examine the data and determine what typical overbreak values are for both primary and secondary stopes. Figure 4.11 and Figure 4.12 show histogram plots of the actual DD_{MAX} values for stopes mined at Lapa mine. These values are calculated based on CMS volumes captured once a stope has been mined out.

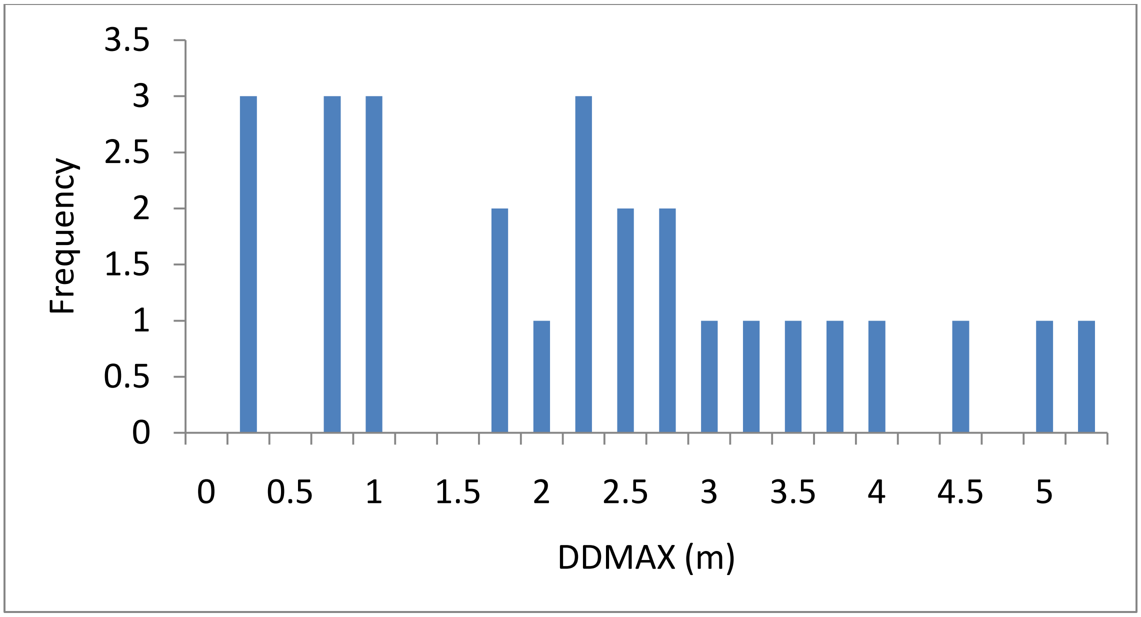

Figure 4.11 Histogram showing DDMAX (South) values for primary stopes.

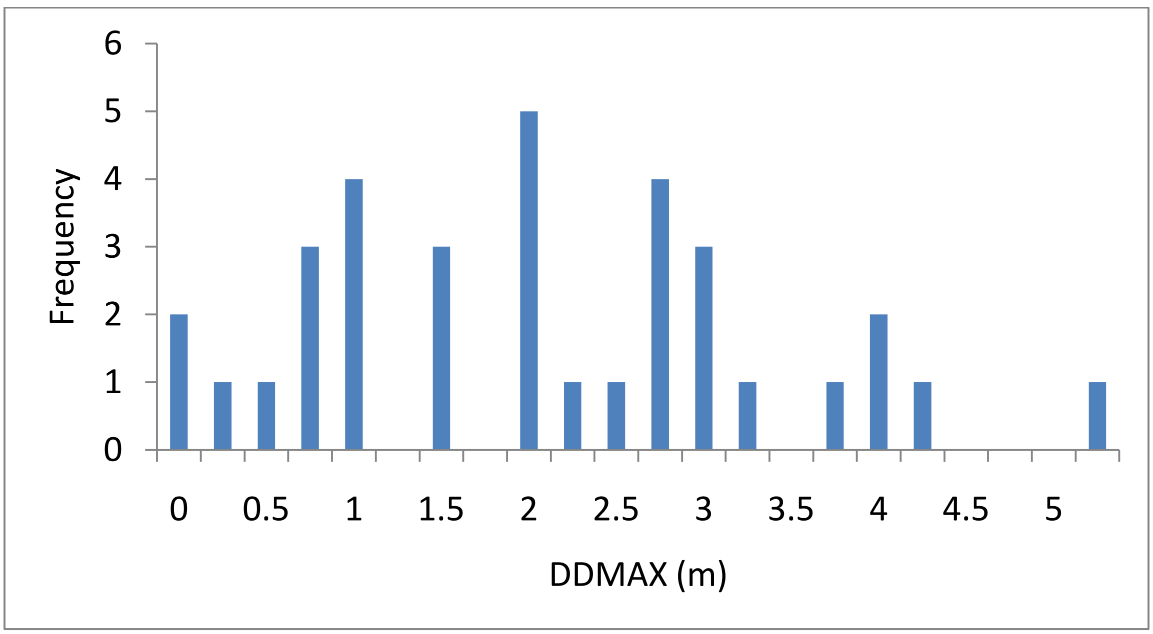

Figure 4.12 Histogram showing DDMAX (South) values for secondary stopes.

By examining the data presented in Figure 4.11 and Figure 4.12 an average DD_{MAX} of 2.20m and 1.98m for primary and secondary stopes respectively can be established.

At the skin surface of the stope walls, the minor principal stress is equal to zero, in reality, as unraveling would occur this would remain true for the wall. With that in mind, it is very likely that it is the major principal stress which is governing the degree of overbreak. By using the base 12m stope strike length case and the averages for primary and secondary stopes it is possible to find the major principal stress contour which describes the desired overbreak envelopes.

After examining the model, it was found that the maximum principal stress contour of 1.5 MPa described the desired overbreak envelope for both primary and secondary stopes. This value is approximately 5% of the footwall rock mass UCS and likely represents a stress state which provides enough clamping force to prevent unraveling of the rock mass. A sample of the contour is shown below in Figure 4.13.

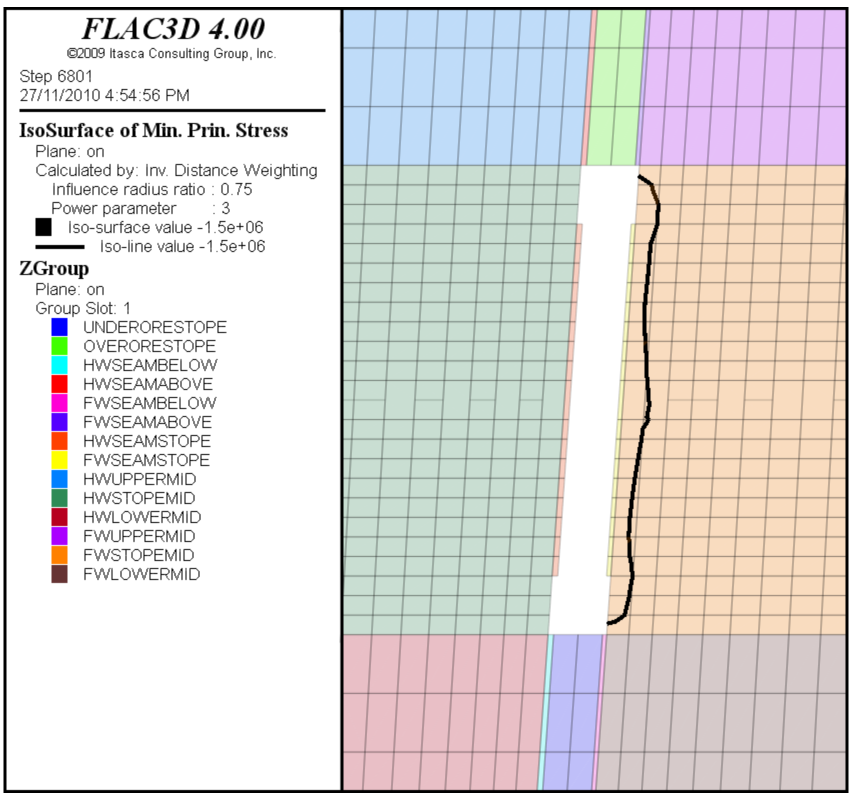

Figure 4.13 Major principal stress contour at 1.5MPa.

By using this criterion it is possible to determine the modelled overbreak for each stope length. With footwall overbreak being vastly more significant than hanging wall overbreak at Lapa mine this study focuses solely on the footwall. While two secondary stopes were modelled in each run, it was found that their overbreak contours were nearly identical in all cases. This was expected at the outset of the study and shows that the backfill is behaving properly. The results of this study are shown below in Figure 4.14.

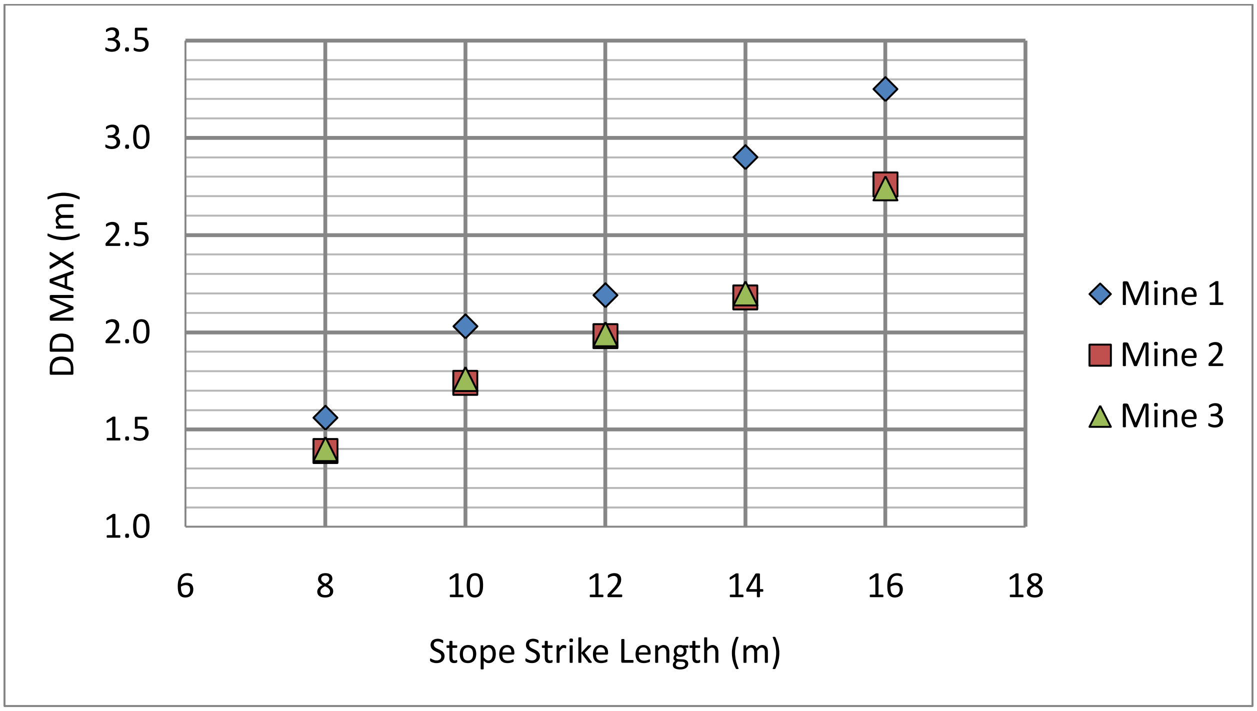

Figure 4.14 Modelled DDMAX with respect to stope strike length.

Mine 1, Mine 2, and Mine 3 refer to the sequence employed in the model. Mine 1 refers to the very first stope having been extracted, this is considered to be a primary stope. Mine 2 and Mine 3 are the second and third stopes, respectively, mined out in longitudinal retreat; these stopes are considered to be secondary stopes. The measurement is taken based on the criteria discussed in previous sections.

Quite clearly, there is a noticeable correlation between stope strike length and DD_{MAX}. Increasing strike length results in a larger degree of footwall instability. Increasing strike length by 1 meter results in an increase in DD_{MAX} of 0.21 and 0.16 meters for primary and secondary stopes respectively. As anticipated, secondary stopes see less overbreak in general compared to primary stopes.

Strike length was studied previously by the author using a two-dimensional model. This model yielded similar results (presented below in Figure 4.15) but the effect of sequence did not emerge.

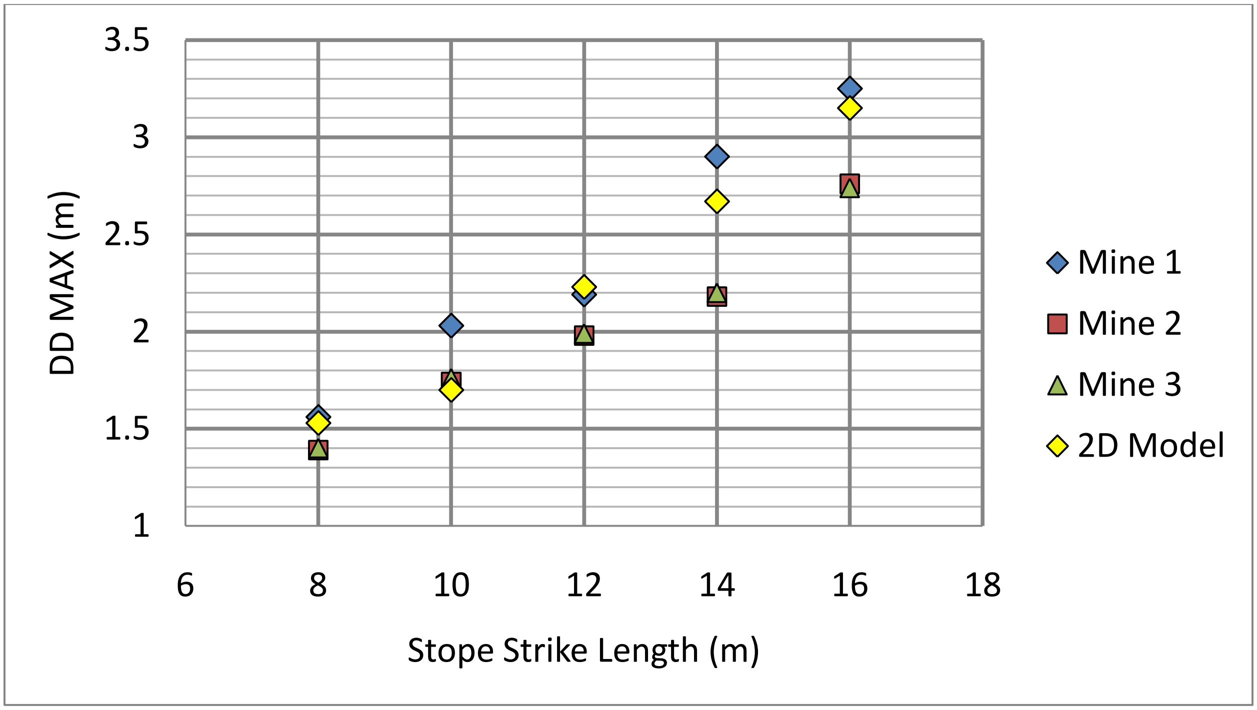

Figure 4.15 Comparing the results of the two studies.

In the previous study, there was no discernable difference in the degree of overbreak between the primary and secondary stopes, despite that, the values of the two studies are quite comparable with the 2D values lying between the primary and secondary values from the 3D model. The next three figures show how the 3D model behaves with respect to the mining sequence. The first stope (Figure 4.16) mined creates a large zone of relaxation in the surrounding rock mass. This large disturbance creates a larger DD_{MAX} for the primary stopes. The second and third stopes mined in sequence (Figure 4.17 and Figure 4.18) are secondary stopes. The backfill helps prevent any further relaxation and subsequent stopes present a smaller disturbance in the rock mass. This effect is the cause of the slightly smaller secondary stope DD_{MAX} values.

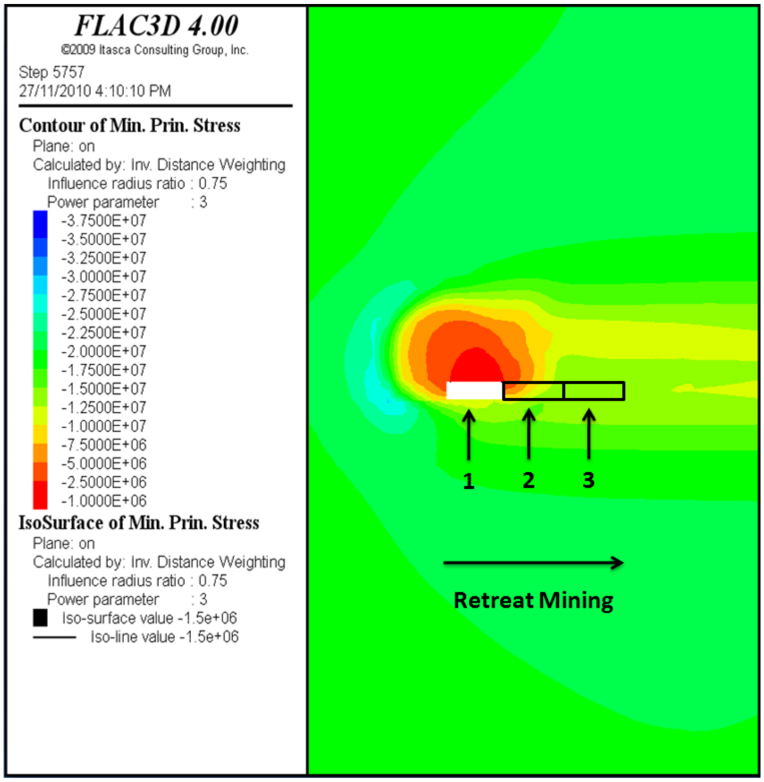

Figure 4.16 Relaxation around a primary stope (Mine 1).

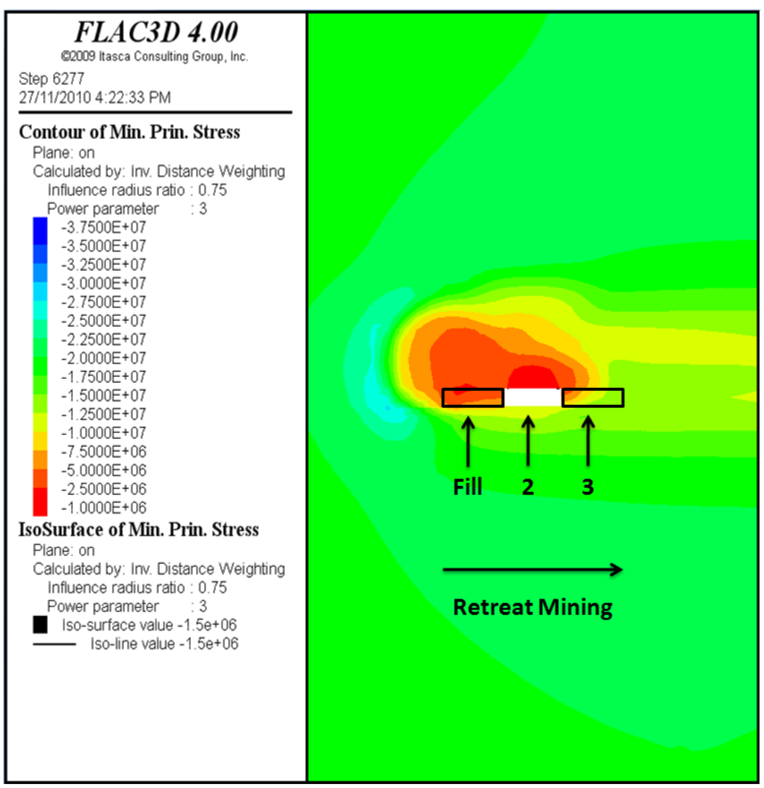

Figure 4.17 Relaxation around a secondary stopes (Mine 2).

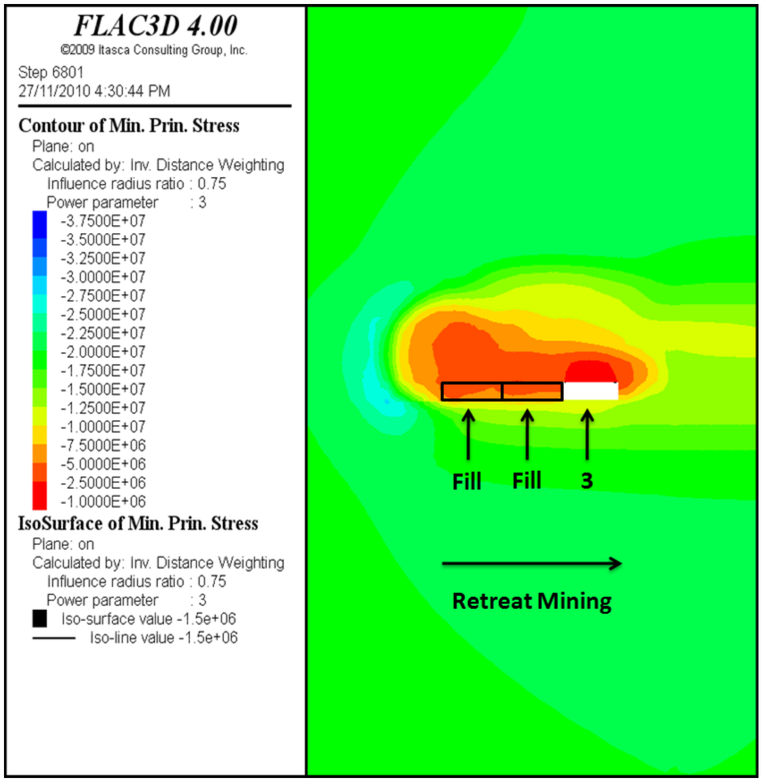

Figure 4.18 Relaxation around a secondary stope (Mine 3).

4.6 Discussion and recommendations

Based on this study it has become clear that shortening stope strike length results in higher confining stresses in the footwall. These higher confining stresses increase the stability of the footwall. Shortened strike lengths will most likely decrease overbreak in the footwall at Lapa mine. While the effects of shortening strike length are less pronounced than decreasing the greatest dimension of the stope (height), during the operating life of a mine it is simpler to adjust strike length compared to adjusting stope height.

The extent to which stope length can be decreased depends on the number of mining fronts available to meet production requirements and the optimization of stope cycle time. While shorter strike lengths require less time to drill production patterns, it is still necessary to develop a slot for each stope, this, along with reduced stope tonnages could make it difficult to reach production goals. On the operational level it is necessary to optimize these factors in order to achieve the best possible results.

Chapter 5 – An Empirical Model to Quantify Dilution at Lapa Mine

5.1 Introduction

Some empirical methods, such as Matthews (1981) or Potvin (1988), provide a general idea of stope stability. Unfortunately, these methods do not quantify the degree of expected dilution. O'Hara (1980) provides as estimate of the degree of dilution but only considers mining method, dip, and stope width. While these factors will certainly influence overbreak, they are generalizations and the effect of these parameters will likely vary between mining operations.

Fortunately, using data which is often at disposal, it is possible to tune these generalizations to specific operations. A properly tuned model can be of great benefit to an operation as it allows planners and production personnel to pre-empt challenges and to reach proactively.

The first several sections of this chapter are dedicated to outlining the generalized approach used in the final model iterations. The development of the Lapa empirical dilution model was an iterative learning process. This process is described in detail in the Case Study section of this chapter (see Section 5.9).

5.2 Developing an empirical model

The development of the empirical model has been undertaken in a six step process.

1) Collect Data
2) Process Data
3) Find Key Factors
4) Examine Trends with Numerical Modelling
5) Construct Empirical Model
6) Re-Evaluate the Model

These stages are described in further detail in the remainder of this chapter.

5.3 Data collection and integration

Modern mining operations are equipped with highly accurate survey equipment. Tools such as Total Stations, Cavity Monitoring Surveys (CMS) are often used to measure overbreak off specific stope walls. Extensive diamond drilling and lab testing provide the engineer with extensive data regarding the rock mass and its mechanical properties. These, along with modern instrumentation to measure rock stress and deformation (i.e. SMART Cables, Multipoint borehole extensometers, etc.) can result in enormous amounts of information stored across several computers or departments. In order to develop an empirical model it is necessary to bring all this data together.

Data integration was achieved through the development of the Lapa DIMAND (described in Chaper 3). The development of a central repository for the large variety of data amassed was instrumental in identifying and studying key influential factors.

5.4 Identifying potential factors

An empirical model is based on the varying influence of several factors which are judged to have significant impact on the final outcome. Determining which factors may influence overbreak requires careful consideration of the parameters influencing stope stability. Past work by Mitri and Henning (2007; 2008), Zniber et al. (2009), Potvin (1988), and Mathews (1981) indicate that stope stability is dependent on a plethora of factors.

Stope geometry, such as height, length, width, dip, and undercut can all play a significant role. Rock mechanical properties, such as the strength of the rock mass, as well as geological characteristics, such as RQD, joint structures, and rock type can all influence stability as well. Both the magnitude and orientation of the in-situ stress regime will undoubtedly affect wall stability.

By examining the specific problem at hand (i.e. unplanned dilution at Lapa mine), it is possible to make initial assessments of the importance of each of these factors. Using the data stored within the Lapa DIMAND, simple first-order relationships can be examined. These first order relationships are examining the influence of a single variable on wall overbreak (measured in terms of DD_{MAX}).

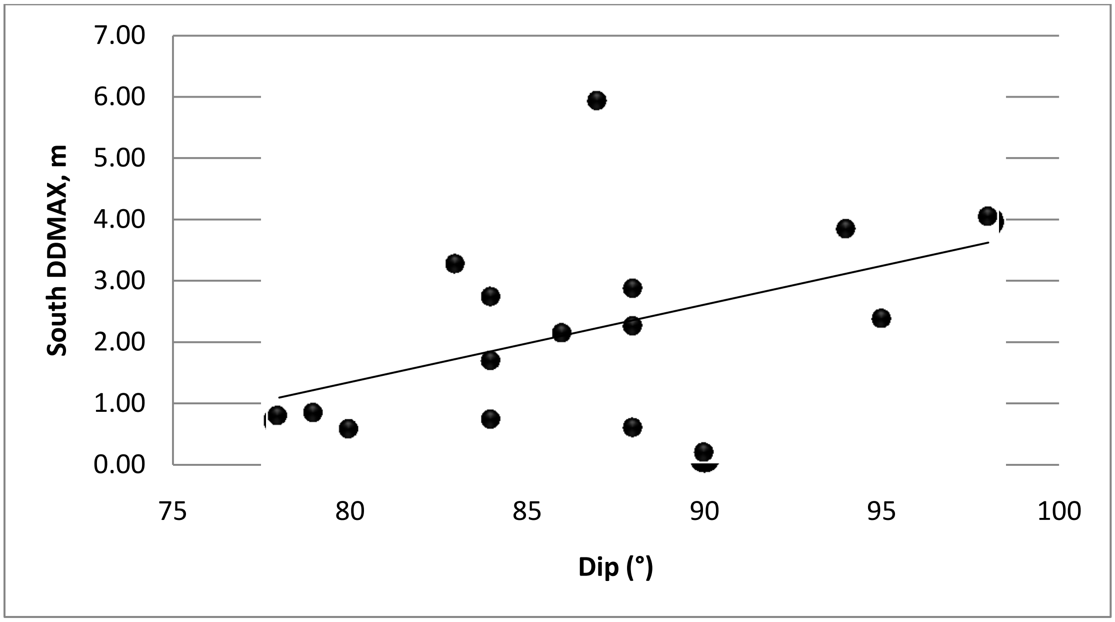

Figure 5.1 Example of a first order relationship.

5.5 Coupling factors

While examining each factor individually may yield some preliminary predictions, it completely ignores the interaction that parameters may have on each other. That is to say, while stope length may not seem to exhibit a trend, it is very possible that the products of stope length and stope height or of stope length and width, etc. may yield interesting trends. In order to fully explore these types of relationships, it is best to test all combinations of parameters. It is also very possible that the coupling of several (i.e. three or more) parameters may have an influence. Figure 5.2 shows an example of all the possible couplings between three parameters (Width, Dip, and RQD).

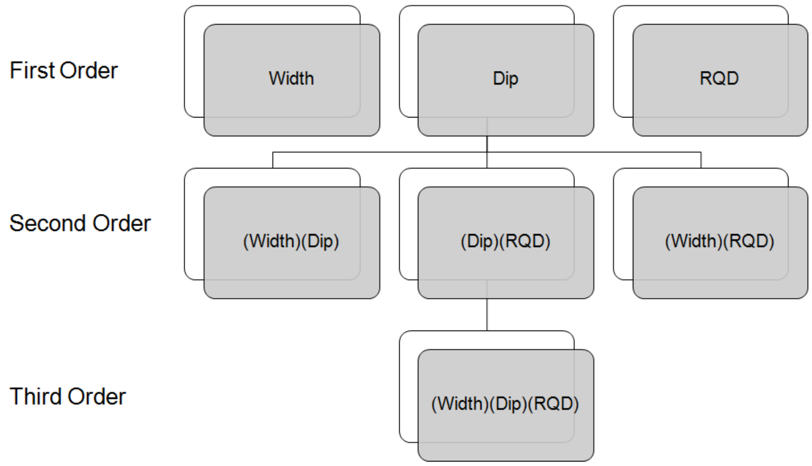

Figure 5.2 Example of coupled parameters.

5.6 Grouping data

Coupling may help identify some numerical trends but trends which are more Boolean in nature are best examined by grouping the data according to a common property. Groups based on properties such as mining method or mining sequence will certainly help illustrate the effects of those factors on overbreak.

Since the mining method at Lapa mine is for the most-part longitudinal retreat, groups based on mining sequence were developed. After examining the mining method, it was decided that the stopes could be divided into (at most) four groups. These groups are:

1) Level-Primary (refer to Figure 5.3)
2) Sublevel-Primary (refer to Figure 5.4 and Figure 5.5)
3) Level-Secondary (refer to Figure 5.6 and Figure 5.7)
4) Sublevel-Secondary (refer to Figure 5.8 and Figure 5.9)

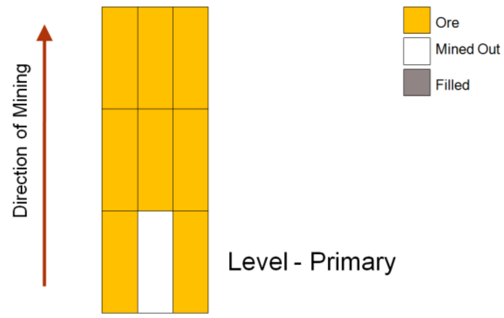

Figure 5.3 Level-Primary sequence division.

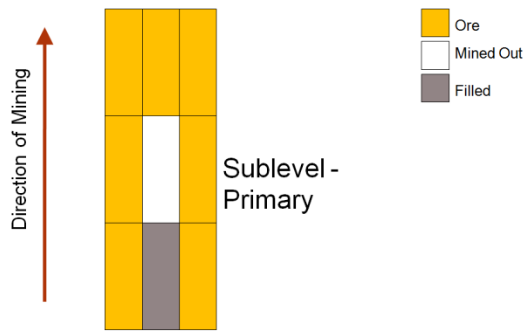

Figure 5.4 Sublevel-Primary sequence division.

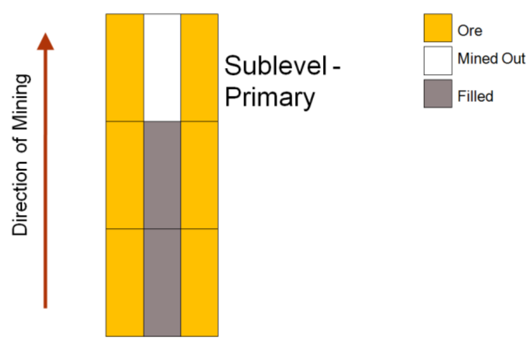

Figure 5.5 Sublevel-Primary sequence division.

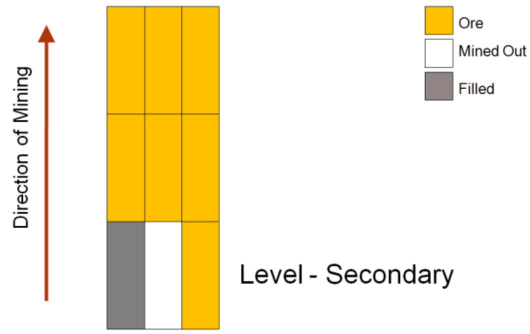

Figure 5.6 Level-Secondary sequence division.

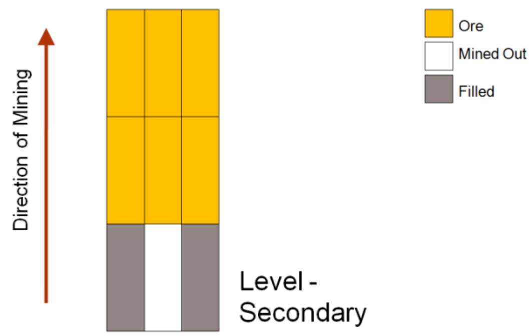

Figure 5.7 Level-Secondary sequence division.

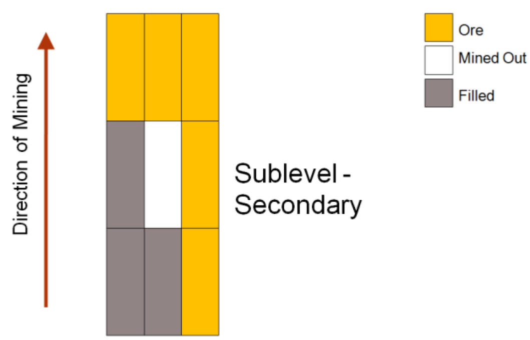

Figure 5.8 Sublevel-Secondary sequence division.

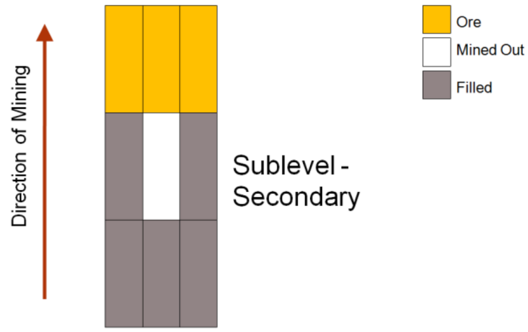

Figure 5.9 Sublevel-Secondary sequence division.

By dividing stopes into groups such as these, it is possible to examine and better understand the effects of sequence. It is important to ensure that the groupings do not have a very small number of samples as this can introduce statistical bias into the model. Since the model is intended to be predictive, this type of bias can be extremely detrimental.

5.7 Attribute evaluation

An empirical model can be constructed using all of the possible combinations of parameters but it is very likely that not all combinations are necessarily relevant. It is necessary to determine which factors have the ability to predict the degree of overbreak.

A statistical tool, known as attribute evaluation, can be employed as a means to determine which attributes are the most predictive. By employing a cross-validation analysis it is also possible to help reduce the effects of sample set bias and to keep the model predictive rather than reactive. This analysis selects a variable number of samples and performs a regression for each set of samples. By repeating this process many times eventually a set of attributes emerge (in these many regressions) as the most predictive.

This process is achieved using a machine learning algorithm software package, named WEKA, developed at the University of Waikato, New Zealand.

Once the most predictive attributes are determined, it is possible to move forward and construct the empirical model.

5.8 Constructing an empirical model

The empirical model is based on a multiple linear regression of the most predictive attributes. The regression coefficients are determined using the regression tool found within Excel. The empirical model is represented by an equation taking the following form:

$DD_{MAX} = A + B \bullet X1 + C \bullet X2 + \ldots$ (12)

Where A, B, C are regression coefficients and X1, X2 are the predictive attributes. X1, X2, etc can also represent coupled parameters.

Models are created for both the South and North walls using the respective DD_{MAX} values as the scalar value. The variable values for each stope are the same for both the North and South walls, with the exception of RQD for which the wall RQD is used. That is to say, for North DD_{MAX}, the North wall RQD value is used and vice-versa for the South wall.

For the purpose of these empirical models, the variables have each been normalized using a constant. The constants are usually based on average values (i.e. the width constant is 3.2 m, the length constant is 12 m) but in some cases peak values have been employed (i.e. the dip constant is 90 degrees, the RQD constant is 100). Examples of this normalization are as follows:

$$\text{Dip} = \text{Dip}/90 \qquad (13)$$

$$\text{Width} = 3.2/\text{Width} \qquad (14)$$

$$\text{RQD} = 100/\text{RQD} \qquad (15)$$

$$\text{Length} = \text{Length}/12 \qquad (16)$$

It should be noted that most stopes dip to the North (i.e. having positive dip values) but several stopes dip to the South (i.e. having negative dip values) which are translated by adding 180 degrees to the negative values.

To best illustrate this section, an example construction of an empirical model could take the following form where the normalized values for Dip, Width, RQD, and Length are represented by X1, X2, X3, and X4 and A, B, C, D, E, F, and G are the regression coefficients.

$DD_{MAX} = A + B \bullet X_1 + C \bullet X_4 + D \bullet (X_1 \bullet X_4) + E \bullet (X_2 \bullet X_4) + F \bullet (X_1 \bullet X_3) + G \bullet (X_1 \bullet X_2 \bullet X_4)$ (17)

Notice how some factors (i.e. Dip and Length) are uncoupled yet also appear as coupled factors with other terms. This indicates that Dip and Length are likely very important factors. It should be noted that this is only an example; in reality more than four factors were included in the attribute selection process. In many cases, most factors were selected to have at least some influence (i.e. as part as a coupled parameter term) but if a factor is deemed unimportant by the attribute selection process then it is left out of the regression.

5.9 Case study

In order to aid in stope design and mine planning, an empirical model was to be created which would be capable of allowing planners to predict the degree of dilution with reasonable accuracy. Initially the data set was not very large and the model was very simple in nature. As the project continued, the structure of the model evolved. This evolution was spurred by an ever-growing stope database as well as lessons learned from previous models. This section focuses on the evolution of the empirical model and lessons learned from each iteration.

5.9.1 The First Model

The first iteration of the empirical model was created in March 2010 and was based on data from roughly 25 stopes. It was initially believed that a simple linear combination of several key factors would best represent dilution. The construction of the model resembled the following:

$DD_{MAX} = (X_1)(X_2)(X_3)A + B$ (18)

Where X_1, X_2, and X_3 are normalized factors and A and B are regression coefficients.

The three key factors employed in this model were identified by examining each suspected factor against DD_{MAX} values for the South and North walls. Examples of this technique are shown below.

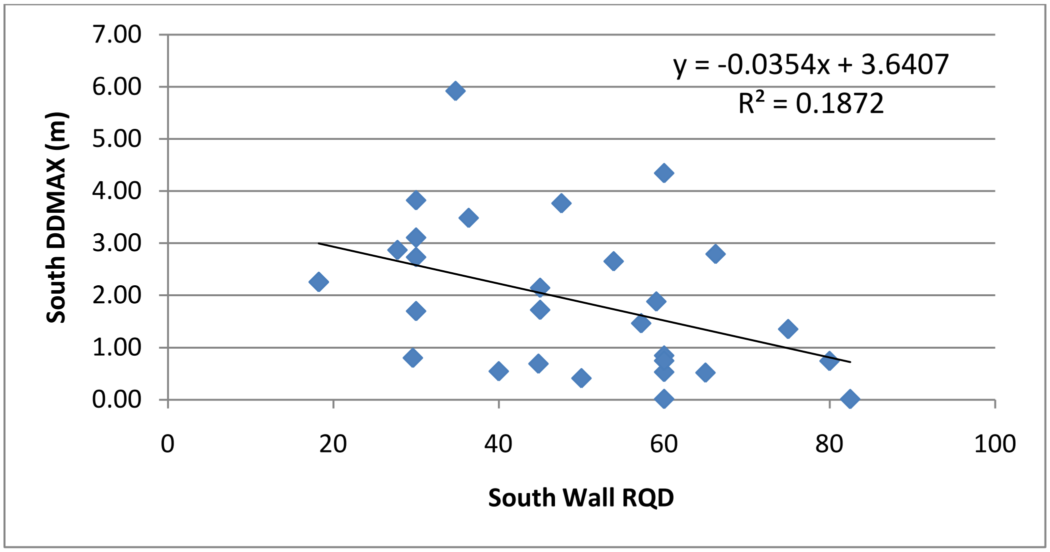

Figure 5.10 A trend between DD_{MAX} and RQD.

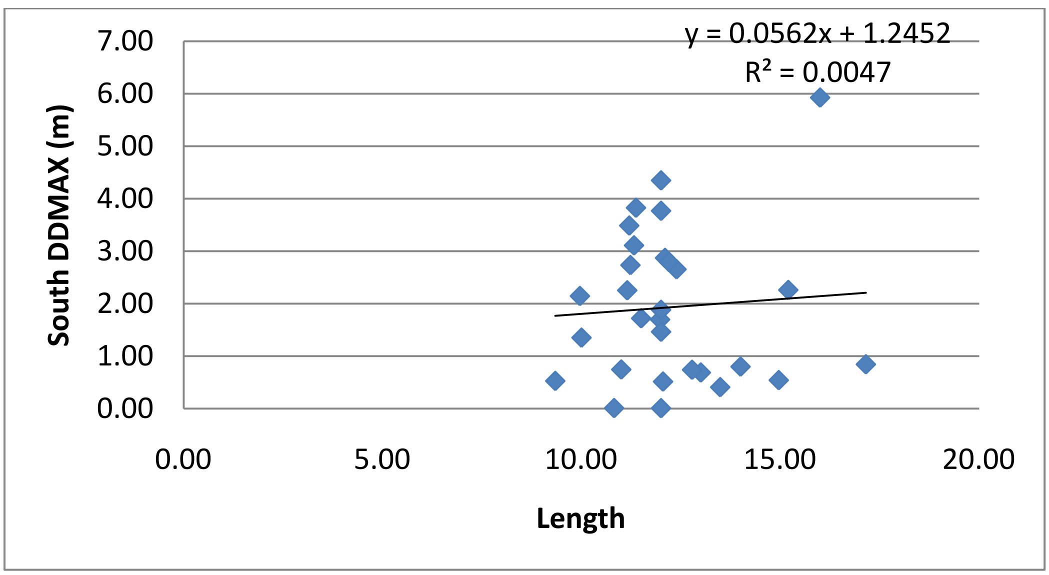

Figure 5.11 An unclear trend between DDMAX and stope strike length.

Figure 5.10 shows a fairly clear trend between DD_{MAX} and RQD whereas Figure 5.11 does not present any clear trend. Using this type of analysis, three key parameters were identified:

1) Undercut

2) Dip

3) RQD

In the case of RQD for this model, the North wall RQD was used for both the North and South models. While this is not ideal, limited South wall drill hole data provided poor RQD values. The concept of using the North wall RQD for both is somewhat justified in that the North and South wall RQD values display an inverse relationship. That is to say, in the westernmost portion of the mine, the south wall RQD is low while the North wall RQD is high. Moving eastward the South wall improves in quality while the North wall deteriorates.

The three factors were normalized for both the North and South models. The normalization was done in such a way that the best factor value would result in the normalized value being equal to one. If the factor value was detrimental to stability then the normalized value would increase above one. For the North (hanging) wall, the normalized dip value is represented by (90°/Dip) such that a shallower dipping stope would worsen stope stability. For the South (footwall) wall, the normalized dip value is represented by (Dip/90°) such that a shallower dipping stope would improve stope stability.

The product of these three normalized factors was regressed against DD_{MAX} values for both the North and South walls. Two equations were proposed as a means to estimate dilution:

$$DD_{MAX\ North} = \left(\frac{Undercut_{North}}{0.4m}\right)\left(\frac{90°}{Dip}\right)\left(\frac{100}{RQD_{North}}\right) \times 0.174 + 0.567 \quad (19)$$

$$DD_{MAX\ South} = \left(\frac{Undercut_{South}}{0.3m}\right)\left(\frac{Dip}{90°}\right)\left(\frac{RQD_{North}}{100}\right) \times 0.310 + 1.601 \quad (20)$$

The quality or fit of these models is evaluated using the coefficient of determination (R^2), values range between 0% and 100% with 100% indicating a perfect model fit. The coefficient of determination is a measure of the amount of statistical variance that is accounted for in the statistical model and gives an indication of how well future outcomes can be predicted (Steel and Torrie 1960).

The North model showed a strong correlation (R^2=89%) but unfortunately the South model was very poor (R^2=18%).

With overbreak from the South wall being of greater concern at Lapa mine it was quite clear that the First model was inadequate. It was also clear that a simple linear regression was not a good approach. By assigning a single coefficient to a group of factors they are all essentially deemed to be equally significant. A multilinear regression approach would allow for different weighting to be assigned to each factor, likely increasing the model correlation.

Challenges in actually gaining a good measurement of the undercut led to the use of planned stope width in place of undercut. Stope width still provides some measure of the degree of undercut in that very narrow stopes (i.e. less than 3.5 m wide) required undercutting greater than the design (in order to achieve the nominal 4.2 m wide drift). Stopes wider than 3.5 m require only the minimum undercut to achieve nominal drift width.

5.9.2 The Second Model

The Second Model was based on the same stope data set except that additional drillhole data was provided by Lapa. The addition of this drill hole data allowed for better estimates of RQD values. Significant factors were determined in a similar fashion as the First Model, examination of each individual factor compared to DD_{MAX}. Once again, dip, width (replacing undercut), and RQD were used as the significant factors.

This model included all possible couplings of these three factors which resulted in a total of seven terms. A multi-linear regression was performed on all of these factors and couplings in order to generate regression coefficients for each term. Models for both the North and South walls were created in the following form:

$$DD_{MAX}=A+B\bullet X_1+C\bullet X_2+D\bullet X_3+E\bullet(X_1\bullet X_2)+F\bullet(X_2\bullet X_3)+G\bullet(X_1\bullet X_3)+H\bullet(X_1\bullet X_2\bullet X_3) \quad (21)$$

Where:

X_1 = Dip/90

X_2 = 3.2/Width

X_3 = 100/RQD

And A, B, C, D, E, F, G, and H are regression coefficients

With eight regression coefficients emerging for each model the equations were fairly complex and very cumbersome. A simple Excel spreadsheet was employed to manage these equations.

Stope	Dip	Undercut North	Undercut South	RQD North	RQD South
	87	0.5	0.35	75	50

North	Coefficients	X	Multiplied
A	-50.6003086		-50.60031
B	47.08795364	**1.034483**	48.711676
C	30.46443167	**1.25**	38.08054
D	26.48570242	**1.333333**	35.31427
E	-28.1555524	***1.293103***	-36.40804
F	-15.6588041	***1.666667***	-26.09801
G	-24.0798902	***1.37931***	-33.21364
H	14.40376708	***1.724138***	24.834081
NORTH DDMAX			**0.6205679**

South	**Coefficients**	**X**	**Multiplied**
A	-9.8354695		-9.835469
B	11.33076855	**0.966667**	10.953076
C	14.76038873	**0.35**	5.1661361
D	-3.09527377	**2**	-6.190548
E	-15.5643409	***0.338333***	-5.265935
F	-3.47422444	***0.7***	-2.431957
G	3.452722627	***1.933333***	6.6752637
H	3.711401294	***0.676667***	2.5113815
SOUTH DDMAX			**1.5819481**

Figure 5.12 Modelled equations for the Second Model.

The new models were fairly cumbersome but the correlation for the crucial South wall increased to 35%. Unfortunately the North wall decreased to 16%. The revised approach was improving the South wall results but it was still clear that there were problems.

The multi-linear regression with coupled factors offered improved results. Unfortunately the dataset was still very small, it was believed that by increasing the dataset better correlation could be achieved and that other (i.e. missing) factors would emerge. The Second Model also required that all possible combinations of couplings be assigned a coefficient; in reality it is very likely that not all combinations are relevant.

5.9.3 The Third Model

The Third Model included an expansion of the stope database to just over 50 stopes. This expansion revealed that stope length may also be a factor. With this expanded database it was possible to examine the effects of sequence.

The effects of sequence were examined using the technique of grouping which was described in Section 5.6. Since the process of actually performing the regression is very simple, it was possible to evaluate a series of groupings in order to compare their effects. Three complete models were examined:

1) All stopes included in one group.
2) Stopes divided into two groups, Level and Sublevel, with one model for each case.
3) Stopes divided into four groups, Level and Sublevel (in the vertical direction) and then Primary and Secondary (in the horizontal direction).

The Third Model also introduced attribute evaluation and employed only the most predictive attributes in the multi-linear regression. All combinations of factors were fed into the attribute evaluation algorithm and unlike the past models, a total of four normalized factors were employed. These factors were:

1) Dip = Dip/90°
2) Width = 3.2m/Width
3) RQD = 100/RQD
4) Length = Length/12m

Within the new stopes added to the model, it was observed that some of the stopes dipped to the South, these negatively dipping stopes are corrected by adding 180°. Unlike the previous models, the normalized dip factor is no longer inverted (i.e. Dip/90° for South and 90°/Dip for North). This was done in order to simplify the model.

A total of six models, two sets of three groupings, one set for both the South and North walls were created using this process. This process results in models taking a form which may be similar to the following example:

$DD_{MAX} = A + B \cdot X_1 + C \cdot X_4 + D \cdot (X_1 \cdot X_4) + E \cdot (X_2 \cdot X_4) + F \cdot (X_1 \cdot X_2 \cdot X_3) + G \cdot (X_1 \cdot X_2 \cdot X_4)$ (22)

Where A, B, C, D, E, F, and G are regression coefficients and X_1, X_2, X_3, and X_4 are the normalized values for dip, width, RQD, and length. The number of parameters and their combinations are dependent on the results of the attribute selection process.

5.9.3.1 All stopes included – South wall

The strongest model is based on the linear combination of the following factors and their regression coefficients.

For the case where no subgroups have been created and all stopes are represented by one model ($R^2 = 38.9\%$):

$DD_{MAX} = A + B \cdot Dip + C \cdot Length + D(Dip \cdot Length) + E(Width \cdot Length) + F(Dip \cdot Width \cdot RQD) + G(Dip \cdot Width \cdot Length)$ (23)

Where the terms Dip, Length, Width, and RQD are the normalized values of these factors and where A, B, C, D, E, F, and G are the regression coefficients.

5.9.3.2 Divided in two groups – South wall

The strongest model is based on the linear combination of the following factors and their regression coefficients:

For **Level Stopes** ($R^2 = 58.5\%$):

$DD_{MAX} = A + B \cdot Dip + C \cdot RQD$ (24)

For **Sublevel Stopes** ($R^2 = 51.2\%$):

$DD_{MAX} = A + B \cdot Dip + C(Dip \cdot Width)$ (25)

Where the terms Dip, Width, and RQD are the normalized values of these factors and where A, B and C are the unique regression coefficients for each model.

5.9.3.3 Divided in four groups – South wall

For four groupings, the strongest models are based on the linear combination of the following factors and their regression coefficients:

For **Level-Primary Stopes** (R^2 = 92.0%):

$$DD_{MAX} = A + B \cdot Dip + C \cdot Length + D(Dip \cdot Length) + E(Dip \cdot Width \cdot Length) \quad (26)$$

For **Level-Secondary Stopes** (R^2 = 44.1%):

$$DD_{MAX} = A + B(Dip \cdot Length) + C(Width \cdot Length) + D(Dip \cdot RQD \cdot Length) \quad (27)$$

For **Sublevel-Primary Stopes** (R^2 = 78.8%):

$$DD_{MAX} = A + B \cdot Dip + C \cdot Length + D(Width \cdot Length) \quad (28)$$

For **Sublevel-Secondary Stopes** (R^2 = 50.4%):

$$DD_{MAX} = A + B(Dip \cdot Width) + C(RQD \cdot Length) \quad (29)$$

Where the terms Dip, Width, Length and RQD are the normalized values of these factors and where A, B and C, and D are the unique regression coefficients for each model.

5.9.3.4 Reviewing South wall models

A summary of the three South wall models are presented below in Table 5.1.

Table 5.1 The Third Model - South wall models

Division	Model	Number of attributes	Number of stopes in model	R^2
All Stopes	1	6	35	38.90%
Level	2	3	19	58.50%
Sublevel		2	16	51.20%
Level – Primary	3	4	9	92.00%
Level – Secondary		3	10	44.10%
Sublevel – Primary		3	9	78.80%
Sublevel - Secondary		2	7	50.40%

If the weighted average of R^2 for each of the three models (using the number of stopes as the weight) then the three models have collective R^2 values of: 38.9%, 55.2%, and 66.6% respectively.

It is quite clear that employing these subgroups results in improved correlations. This indicates that stope sequence has a distinct effect on unplanned stope dilution. Unfortunately, while the four group subdivision provides the best correlation, the number of stopes in each group is quite small. A small population size introduces heavy bias on the population and results in a model which is not robust. At this time, the divided in two grouping provides the best option. With larger group sample sizes the effect of bias is somewhat reduced. The modeled equations are provided below:

For **Level Stopes** (R^2 = 58.5%):

$$DD_{MAX} = 19.52 - 18.17\left(\frac{Dip}{90^{\circ}}\right) + 0.27\left(\frac{100}{RQD}\right) \quad (30)$$

For **Sublevel Stopes** (R^2 = 51.2%):

$$DD_{MAX} = -9.06 + 8.86\left(\frac{Dip}{90^{\circ}}\right) + 3.34\left(\frac{Dip}{90^{\circ}}\frac{3.2m}{Width}\right) \quad (31)$$

5.9.3.5 All stopes included – North wall

The strongest model is based on the linear combination of the following factors and their regression coefficients (R^2 = 31.1%):

$DD_{MAX} = A + B(Width \cdot RQD \cdot Length)$ (32)

Where the terms Length, Width, and RQD are the normalized values of these factors and where A and B are the regression coefficients.

5.9.3.6 Divided in two groups – North wall

The strongest model is based on the linear combination of the following factors and their regression coefficients:

For **Level Stopes** (R^2 = 13.9%):

$DD_{MAX} = A + B \cdot Dip + C \cdot Width + D(Dip \cdot Length) + E(Width \cdot Length)$ (33)

For **Sublevel Stopes** (R^2 = 57.6%):

$DD_{MAX} = A + B \cdot Dip + C \cdot Width$ (34)

Where the terms Dip, Width, and Length are the normalized values of these factors and where A, B, C, D, and E are the unique regression coefficients for each model.

5.9.3.7 Divide in four groups – North wall

For four groupings, the strongest models are based on the linear combination of the following factors and their regression coefficients:

For **Level-Primary Stopes** (R^2 = 25.7%):
$DD_{MAX} = A + B \cdot Width + C \cdot Length + D(Dip \cdot Length)$ (35)

For **Level-Secondary Stopes** (R^2 = 28.1%):

$DD_{MAX} = A + B \cdot Length + C(Width \cdot Length)$ (36)

For **Sublevel-Primary Stopes** (R^2 = 84.8%):

$DD_{MAX} = A + B \cdot Length + C(Width \cdot Length)$ (37)

For **Sublevel-Secondary Stopes** (R^2 = 82.2%):

$DD_{MAX} = A + B(Dip \cdot Length) + C(Dip \cdot RQD \cdot Width)$ (38)

Where the terms Dip, Width, Length and RQD are the normalized values of these factors and where A, B and C, and D are the unique regression coefficients for each model.

5.9.3.8 Reviewing North wall models

A summary of the three North wall models is presented in the table below:

Table 5.2 The Third Model - North wall models.

Division	Model	Number of Attributes	Number of stopes in model	R^2
All Stopes	1	2	40	33.10%
Level	2	4	26	13.90%
Sublevel		2	14	57.60%
Level – Primary	3	3	12	25.70%
Level – Secondary		2	14	28.10%
Sublevel – Primary		2	8	84.80%
Sublevel - Secondary		2	6	82.20%

If the weighted average of R^2 for each of the three models (using the number of stopes as the weight) then the three models have collective R^2 values of: 33.1%, 29.2%, and 53.5% respectively.

The results of the Third Model for the North wall are quite mixed. Again, it is worth noting that the North wall is of less concern at Lapa mine, nevertheless, efforts were made to develop a good model. On first inspection, the two group subdivision appears to have yielded worse results than the model that did not include the effects of sequence. Closer inspection of the grouped models (both the two and four) reveals that poor correlation exists mainly for the Level stope models. The Sublevel models provided much improved correlations. Due to the nature of the longitudinal retreat mining method, as mining progresses, sublevel stopes will eventually represent the majority of stopes. With this in mind there is some justification to push forward with the two division model. While the four division model provides better correlation values, as before this is due to the small sample group size. The modeled equations are provided below:

For **Level Stopes** (R^2 = 13.9%):

$$DD_{MAX} = 2.45 - 13.08\left(\frac{Dip}{90^{\circ}}\right) + 10.37\left(\frac{3.2m}{Width}\right) + 11.28\left(\frac{Dip}{90^{\circ}}\frac{Length}{12m}\right) - 10.13\left(\frac{3.2m}{Width}\frac{Length}{12m}\right) \quad (39)$$

For **Sublevel Stopes** (R^2 = 57.6%):

$$DD_{MAX} = 6.47 - 7.91\left(\frac{Dip}{90^{\circ}}\right) + 3.38\left(\frac{3.2m}{Width}\right) \quad (40)$$

5.9.4 The Fourth Model

The Third Model with the addition of stope sequence, stope length, and an overall increase in the number of data points provided better results than previous models. The use of attribute selection to eliminate unnecessary factors (or couplings) helps to maintain some degree of simplicity to the model. Based on the success of the Third Model it was decided to maintain the same construction and procedure throughout the development of the Fourth Model. It was hoped that additional stopes would result in better results.

The Fourth Model included the expansion of the stope database to 46 stopes and an addition of roughly 5,000 drill hole database samples (bringing to total number of drill hole samples to roughly 60,000). The Third model identified four factors which influence dilution: Width, Length, Dip, and RQD. Between the development of the Third and Fourth models, Lapa mine started production from deeper sections of the mine. Since mining horizons had expanded and now covered a greater vertical expanse, it was decided to include a factor representative of depth.

The depth parameter used is simple the Level number normalized by the deepest level:

$$Depth = \frac{Level}{128}$$

In addition to the new concept of depth, it was decided to add another stope division. A total of four complete models were developed:

1) All stopes included in one group.
2) Stopes divided into two groups, Level and Sublevel, with one model for each case.
3) Stopes divided into two groups, Primary and Secondary, with one model for each case.
4) Stopes divided into four groups, Level and Sublevel (in the vertical direction) and then Primary and Secondary (in the horizontal direction).

5.9.4.1 All stopes included – South wall

The strongest model is based on the linear combination of the following factors and their regression coefficients.

For the case where no subgroups have been created and all stopes are represented by one model (R^2 = 38.7%):

$$DD_{MAX} = A + B \cdot Dip + C(Width \cdot Length) + D(Width \cdot Dip) + E(Width \cdot Depth) + F(Length \cdot Dip) + G(Width \cdot Length \cdot Dip) + H(Width \cdot Length \cdot Depth) + I(Width \cdot Dip \cdot Depth) + J(Width \cdot Length \cdot Dip \cdot Depth) + K(Width \cdot Dip \cdot Depth \cdot RQD) \quad (41)$$

Where the terms Dip, Length, Width, and RQD are the normalized values of these factors and where A, B, C, D, E, F, G, H, I, J, and K are the regression coefficients.

5.9.4.2 Divided in two groups, Level and Sublevel – South wall

The strongest model is based on the linear combination of the following factors and their regression coefficients:

For **Level Stopes** (R^2 = 49.4%):

$DD_{MAX} = A + B \cdot Dip + C(Width \cdot Dip) + D(Width \cdot Depth) + E(Width \cdot Length \cdot Depth) + F(Width \cdot Dip \cdot Depth) + G(Width \cdot Length \cdot Dip \cdot Depth) + H(Width \cdot Dip \cdot Depth \cdot RQD)$ (42)

For **Sublevel Stopes** (R^2 = 51.6%):

$DD_{MAX} = A + B \cdot Dip + C(Dip \cdot Length) + D(Width \cdot Length \cdot Dip \cdot RQD)$ (43)

Where the terms Dip, Width, and RQD are the normalized values of these factors and where A, B, C, D, E, F, G, and H are the unique regression coefficients for each model.

5.9.4.3 Divided in two groups, Primary and Secondary – South wall

The strongest model is based on the linear combination of the following factors and their regression coefficients:

For **Primary Stopes** (R^2 = 54.3%)**:**

$DD_{MAX} = A + B \cdot Width + C \cdot Dip + D(Width \cdot Dip) + E(Width \cdot Depth) + F(Width \cdot Length \cdot Depth) + G(Width \cdot Dip \cdot Depth) + H(Width \cdot Length \cdot Dip \cdot Depth) + I(Width \cdot Dip \cdot Depth \cdot RQD)$ (44)

For **Secondary Stopes** (R^2 = 27.7%)**:**

$DD_{MAX} = A + B \cdot Dip + C(Width \cdot Dip) + D(Length \cdot Dip) + E(Dip \cdot Depth \cdot RQD)$ (45)

Where the terms Dip, Width, and RQD are the normalized values of these factors and where A, B, C, D, E, F, G, H, and I are the unique regression coefficients for each model.

5.9.4.4 Divided in four groups – South wall

For four groupings, the strongest models are based on the linear combination of the following factors and their regression coefficients:

For **Level-Primary Stopes** (R^2 = 99.5%)**:**

$DD_{MAX} = A + B \cdot Length + C(Width \cdot Depth) + D(Width \cdot Length \cdot Depth) + E(Width \cdot Dip \cdot Depth) + F(Width \cdot Length \cdot Dip \cdot Depth) + G(Width \cdot Dip \cdot Depth \cdot RQD)$ (46)

For **Level-Secondary Stopes** (R^2 = 44.0%)**:**

$DD_{MAX} = A + B \cdot Length + C \cdot Dip + D(Dip \cdot Length) + E(Width \cdot Dip \cdot Depth) + F(Width \cdot Dip \cdot Depth \cdot RQD)$ (47)

For **Sublevel-Primary Stopes** (R^2 = 64.7%)**:**

$DD_{MAX} = A + B \cdot Dip + C(Width \cdot Dip) + D(Dip \cdot Depth \cdot RQD)$ (48)

For **Sublevel-Secondary Stopes** (R^2 = 93.7%)**:**

$DD_{MAX} = A + B(Length \cdot Dip) + C(Width \cdot Length \cdot Dip) + D(Width \cdot Length \cdot Depth) + E(Dip \cdot Depth \cdot RQD) + F(Depth \cdot RQD)$ (49)

Where the terms Dip, Width, Length and RQD are the normalized values of these factors and where A, B and C, D, E, and F are the unique regression coefficients for each model.

5.9.4.5 Reviewing South wall models

A summary of the four South wall models are presented below in Table 5.3.

Table 5.3 The Third Model - South wall models.

Division	Model	Number of attributes	Number of stopes in model	R^2
All Stopes	1	10	46	38.70%
Level	2	7	26	49.4%
Sublevel		3	20	51.6%
Primary	3	8	20	54.3%
Secondary		3	26	27.7%
Level – Primary	4	6	9	99.5%
Level – Secondary		5	17	44.0%
Sublevel – Primary		4	11	64.7%
Sublevel - Secondary		6	9	93.7%

If the weighted average of R^2 for each of the three models (using the number of stopes as the weight) then the four models have collective R^2 values of: 38.7%, 50.4%, 39.3% and 69.5% respectively. Table 5.4 shows which of the expected factors were selected for inclusion in the model. In most cases all five factors were employed, this indicates that these predicted factors are indeed influencing stope overbreak.

Table 5.4 Factors included in each model.

South Wall	Width	Length	Dip	Depth	RQD
All	•	•	•	•	•
Level	•	•	•	•	•
Sublevel	•	•	•		
Primary	•	•	•	•	•
Secondary	•	•	•		
Level Primary	•	•	•	•	•
Level Secondary	•	•	•	•	•
Sublevel Primary	•	•	•	•	•
Sublevel Secondary	•	•	•	•	•

It is quite clear that employing these subgroups results in improved correlations. The addition of the Primary-Secondary subdivision did not yield results as promising as the Level-Sublevel division. This indicates that stope sequence has a distinct effect on unplanned stope dilution but that the vertical sequence is of higher importance. Unfortunately, while the four group subdivision provides the best correlation, the number of stopes in each group is quite small. A small population size introduces heavy bias on the population and results in a model which is not robust. At this time, the divided in two grouping by level type (i.e. Level-Sublevel) provides the best option. With larger group sample sizes the effect of bias is somewhat reduced. The modeled equations are provided below:

For **Level Stopes** (R^2 = 49.4%)**:**

$$DD_{MAX} = -16.15 + 16.64\left(\frac{Dip}{90^0}\right) + 0.70\left(\frac{Width}{3.2m}\frac{Dip}{90^0}\right) - 43.98\left(\frac{Width}{3.2m}\frac{Depth}{128}\right) + 69.55\left(\frac{Width}{3.2m}\frac{Length}{12m}\frac{Depth}{128}\right) + 45.66\left(\frac{Width}{3.2m}\frac{Dip}{90^0}\frac{Depth}{128}\right) - 70.71\left(\frac{Width}{3.2m}\frac{Length}{12m}\frac{Dip}{90^0}\frac{Depth}{128}\right) + 0.42\left(\frac{Width}{3.2m}\frac{Dip}{90^0}\frac{Depth}{128}\frac{100}{RQD}\right) \quad (50)$$

For **Sublevel Stopes** (R^2 = 51.6%):

$$DD_{MAX} = -9.02 + 6.79\left(\frac{Dip}{90^0}\right) + 2.84\left(\frac{Length}{12m}\frac{Dip}{90^0}\right) + 2.12\left(\frac{Width}{3.2m}\frac{Length}{12m}\frac{Dip}{90^0}\right) \quad (51)$$

5.9.4.6 All stopes included – North wall

The strongest model is based on the linear combination of the following factors and their regression coefficients (R^2 = 18.6%):

$$DD_{MAX} = A + B \cdot Dip + C \cdot Depth + D(Dip \cdot Depth) + E(Width \cdot Dip \cdot Depth) + F(Length \cdot Dip \cdot Depth) + G(Width \cdot Length \cdot Dip \cdot Depth) + H(Length \cdot Dip \cdot Depth \cdot RQD) \quad (52)$$

Where the terms Length, Width, Dip, Depth and RQD are the normalized values of these factors and where A, B, C, D, E, F, G, and H are the regression coefficients.

5.9.4.7 Divided in two groups, Level and Sublevel – North wall

The strongest model is based on the linear combination of the following factors and their regression coefficients:

For **Level Stopes** (R^2 = 21.0%)**:**

$DD_{MAX} = A + B \cdot Length + C \cdot Dip + D(Length \cdot RQD)$ (53)

For **Sublevel Stopes** (R^2 = 56.2%):

$DD_{MAX} = A + B \cdot Width + C \cdot Length + D \cdot Dip + E(Length \cdot Dip) + F(Length \cdot Dip \cdot Depth) + G(Length \cdot Dip \cdot Depth \cdot RQD)$ (54)

Where the terms Dip, Width, Depth, RQD, and Length are the normalized values of these factors and where A, B, C, D, E, F, and G are the unique regression coefficients for each model.

5.9.4.8 Divided in two groups, Primary and Secondary – North wall

The strongest model is based on the linear combination of the following factors and their regression coefficients:

For **Primary Stopes** (R^2 = 13.0%)**:**

$DD_{MAX} = A + B \cdot Length + C(Dip \cdot Depth) + D(Length \cdot Dip \cdot Depth)$ (55)

For **Secondary Stopes** (R^2 = 4.7%):

$DD_{MAX} = A + B(Length \cdot Depth) + C(Width \cdot Dip \cdot Depth) + D(Length \cdot Dip \cdot Depth) + E(Width \cdot Length \cdot Dip \cdot Depth) + F(Length \cdot Dip \cdot Depth \cdot RQD)$ (56)

Where the terms Dip, Width, Depth, RQD, and Length are the normalized values of these factors and where A, B, C, D, E, F, and G are the unique regression coefficients for each model.

5.9.4.9 Divide in four groups – North wall

For four groupings, the strongest models are based on the linear combination of the following factors and their regression coefficients:

For **Level-Primary Stopes** (R^2 = 60.0%)**:**

$DD_{MAX} = A + B \cdot Length + C \cdot Dip + D(Width \cdot Length \cdot Depth)$ (57)

For **Level-Secondary Stopes** (R^2 = 32.2%)**:**

$DD_{MAX} = A + B \cdot Dip + C(Dip \cdot Depth) + D(Width \cdot Dip \cdot Depth) + E(Width \cdot Length \cdot Dip \cdot Depth) + F(Width \cdot Dip \cdot Depth \cdot RQD)$ (58)

For **Sublevel-Primary Stopes** (R^2 = 71.8%)**:**

$DD_{MAX} = A + B \cdot Width + C(Length \cdot Dip) + D(Length \cdot Dip \cdot Depth) + E(Length \cdot Dip \cdot RQD)$ (59)

For **Sublevel-Secondary Stopes** (R^2 = 24.9%)**:**

$DD_{MAX} = A + B(Dip \cdot RQD) + C(Width \cdot Dip \cdot Depth) + D(Width \cdot Dip \cdot RQD) + E(Width \cdot Length \cdot Dip \cdot Depth$ (60)

Where the terms Dip, Width, Length, Depth and RQD are the normalized values of these factors and where A, B and C, D, E, and F are the unique regression coefficients for each model.

5.9.4.10 Reviewing North wall models

A summary of the three North wall models is presented in the table below:

Table 5.5 The Fourth Model - North wall models.

Division	Model	Number of Attributes	Number of stopes in model	R^2
All Stopes	1	7	46	18.6%
Level	2	4	27	21.0%
Sublevel		6	19	56.2%
Primary	3	3	18	13.0%
Secondary		5	28	4.7%
Level – Primary	4	3	9	60.0%
Level – Secondary		5	18	32.2%
Sublevel – Primary		4	10	78.1%
Sublevel - Secondary		4	9	24.9%

If the weighted average of R^2 for each of the four models (using the number of stopes as the weight) then the four models have collective R^2 values of: 18.6%, 35.5%, 7.95% and 46.19% respectively. Table 5.6 shows which of the expected factors were selected for inclusion in the model.

Table 5.6 Factors included in each model.

North wall	Width	Length	Dip	Depth	RQD
All	•	•	•	•	•
Level	•	•	•	•	•
Sublevel	•	•	•	•	•
Primary		•	•	•	
Secondary	•	•	•	•	•
Level Primary	•	•	•	•	
Level Secondary	•	•	•	•	•
Sublevel Primary	•	•	•	•	•
Sublevel Secondary	•	•	•	•	•

As with the South model, the addition of sequence subgroups improved the correlation results. Unfortunately the correlation values are generally quite lower than those found for the South model. The Level and Sublevel yielded the best correlation results while maintaining a reasonable sample group size. These two models also employed all the potential factors. The model is presented below:

For **Level Stopes** (R^2 = 21.0%)**:**

$$DD_{MAX} = -3.90 - 0.65\left(\frac{Length}{12m}\right) + 4.58\left(\frac{90^0}{Dip}\right) + 1.12\left(\frac{Width}{3.2m}\frac{90^0}{Dip}\frac{Depth}{128}\right) - 0.08\left(\frac{Length}{12m}\frac{100}{RQD}\right)$$
(61)

For **Sublevel Stopes** (R^2 = 56.2%)**:**

$$DD_{MAX} = 84.76 - 2.43\left(\frac{Width}{3.2m}\right) - 86.91\left(\frac{Length}{12m}\right) - 79.15\left(\frac{90^0}{Dip}\right) + 84.60\left(\frac{Length}{12m}\frac{90^0}{Dip}\right) - 0.55\left(\frac{Length}{12m}\frac{90^0}{Dip}\frac{Depth}{128}\right) + 0.63\left(\frac{Length}{12m}\frac{90^0}{Dip}\frac{Depth}{128}\frac{100}{RQD}\right)$$ (62)

5.9.5 The Fifth Model

The Fifth model was constructed in the same fashion as the Fourth model. While the Fourth model used only 46 stopes, the Fifth model employed 86 stopes. The sudden swell of the database is due to two factors. Firstly, about 30 new stopes were added to the database following an update from Lapa mine. Secondly, a review of stopes eliminated from previous models showed that some of these "erroneous" stopes were unnecessarily removed from the sample group. In the past, stopes were eliminated based on what was considered 'unusual' geometry (i.e. long stopes, very wide stopes, etc.) and not necessarily due to the degree of their overbreak. The problem with this technique being that these unusual stopes were not consistently high or low overbreak values; that is to say, factors other than geometry were governing overbreak. Removing stopes based on this criteria was felt to be inappropriate, nevertheless, it is still necessary to remove stopes which suffered enormous overbreak due to unusual circumstances.

By examining the distributions of DD_{MAX} values for the South wall, it was possible to identify four outlying stopes. These four stopes all had DD_{MAX} values in excess of 6.0m and are shown below in Figure 5.13.

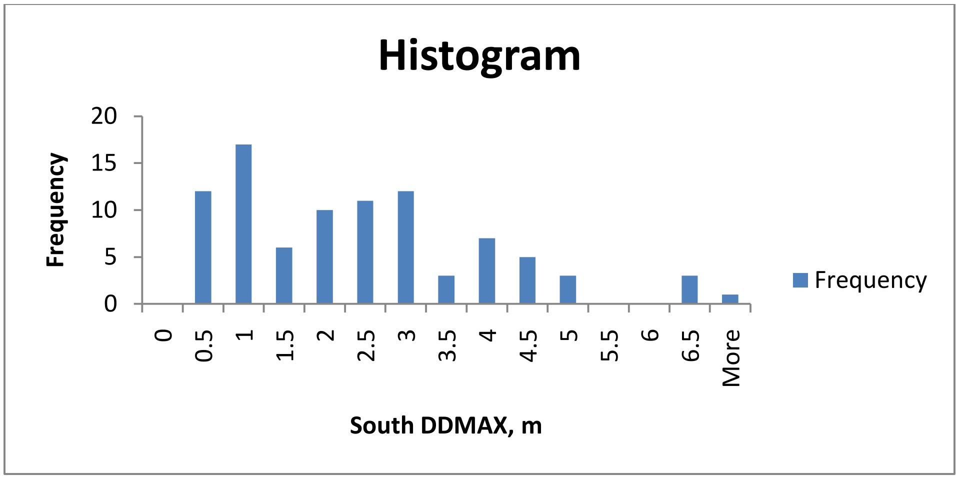

Figure 5.13 Histogram of South Wall DD_{MAX} values.

The major addition to the Fifth model is the revision of the measure used to assess the impact of sequence. In the models previous to this, the effects of sequence were treated through groupings without any measure relating to previously mined surrounding stopes.

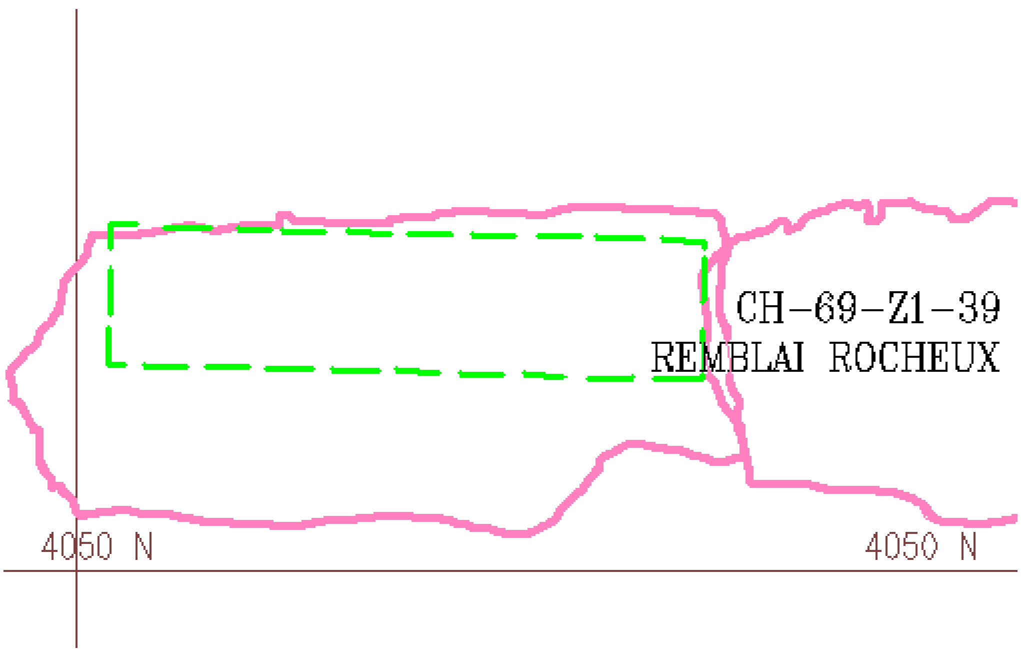

Figure 5.14 Example of sequence influence, mid-stope height CMS contour (pink) and planned stope outline (green), South wall is at the bottom.

Figure 5.14 shows an example of how the overbreak of a previously mined stope appears to directly influence the next stope in the sequence. The overbreak contours of the previous stope (69-Z1-39) extend to approximately the same depth as the overbreak contours of the next stope.

This effect appears to impact stopes both positively and negatively; in cases where the previous stope experienced a large degree of overbreak the effect is negative whereas if the overbreak on the previous stope was slight (as in the North face of Figure 5.14) then this can have a positive effect. In order to include this factor in the model it is necessary to introduce a new term. To assess the independent effects of both the horizontal and vertical sequence effects two separate terms are required.

$$DD_{Below} = 1 + DD_{MAX\ Below}$$

$$DD_{Adjacent} = 1 + DD_{MAXAdjacent}$$

Where DD_{Below} and $DD_{Adjacent}$ are the factors used in the model. $DD_{MAXBelow}$ is the DD_{MAX} value of the stope mined out immediately underneath the new stope. $DD_{MAXAdjacent}$ is the DD_{MAX} value of the stope mined out immediately next to (on the same level) as the new stope. In cases where the new stope is an S2 (i.e. backfill on both sides) then $DD_{MAXAdjacent}$ is the average DD_{MAX} of those two stopes. For Primary stopes or Level stopes (i.e. stopes without adjacent stopes or stopes underneath) the $DD_{MAXBelow}$ or $DD_{MAXAdjacent}$ values are set to zero, resulting in a factor of 1. A total of seven factors are now included in the model:

a) Width
b) Length
c) Dip
d) Depth
e) RQD
f) DD_{Below}
g) $DD_{Adjacent}$

The addition of this factor accounts for the effects of sequence. Since the effects of sequence are considered by these new factors, the division of stopes into groups is redundant and ultimately unnecessary. Only one model for both the South and North wall are required.

5.9.5.1 South wall model

For the South wall, the most predictive attributes, as well as their correlation coefficients are shown below in Table 5.7.

Table 5.7 The Fifth Model – South wall model.

Factor	Coefficient
Constant	-24.68
+Length	23.77
+Dip	29.52
+(Width•Length)	0.19
+(Length•Dip)	-27.53
+(Dip•Depth)	-0.34
+(Dip•DD_{Below})	0.15
+(Dip•Depth•RQD)	0.27
+(Width•Dip•Depth•DD_{Adj})	0.22
+(Width•Dip•Depth•DD_{Below})	-0.13

Where Length, Dip, Width, Depth, and RQD are the normalized variables of the actual values:

1) Length = Length/12m
2) Dip=Dip/90°
3) Width=Width/3.2m
4) Depth=Depth/128
5) RQD=100/RQD_{South}

5.9.5.2 North wall model

For the North wall, the most predictive attributes, as well as their correlation coefficients are shown below in Table 5.8.

Table 5.8 The Fifth Model – North wall model.

Factor	Coefficient
Constant	-23.67
+Width	15.35
+Dip	21.98
+(Width•Dip)	-11.25
+(Length•Dip)	-3.43
+(Width•Length•Dip)	0.42
+(Width•Dip•Depth)	-4.42
+(Length•Dip•Depth)	5.36
+(Width•Length•Dip•RQD)	-0.04
+(Width•Length•Depth•DD_{Adj})	0.57
+(Length•Dip•Depth•RQD•DD_{Below})	0.38
+(Width•Length•Dip•Depth•RQD•DD_{Below}•DD_{Adj})	-0.19

Where Length, Dip, Width, Depth, and RQD are the normalized variables of the actual values:

1) Length = Length/12m
2) Dip= 90°/Dip
3) Width=Width/3.2m
4) Depth=Depth/128
5) RQD=100/RQD_{North}

5.9.5.3 Extending the usefulness of the Fifth Model

The models that use the measurable effects of dilution (i.e. $DD_{Adjacent}$ and DD_{Below}) provide good correlation values. The South and North wall models have R^2 values of approximately 54% and 55% respectively. While these values are similar to those obtained in the fourth model, the sample size of the new models is much larger. Larger not only due to the addition of new stopes but also because the stopes are not divided into smaller sub groups in order to account for the effects of sequence.

The new strategy for considering the influence of sequence is effective but it suffers from one major drawback. In order to be able to use the new method, it is necessary to have the dilution data from the stopes mined underneath and adjacent to the new stope. This limitation prevents the new model from being used in long term planning exercises. When the grouping strategy was employed it was not necessary to have exact values for the behavior of surrounding stopes, an understanding of the mining sequence was all that was required.

With that in mind, it was decided to provide two sets of models, the first set (presented in Sections 5.9.5.1 and 5.9.5.2) that can be used as a short term planning tool, and the second set of models (presented below) which are a long range planning tool.

5.9.5.4 Long range models

As with the fourth model (presented in Section 5.9.4) the effects of sequence were included in the model by grouping the stopes according to their position in the mining sequence. The following sections present models which have sufficiently high correlations that they could be employed with some degree of confidence. Nevertheless, a variety of models were provided in order to allow the end-user to select the appropriate model(s) of their choosing.

5.9.5.5 Divided in two groups, Level and Sublevel – South

The strongest model is based on the linear combination of the following factors and their regression coefficients:

For **Level Stopes** (R^2 = 52.7%)**:**

$$DD_{MAX} = 2.44 - 0.43\left(\frac{Width}{3.2m}\right) + 0.67\left(\frac{Depth}{128}\right) - 1.56\left(\frac{Length}{12m}\frac{Dip}{90^0}\right) + 0.59\left(\frac{Dip}{90^0}\frac{Depth}{128}\frac{100}{RQD}\right) \text{ (63)}$$

For **Sublevel Stopes** (R^2 = 47.7%)**:**

$$DD_{MAX} = -1.27 - 3.17\left(\frac{Length}{12m}\right) + 6.22\left(\frac{Dip}{90^0}\right) + 0.19\left(\frac{Width}{3.2m}\frac{Dip}{90^0}\frac{Depth}{128}\frac{100}{RQD}\right) \text{ (64)}$$

5.9.5.6 Divided in two groups, Primary and Secondary – South

The strongest model is based on the linear combination of the following factors and their regression coefficients:

For **Primary Stopes** (R^2 = 53.7%):

$$DD_{MAX} = 3.36 - 0.71\left(\frac{Length}{12m}\right) - 1.67\left(\frac{Length}{12m}\frac{Dip}{90^0}\right) + 0.55\left(\frac{Dip}{90^0}\frac{Depth}{128}\frac{100}{RQD}\right) \text{ (65)}$$

For **Secondary Stopes** (R^2 = 46.8%)**:**

$$DD_{MAX} = -0.23 - 2.70\left(\frac{Length}{12m}\right) + 3.64\left(\frac{Dip}{90^0}\right) + 1.22\left(\frac{Width}{3.2m}\frac{Dip}{90^0}\frac{Depth}{128}\right) + 0.18\left(\frac{Dip}{90^0}\frac{Depth}{128}\frac{100}{RQD}\right) \text{ (66)}$$

5.9.5.7 Divided in four groups - South

For four groupings, the strongest models are based on the linear combination of the following factors and their regression coefficients:

For **Level-Primary Stopes** (R^2 = 63.3%)**:**

$$DD_{MAX} = 177.53 - 158.94\left(\frac{Length}{12m}\right) - 181.82\left(\frac{Dip}{90^0}\right) + 162.25\left(\frac{Length}{12m}\frac{Dip}{90^0}\right) + 0.66\left(\frac{Depth}{128}\frac{100}{RQD}\right) + 1.59\left(\frac{Width}{3.2m}\frac{Length}{12m}\frac{Dip}{90^0}\frac{Depth}{128}\right) \quad (67)$$

For **Level-Secondary Stopes** (R^2 = 53.5%)**:**

$$DD_{MAX} = -5.86 - 1.84\left(\frac{Length}{12m}\right) + 7.72\left(\frac{Dip}{90^0}\right) - 63.94\left(\frac{Depth}{128}\right) + 65.61\left(\frac{Width}{3.2m}\frac{Depth}{128}\right) + 64.61\left(\frac{Dip}{90^0}\frac{Depth}{12m}\right) - 64.60\left(\frac{Width}{3.2m}\frac{Dip}{90^0}\frac{Depth}{128}\right) + 0.50\left(\frac{Dip}{90^0}\frac{Depth}{128}\frac{100}{RQD}\right) \quad (68)$$

For **Sublevel-Primary Stopes** (R^2 = 48.9%):

$$DD_{MAX} = -22.26 + 24.83\left(\frac{Dip}{90^0}\right) + 22.88\left(\frac{Depth}{128}\right) - 23.82\left(\frac{Dip}{90^0}\frac{Depth}{128}\right) + 0.40\left(\frac{Dip}{90^0}\frac{Depth}{128}\frac{100}{RQD}\right) \quad (69)$$

For **Sublevel-Secondary Stopes** (R^2 = 62.3%):

$$DD_{MAX} = -2.39 - 3.95\left(\frac{Length}{12m}\right) + 7.96\left(\frac{Dip}{90^0}\right) + 0.17\left(\frac{Width}{3.2m}\frac{Dip}{90^0}\frac{100}{RQD}\right) \quad (70)$$

5.9.5.8 Divided in two groups, Level and Sublevel – North

The strongest model is based on the linear combination of the following factors and their regression coefficients:

For **Level Stopes** (R^2 = 51.1%)**:**

$$DD_{MAX} = -6.08 + 6.00\left(\frac{90^0}{Dip}\right) + 1.14\left(\frac{Width}{3.2m}\frac{Length}{12m}\frac{90^0}{Dip}\frac{Depth}{128}\right) \quad (71)$$

For **Sublevel Stopes** (R^2 = 36.8%):

$$DD_{MAX} = -1.93 - 1.06\left(\frac{Width}{3.2m}\right) + 3.63\left(\frac{90^0}{Dip}\right) + 0.36\left(\frac{90^0}{Dip}\frac{Depth}{128}\frac{100}{RQD}\right) \quad (72)$$

5.9.5.9 Divided in two groups, Primary and Secondary – North

The strongest model is based on the linear combination of the following factors and their regression coefficients:

For **Primary Stopes** (R^2 = 42.1%):

$$DD_{MAX} = -5.76 + 6.31\left(\frac{90^0}{Dip}\right) + 0.04\left(\frac{90^0}{Dip}\frac{100}{RQD}\right) + 0.30\left(\frac{Width}{3.2m}\frac{Length}{12m}\frac{90^0}{Dip}\right) \quad (73)$$

For **Secondary Stopes** (R^2 = 25.0%):

$$DD_{MAX} = -4.48 + 4.15\left(\frac{90^0}{Dip}\right) + 1.52\left(\frac{Length}{12m}\frac{90^0}{Dip}\frac{Depth}{128}\right) \quad (74)$$

5.9.5.10 Divided in four groups - North

For four groupings, the strongest models are based on the linear combination of the following factors and their regression coefficients:

For **Level-Primary Stopes** (R^2 = 58.1%):

$$DD_{MAX} = -3.57 + 3.59\left(\frac{90^0}{Dip}\right) + 0.95\left(\frac{Width}{3.2m}\frac{90^0}{Dip}\right) \quad (75)$$

For **Level-Secondary Stopes** (R^2 = 39.3%):

$$DD_{MAX} = -14.06 + 5.91\left(\frac{90^0}{Dip}\right) + 6.72\left(\frac{Width}{3.2m}\frac{90^0}{Dip}\right) + 7.22\left(\frac{Length}{12m}\frac{90^0}{Dip}\right) - 7.22\left(\frac{Width}{3.2m}\frac{Length}{12m}\frac{90^0}{Dip}\right) + 5.30\left(\frac{Width}{3.2m}\frac{Length}{12m}\frac{Depth}{128}\right) + 1.92\left(\frac{Width}{3.2m}\frac{90^0}{Dip}\frac{Depth}{128}\right) + 0.11\left(\frac{Length}{12m}\frac{90^0}{Dip}\frac{100}{RQD}\right) - 4.66\left(\frac{Width}{3.2m}\frac{Length}{12m}\frac{90^0}{Dip}\frac{Depth}{128}\right) \quad (76)$$

For **Sublevel-Primary Stopes** (R^2 = 69.2%):

$$DD_{MAX} = -0.35 + 0.89\left(\frac{Width}{3.2m}\right) + 1.78\left(\frac{90^0}{Dip}\right) - 1.92\left(\frac{Width}{3.2m}\frac{Depth}{128}\right) + 3.09\left(\frac{Length}{12m}\frac{Depth}{128}\right) - 2.26\left(\frac{Width}{3.2m}\frac{Length}{12m}\frac{Depth}{128}\right) \quad (77)$$

For **Sublevel-Secondary Stopes** (R^2 = 41.1%):

$$DD_{MAX} = 1.10 - 1.25\left(\frac{Width}{3.2m}\right) + 1.50\left(\frac{Length}{12m}\frac{90^0}{Dip}\frac{Depth}{128}\right) \quad (78)$$

5.9.5.11 Reviewing the South wall models

A summary of the South wall models is presented below in Table 5.9

Table 5.9 The Fifth Model - South wall.

Division	Model	Number of Attributes	Number of stopes in model	R^2
Level	1	4	50	52.7%
Sublevel		3	36	47.7%
Primary	2	3	32	53.7%
Secondary		4	54	46.8%
Level – Primary	3	5	16	63.3%
Level – Secondary		7	34	53.5%
Sublevel – Primary		4	16	48.9%
Sublevel - Secondary		3	20	62.3%
New Sequence Model	4	9	86	54.0%

If the weighted average of R^2 for each of the four models (using the number of stopes as the weight) then the four models have collective R^2 values of: 50.6%, 49.4%, 56.5%, and 54.0% respectively. Table 5.10 shows which of the expected factors were selected for inclusion in the model.

Table 5.10 Factors included in each model.

South Wall	Width	Length	Dip	Depth	RQD	DD_{Adj}	DD_{Bel}
Level		•	•	•	•	n/a	n/a
Sublevel	•	•	•	•	•	n/a	n/a
Primary		•	•	•	•	n/a	n/a
Secondary	•	•	•	•	•	n/a	n/a
Level Primary	•	•	•	•	•	n/a	n/a
Level Secondary	•	•	•	•	•	n/a	n/a
Sublevel Primary			•	•	•	n/a	n/a
Sublevel Secondary	•	•	•		•	n/a	n/a
New Sequence Model	•	•	•	•	•	•	•

The bulk of the models employ all of the factors. Three of the models are missing one of the factors while one model (Sublevel-Primary) does not contain two of the expected factors. The Sublevel-Primary model has one of the smaller sample groups and also a very low correlation value.

5.9.5.12 Reviewing North wall models

A summary of the North wall models is presented below in Table 5.11

Table 5.11 The Fifth Model - North wall.

Division	Model	Number of Attributes	Number of stopes in model	R^2
Level	1	2	48	51.1%
Sublevel		3	38	36.8%
Primary	2	3	30	42.1%
Secondary		2	56	25.0%
Level – Primary	3	2	15	58.1%
Level – Secondary		8	33	39.3%
Sublevel – Primary		5	15	69.2%
Sublevel - Secondary		2	23	41.1%
New Sequence Model	4	11	86	55.0%

If the weighted average of R^2 for each of the four models (using the number of stopes as the weight) then the four models have collective R^2 values of: 44.8%, 30.9%, 48.3%, and 55.0% respectively. Table 5.12 shows which of the expected factors were selected for inclusion in the model.

Table 5.12 Factors included in each model.

South Wall	Width	Length	Dip	Depth	RQD	DD_{Adj}	DD_{Bel}
Level	•	•	•	•		n/a	n/a
Sublevel	•		•	•	•	n/a	n/a
Primary	•	•	•		•	n/a	n/a
Secondary		•	•	•		n/a	n/a
Level Primary	•		•			n/a	n/a
Level Secondary	•	•	•	•	•	n/a	n/a
Sublevel Primary	•	•	•	•		n/a	n/a
Sublevel Secondary	•	•	•	•		n/a	n/a
New Sequence Model	•	•	•	•	•	•	•

The bulk of these models do not employ all of the expected factors. The new sequence model contains all of the expected factors and boasts the highest correlation (in terms of complete models). A user would need to be very selective of the long-range model they employ to estimate dilution. Nevertheless, there is still a good selection of models with decent correlation values.

5.10 Discussion and conclusions

A series of five complete models were developed. Each iteration brought a new approach and (in many cases) more data. Figure 5.15 shows the correlation values and number of stopes for each model iteration included in the best model. Quite clearly, as work progressed, results were generally improved. While models 3, 4, and 5 did not see significant improvements in South wall correlation vales, the sample group more than doubled in size.

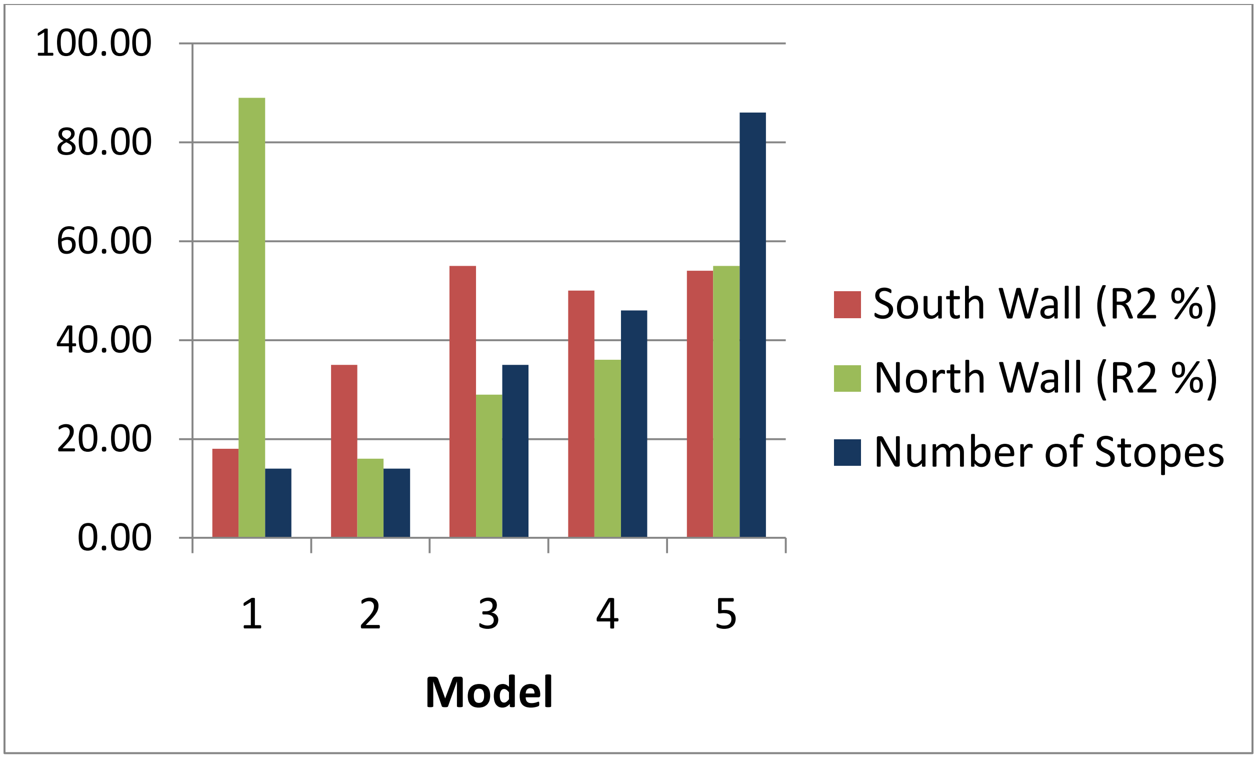

Figure 5.15 The progression of the empirical model.

While this shows that the approach was sound and unbiased, it also reveals the possibility that some influential factors were missed altogether in the model. Blast design, for example, was not examined in any detail, variation in powder factor, drill hole layouts, etc. all could have an influence on overbreak. In terms of geology, only RQD was employed, a more comprehensive measure, such as RMR or Q may have better reflected the impact of rock wall quality.

If these types of trends are to be explored then the database of data would need to undergo significant expansion and it is also necessary to create factors which can easily be measured or estimated. Reducing something as complex as "blast design" to some sort of measurable value may be a very complex and ultimately (if determined so using attribute evaluation) useless.

There is also the probable case that the mathematical model employed to represent the factors is a poor fit to the actual data. The model employed for this study was based on linear regressions but in reality dilution may be related to a factor though a power, logarithmic, sinusoidal, etc. type function. Also, it is assumed that the coupling between parameters is represented by multiplying the factors together; it is also possible that some factors are inversely related or are coupled with themselves (i.e. raised to some power).

Lastly, natural variance (i.e. randomness) in parameters (and results) as well as measurement error can contribute to challenges in obtaining high correlation values. This type of variance was hopefully minimized by using consistent strategies (as well as highly accurate survey equipment) to obtain values for each stope.

In order to make the model accessible and simple to use, the development of a DIMAND (refer to Chapter 3) feature which allows a user to select which model, input data, and retrieve estimates is recommended. Periodic updates of the model, using the same procedure outlined in this chapter but with additional data may also help refine and improve the models. That being said, increases in correlation are not necessarily expected due to the reasons explored earlier in this section.

To aid in the visualization of model accuracy and performance, two plots (one for the South wall, Figure 5.16 and one for the North wall, Figure 5.17) were produced using the New Sequence Model. On the horizontal axis, DD_{MAX} Measured refers to the actual DD_{MAX} values obtained through CMS surveys of the mined stope. The vertical axis, DD_{MAX} Predicted is the DD_{MAX} value predicted for each stope, based on the New Sequence Model and stope construction details. A red line has been superimposed on each plot; a perfect prediction would sit on the red line while poor predictions will lie far away from the red line.

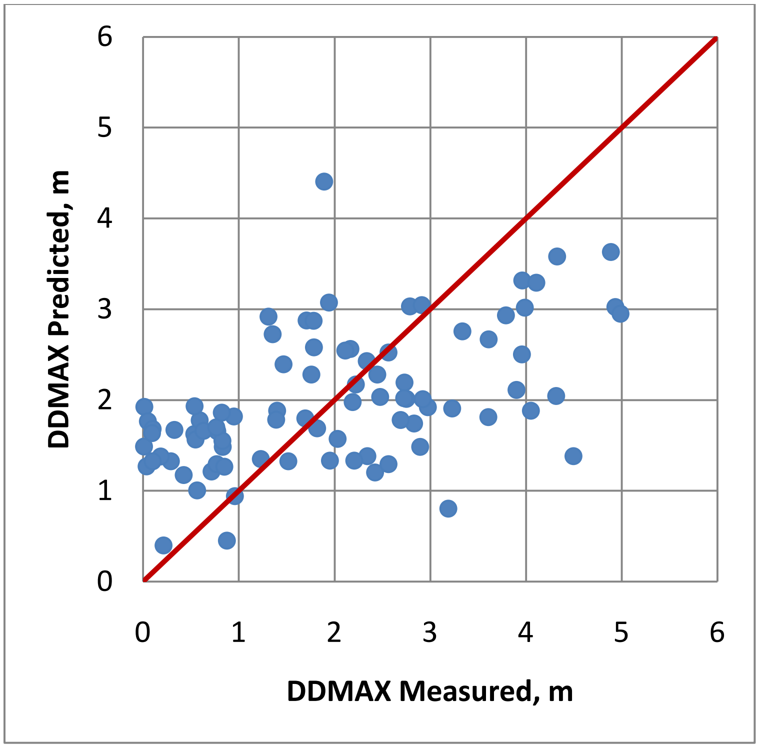

Figure 5.16 Evaluating model predictions for the South Model.

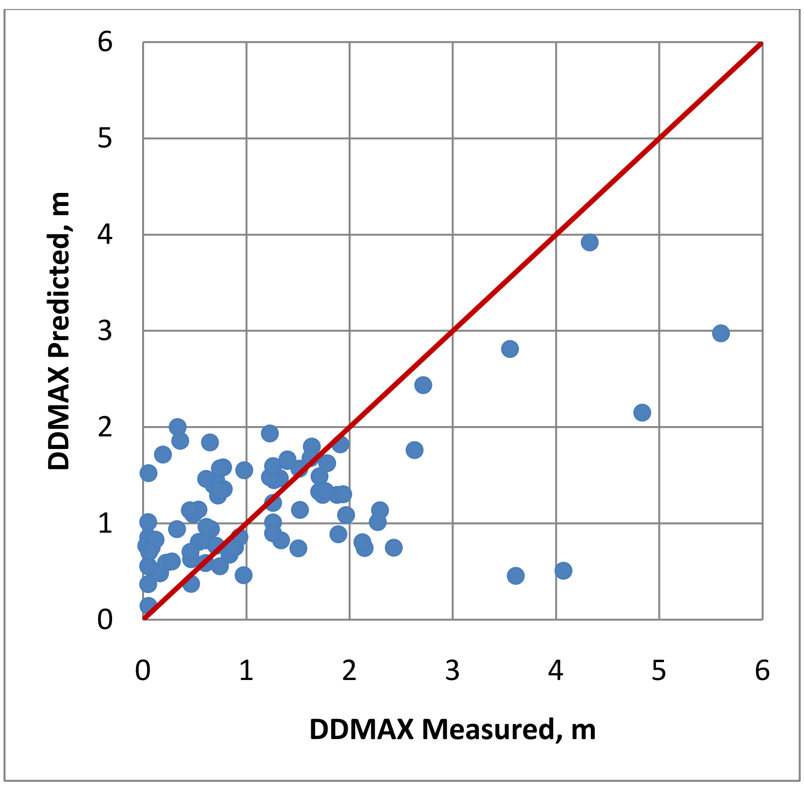

Figure 5.17 Evaluating model predictions for the North Model.

Examining Figure 5.16 and Figure 5.17 can help reveal prediction trends. Points that lie below the red line are values which were underestimated while points that lie above the red line are values which have been overestimated. Both models reveal a tendency to overestimate DD_{MAX} values when low dilution occurs (i.e. DD_{MAX} Measured less than 1m) as well as the tendency to underestimate DD_{MAX} when high dilution occurs (i.e. DD_{MAX} Measured greater than 3m). Overall, of the stopes plotted, the South Model overestimated 52% of the values and underestimated 48% of the time. The North Model showed a higher tendency (60%) to overestimate. Identifying these types of model behaviours aids the user in interpreting model predictions.

Chapter 6 – Summary and Conclusions

6.1 Summary

Longitudinal narrow vein retreat mining stopes can be prone to large amount of unplanned ore dilution. If unchecked, this excess dilution can threaten the economic integrity of a mining operation. This thesis examines a case study of Lapa mine in Preissac, Quebec and shows the steps necessary to develop an empirical model that can be employed to estimate dilution on a stope by stope basis.

The procedure outlined in this thesis can be extended to other operations providing a similar approach is employed.

- Collecting enough data to establish a geomechanical and stope reconciliation database.
- Identifying factors which may influence overbreak and gaining a better understanding of their impact through the use of numerical models.
- Employing statistical software to find relevant factors and their couplings.
- Performing a multi-linear regression of these relevant factors to determine the coefficients of the mathematical model that represents dilution as a function of the relevant factors.
- Periodically updating the model with new data and revising the model as necessary.

6.2 Conclusions

The following are the key conclusions of this study:

- Developing a useful and accessible database is paramount in this type of exercise. The time invested in the initial database development and set-up is repaid many times over during its use. This study could not have been completed within this timeframe without the use of the Lapa DIMAND.
- A variety of means exist to quantify dilution but simple percentages and even the slightly more advanced ELOS fail to capture the true shape and the actual effect of overbreak on

the rockmass. Dilution density reveals the extent of damage to the rockmass and is not inadvertently affected by stope widths.

- A large number of factors which influence overbreak were revealed, by carefully considering the problem it was possible to reduce this (i.e. stope height is constant at Lapa mine so it will not have an influence) to a manageable number of factors to consider. Dilution at Lapa mine seems to be primarily influenced by: stope length, stope width, stope dip, RQD, mining depth, and mining sequence.
- Careful study of stope strike length (a controllable parameter) showed that it has the ability to influence dilution. Based on the numerical model, reducing stope strike length will increase stope wall stability. The degree to which the stope strike length can be shortened will ultimately depend on the economics of reducing stope tonnages, increasing setup costs per each shorter stope (due to a fixed cost associated with developing the raise), and the overall savings resulting from lower dilutions.
- The development of a strategy for creating empirical dilution models allows a mine operator to better weigh the various factors influencing dilution and to optimize stope construction in order to minimize the potential for excessive dilution.

6.3 Recommendations for further research

The following are recommendations for future topics of study:

- A longitudinal retreat mining method employs a large amount of backfill. The performance of these backfill materials (especially cemented rock fill) needs to be studied and better understood.
- From a static standpoint, backfill dilution in narrow vein mining should not be of very significant concern. The exposed backfill face is quite small compared to the other exposed faces, despite this, many stopes at Lapa experienced dilution due to backfill. A study focused on exploring causes of backfill failure is recommended.
- The empirical dilution models presented in this study did not consider the effects of blasting on overbreak. Factors such as: powder factor, burden, spacing, and drill hole deviation may all influence overbreak.

- Examine the effects of vertical sequencing. As mining progresses an increased number of stopes will have been previously undermined. With footwall overbreak increasing the degree to which subsequently mined stopes are undercut, the effects of undercutting can be compounded as mining proceeds upwards. This phenomenon should be examined in three dimensions and the ability of pattern cablebolting to reduce this effect should be assessed.
- The degree to which the stope strike length can be shortened will ultimately depend on the economics of reducing stope tonnages, increasing setup costs per each shorter stope (due to a fixed cost associated with developing the raise), and the overall savings resulting from lower dilutions. Economic analysis of these factors could aid in stope optimization.

References

Barton, N. R., R. Lien, Lunde, J.. (1974). "Engineering classification of rock masses for the design of tunnel support." Rock Mech Min Sci (6): 189-239.

Bieniawski, Z. (1989). Engineering Rock Mass Classifications. New York, Wiley**:** 251.

Coulomb, C. (1776). "Essai sur une application des règles des maximis et minimis à quelques provblèmes de statique relatifs à l'architecture." Mem. Acad. **5**(7).

Dunne, K. and R. Pakalnis (1996). Dilution aspects of a sublevel retreat stope at Detour Lake Mine. Rock Engineering for Underground Civil Construction; Rock Mechanics. M. Aubertin, F. Hassani and H. S. Mitri, Balkema Rotterdam**:** 305-313.

Elbrond, J. (1994). "Economic effects of orelosses and rock dilution." CIM Bulletin **89**(978): 131-134.

Forsyth, W., T. Kleine, Cameron, A. (1994). Inaccurate blasthole drilling, Golder Associates Ltd.

Hassani, F. and J. Archibald (1998). "Mine Backfill." Canadian Institute of Mining, Metallurgy, and Petroleum.

Henning, J. G. and H. S. Mitri (2007). "Numerical modeling of ore dilution in blasthole stoping." International Journal of Rock Mechanics and Mining Sciences **44**: 692-703.

Henning, J. G. and H. S. Mitri (2008). "Assessment and control of ore dilution in long hole mining - case studies." Geotechnical and Geological Engineering: 349-366.

Hoek, E. and E. Brown (1980). "Underground excavation in rock." The Institution of Mining and Metallurgy.

Hoek, E. and E. Brown (1997). "Practical estimates of rock mass strength." International Journal of Rock Mechanics and Mining Sciences **34**(8): 1165-1186.

Hoek, E., C. Carranza-Torres, Corkum, B.. (2002). Hoek-Brown Failure Criterion—2002 Edition. 5th North American Rock Mechanics Symposium and the 148 17th Tunnelling Association of Canada Conference—NARMS-TAC. Toronto, Ontario, University of Toronto Press**:** 267-271.

Hoek, E. and M. Diederichs (2006). "Empirical estimation of rock mass modulus." International Journal of Rock Mechanics and Mining Sciences **43**(2): 203-215.

Mathews, K., E. Hoek,Wyllie, D.C., Steward S.B.V. (1981). Prediction of stable excavations for mining at depths below 1000 metres in hard rock. Ottawa, Department of Energy, Mines and Resources.

Mitri, H. S., R. Hughes, Lecomte, E. (2010). Factors influencing unplanned ore dilution in narrow vein longitudinal mining. 2010 SME Annual Meeting. Phoenix, Arizona.

O'Hara, T. (1980). "Quick Guides to the Evaluation of Orebodies." CIM Bulletin.

Pakalnis, R. (1986). Empirical stope design in Canada. Vancouver, British Columbia, University of British Columbia. **PhD:** 276.

Potvin, Y. (1988). Empirical open stope design in Canada. Vancouver, British Columbia, University of British Columbia. **PhD**.

Steel, R. G. D. and J. H. Torrie (1960). Principles and Procedures of Statistics. New York, McGraw-Hill**:** 187-287.

Trevor, S. (1991). Dilution control at Hudson Bay mining & smelting, Flin Flon operations. Proceedings of the 93rd CIM annual general meeting, Vancouver, British Columbia.

Vallée, M., M. David, Dagbert, M., Desrochers, C. (1992). "Guide to the evaluation of gold deposits." CIM **45**.

Wang, J. (2004). Influence of stress, undercutting, blasting and time on open stope stability and dilution. Saskatoon, Saskatchewan, University of Saskatchewan. **PhD**.

Zhao, X. and M. Cai (2010). "A mobilized dilation angle model for rocks." International Journal of Rock Mechanics and Mining Sciences **47**: 368-384.

Zniber El Mouhabbis, H., H. S. Mitri, Berdard, N., Lecomte, E. (2009). Effect of stope undercutting on its wall overbreak. Proc 43rd US Rock Mechanics Symposium. Asheville, North Carolina. **ARMA 09-200**.